

**Post Cerro Grande Fire Channel Morphology
in Lower Pueblo Canyon, Reach P-4 West:
and
Storm Water Transport of Plutonium 239/240
in Suspended Sediments**

Los Alamos County, New Mexico

Dave Englert, Ralph Ford-Schmid, and Kenny Bransford

Department of Energy Oversight Bureau
New Mexico Environment Department
2905 Rodeo Park Drive East
Santa Fe, New Mexico 87505

October 2004



Forward

The mission of the New Mexico Environment Department DOE Oversight Bureau is to assure that activities at DOE facilities in New Mexico are protective of the public health and safety and the environment. The Bureau's activities are funded through a grant from the U.S. Department of Energy in accordance with the provisions set forth in the *Agreement-In-Principle between the State of New Mexico and the U.S. Department of Energy*. One of the primary objectives of the agreement is the development and implementation of a program of independent monitoring and oversight.

Acknowledgements

This report was improved by thoughtful review and comments provided by Bernie Kleinman, Ellen Kleinman, Larry Smolka, Tim Michael, Leonard Lane, Michael Dale, John Till, Jim Rocco, Jill Aanenson, Justin Mohler, Paul Voileque, Joni Arends, and Francisco Apodaca. We would also like to thank Mark Koffman, Kevin Vigil, Tim Michael, Bill Bartels, Michael Dale, Steve Yanicak, Bob Weeks, and Kim Granzow for assisting in storm water collection and geomorphology fieldwork.

Table of Contents

Abstract	1
Introduction	2
Setting	5
Methodology	8
Hydrological Evaluation	8
Field Morphologic Measurements	9
Treatment of Data	9
Global Positioning System (GPS) Use	9
Stream Classification	10
Determination of Bankfull Discharge	11
Storm Water Monitoring	14
Plutonium Analytical Measurements	17
Mass Transport Calculation Methods	18
Hydrologic Data	20
Channel Characteristics and Discussion	24
Sediment and Plutonium-239/240 Transport	32
Summary	47
Recommendations	50
References	52
Appendix A. Historical Perspective	55
Appendix B. Linear and Vertical Field Measurements For Cross Sections and Longitudinal Profile	66
Appendix C. Stream Classification, Dimension, and Hydraulic Summaries	86
Appendix D. Latitude-Longitude Coordinates for Cross Section End Points	92
Appendix E. Cross Section Charts, Dimensions, and Remarks For P-4 West	94
Appendix F. DOE OB 2001 and 2002 Plutonium-239/240 and Suspended Sediment Concentrations in Pueblo Canyon Storm Water	110
Appendix G. Plutonium-239/240 and Suspended Sediment vs Flow Plots For Storm Water Runoff Measured in 2001 and 2002	116

Figures

Figure 1. Stream and rain gages in Pueblo Canyon	8
Figure 2. Bankfull Cross-Sectional Area as a Function of Watershed Area, All New Mexico Sites, (Knight et al., 1999)	11
Figure 3. Bankfull Discharge as a Function of Watershed Area, New Mexico Gage Sites, (Knight et al., 1999)	12
Figure 4. Cross Section 10 demonstrating the water level stage heights for 3 discharge rates	14
Figure 5. Magnitude and frequency of storm water flows greater than 10 cfs at LANL gage E060 in lower Pueblo Canyon	21
Figure 6. Daily cumulative precipitation at North Community rain gage in upper Pueblo Canyon correlated to runoff events greater than 10 cfs in lower Pueblo Canyon. Snowfall is measured in equivalent rainfall units	23
Figure 7. Annual cumulative precipitation and total flow relationship at lower Pueblo Canyon	24
Figure 8. Cross Section 20, most upstream measurement, and representative of the upper and lower stream sections at P-4 West	28
Figure 9. Cross Section 10, representative of the channel within the mid section of P-4 West	29
Figure 10. Longitudinal profile of P-4 West	31
Figure 11. June 22, 2002 hydrograph and associated suspended sediment concentrations	34
Figure 12. June 22, 2002 hydrograph and associated plutonium-239/240 concentrations	35
Figure 13. Total plutonium-239/240 in water compared to plutonium-239/240 in residual sediments	36
Figure 14. Ten year averages of plutonium-239/240 in bed load within the Pueblo Canyon channel	38
Figure 15. Plutonium-239/240 inventory transport correlation to peak flows	40
Figure 16. Sediment yield correlation to peak flows	41

Figure 17. Suspended sediments concentration and plutonium-239/240 concentration relationship	44
Figure 18. Plutonium-239/240 concentration correlation to flow rate.....	45
Figure 19. Suspended Sediment Concentration correlation to flow rate.....	46
Figure 20. Derived plutonium transport inventory and peak flow estimates from all samples collected during sampled storm events	47
Figure A-1. 2000 Plutonium-239/240 in ash from the Cerro Grande fire, and in storm water suspended sediment from reference canyons, Los Alamos Canyon, and Pueblo Canyon	56
Figure A-2. 2001 Plutonium-239/240 in ash from the Cerro Grande fire, and in storm water suspended sediment from reference	57
Figure A-3. 2002 Plutonium-239/240 concentrations in Cerro Grande ash, reference canyons, and Pueblo Canyon.....	58
Figure A-4. Cesium-137 concentrations in Viveash and Cerro Grand ash, and in storm water suspended sediment samples collected in 2000, 2001, and 2002	59
Figure A-5. Strontium-90 measurements in ash collected from the 2000 Viveash and Cerro Grande fires, and in suspended sediments collected from storm water in 200, 2001, and 2002	60
Figure A-6. Annual precipitation in Los Alamos area from 1943 to 1986	63
Figure A-7. Total annual flow in acre feet and the maximum flow for the single greatest runoff event per year in cfs.	64
Figure A-8. Plutonium annual mass transport rates estimated by Graff.....	65
Figure E1. Cross Sections 20 and 19	96
Figure E2. Cross sections 18 and 17.....	97
Figure E3. Cross sections 16 and 15.....	98
Figure E4. Cross sections 14 and 13.....	99
Figure E5. Cross sections 12 and 11a	100
Figure E6. Cross sections 11c and 10.....	101
Figure E7. Cross sections 11 and 8.....	102
Figure E8. Cross sections 9 and 7.....	103
Figure E9. Cross sections 6b and 5d	104
Figure E10. Cross sections 5c and 6.....	105
Figure E11. Cross sections 5b and 5.....	106
Figure E12. Cross sections 5a and 4.....	107
Figure E13. Cross sections 3 and 2.....	108
Figure E14. Cross section 1.....	109
Figure G-1. Plutonium-239/240 and Suspended Sediment Concentration Relationships to Flow during August 11, 2001 Runoff Event.....	117
Figure G-2. Plutonium-239/240 and Suspended Sediment Concentration Relationships to Flow during August 16, 2001 Runoff Event.....	118
Figure G-3. Plutonium-239/240 and Suspended Sediment Concentration Relationships to Flow during June 22, 2002 Runoff Event.....	119
Figure G-4. Plutonium-239/240 and Suspended Sediment Concentration Relationships to Flow during July 18, 2002 Runoff Event.....	120
Figure G-5. Plutonium-239/240 and Suspended Sediment Concentration Relationships to Flow during July 26, 2002 Runoff Event.....	121
Figure G-6. Plutonium-239/240 and Suspended Sediment Concentration Relationships to Flow during September 10, 2002 Runoff Event.....	122

Tables

Table 1. Classification Key for streams (Rosgen 1996)	10
Table 2. Summary table of cross section classifications and stream dimensions	27
Table 3. Plutonium-239/240 and sediment inventory transported beyond E060 during 6 of 37 storm water flows during 2000, 2001, and 2002	39
Table 4. Runoff Dates, peak flows, plutonium and sediment transport estimates, and summations	42
Table A-1. Plutonium-239/240 reference values and concentrations measured in storm water suspended sediments	56

Table A-2. Estimates of plutonium-239/240 and sediment transport into the Rio Grande at lower Los Alamos Canyon (Graff, 1983).....	62
Table B-1. Measurements at Cross Sections 20 and 19.....	71
Table B-2. Measurements at Cross Sections 18 and 17.....	72
Table B-3. Measurements at Cross Sections 16 and 15.....	73
Table B-4. Measurements at Cross Sections 14 and 13.....	74
Table B-5. Measurements at Cross Sections 12 and 11A.....	75
Table B-6. Measurements at Cross Sections 11C and 10.....	76
Table B-7. Measurements at Cross Sections 11 and 8.....	77
Table B-8. Measurements at Cross Sections 9 and 7.....	78
Table B-9. Measurements at Cross Sections 6B and 5D.....	79
Table B-10. Measurements at Cross Sections 5C and 6.....	80
Table B-11. Measurements at Cross Sections 5B and 5.....	81
Table B-12. Measurements at Cross Sections 5A and 4.....	82
Table B-13. Measurements at Cross Sections 3 and 2.....	83
Table B-14. Measurements at Cross Section 1.....	84
Table B-15. Measurements Along Longitudinal Profile, West to East.....	85
Table C-1. Summary table of cross section classifications and stream dimensions.....	87
Table C-2. Summary table of cross section stream dimensions.....	90
Table C-3. Summary table of cross section stream hydraulics.....	91
Table D1. Cross section end point coordinates.....	93
Table F1. NMED DOE OB 2000, 2001, and 2002 Plutonium-239/240 and Suspended Sediment Concentrations in Pueblo Canyon system.....	112
Table F2. Particle Size Distribution for Storm water Samples in Pueblo Canyon.....	115

Plates

Plate 1. Overview of NMED Stream Morphology Project in Lower Pueblo Canyon.....	3
Plate 2. Stream Morphology in P-4 West in Pueblo Canyon.....	26
Plate 3. Cross Section Locations, Channel Classifications, and Profile in P4 West.....	95
Plate 4. Storm Water Sample Locations and LANL Sediment Surveillance Station.....	111

Abstract

In 2002 and 2003, the New Mexico Environment Department characterized the shape and function of a short stream reach in lower Pueblo Canyon called P-4 West. The stream channels in Pueblo Canyon, as well as other channels on the Pajarito Plateau, are adjusting to increased storm water flows. Peak flows and total discharge in canyons on the Pajarito Plateau have increased due to changes in forest floor soil conditions resulting from the May 2000 Cerro Grande fire. The adjustments include channel geometry changes, increased sediment yield, and associated legacy contaminant transport from canyons within the Los Alamos National Laboratory (LANL).

This project was initiated during July of 2002 in Pueblo Canyon reach P-4 West to (1) establish baseline conditions for monitoring changes in the Pueblo Canyon channels, (2) demonstrate a method for evaluating, predicting, and monitoring channel changes, (3) compare channel changes to pre-fire geomorphic mapping of plutonium-239/240 distribution in Pueblo Canyon sediments, and (4) demonstrate methods for estimating sediment and plutonium-239/240 transport from Pueblo Canyon. It is an extension of a project initiated during November of 2001 in P-4 East, a reach downstream of P-4 West.

We measured channel dimensions at 27 cross sections in reach P-4 West, established a stream profile along 3,000 feet of its length, and mapped the pattern of the channel bottom and banks of the floodplains and terraces. These measurements were used to classify the existing stream channel in P-4 West and evaluate channel adjustments to impacts from the Cerro Grande fire. We assessed the channel dimensions, profile, and stream patterns in relationship to geomorphic units and plutonium-239/240 concentrations and inventories in those units measured and mapped by the Los Alamos National Laboratory Environmental Restoration Group. We also collected storm water samples in Pueblo Canyon to determine the rate and mass of sediment and plutonium-239/240 transport from this area.

We found that the rates of normal channel adjustments: degradation, aggradation and subsequent sediment mixing, have accelerated since the Cerro Grande fire. Destabilized channel banks are mostly limited to the pre-fire active channel and lower floodplain banks, where legacy waste contaminant inventories are the smallest. In some areas, floodwaters have flowed over terraces, causing erosion, sediment mixing, and net deposition on them. Where the floodwaters return to the main channel, bank erosion of older sediment units that contain larger plutonium-239/240 concentrations and inventories is common.

We estimate 87 mCi of plutonium-239/240 contained in 22,000 tons of suspended sediment were transported out of Pueblo Canyon from 2000 to 2002. This is equivalent to an average 4.5 pCi/g concentration of plutonium-239/240 in suspended sediments, an order of magnitude greater than plutonium-239/240 concentrations realized in ash created during the Cerro Grande fire, and 2 orders of magnitude greater than background sediment levels. Because legacy plutonium-239/240 overwhelms the contribution of

plutonium from background and Cerro Grande ash sources, they were not differentiated in our inventory calculations.

Contaminant transport rates as large as these have not been seen since the 1950's and 60's, during and shortly after a period LANL was discharging radioactive wastewaters into the Pueblo Canyon system. Prior to the fire, LANL had estimated over 1 curie of plutonium was stored in Pueblo Canyon sediments. We calculate that approximately 9% of the pre-fire plutonium inventory in Pueblo Canyon has been removed. Contaminant transport is closely associated with the increased flooding in Pueblo Canyon and we expect transport to diminish as flood frequencies and intensities diminish.

To control the current transport of sediments and legacy contaminants from Pueblo Canyon, we make several recommendations to the agencies involved in rehabilitation of Cerro Grande Fire impacts. These agencies include the U.S. Department of Energy, Los Alamos National Laboratory, Los Alamos municipality, Los Alamos County, U.S. Forest Service, and the New Mexico Environment Department. The recommendations are: (1) initiate bank stabilization efforts in areas impacted by flooding, (2) enhance sediment deposition on floodplains and terraces, (3) re-evaluate forest rehabilitation in burned watersheds, (4) reduce urban runoff in Pueblo Canyon from the Los Alamos town site, (5) increase and improve storm water monitoring efforts, and (6) continue monitoring channel geometry and stream characteristics.

Introduction

In July and August of 2002, and later in 2003, the Department of Energy Oversight Bureau of the New Mexico Environment Department measured physical variables of the stream in lower Pueblo Canyon, reach P-4 West, that reflect the condition of its channel. This investigation was initiated to evaluate and monitor the May 2000 Cerro Grande fire impacts to the Pueblo Canyon stream channel. We measured channel dimensions, stream pattern, stream profile, and bed features to assess channel stability. We also collected and evaluated storm water samples for sediment and plutonium-239/240 transport during the summer months since the fire. This reach is upstream of P-4 East, an area where we completed a similar investigation in November of 2001 (Ford-Schmid, 2003). Both reaches are downstream of an area burned during the Cerro Grande fire. Exceptionally large deposits of early post-1942 sediment containing legacy contaminants from early LANL operations exist in P-4 West (Reneau, et al, 1998). The plutonium-239/240 inventory and contaminated sediment volumes are relatively larger than other reaches in Pueblo Canyon. See Plate 1 for map of the area.

NMED Stream Morphology Project in Pueblo Canyon

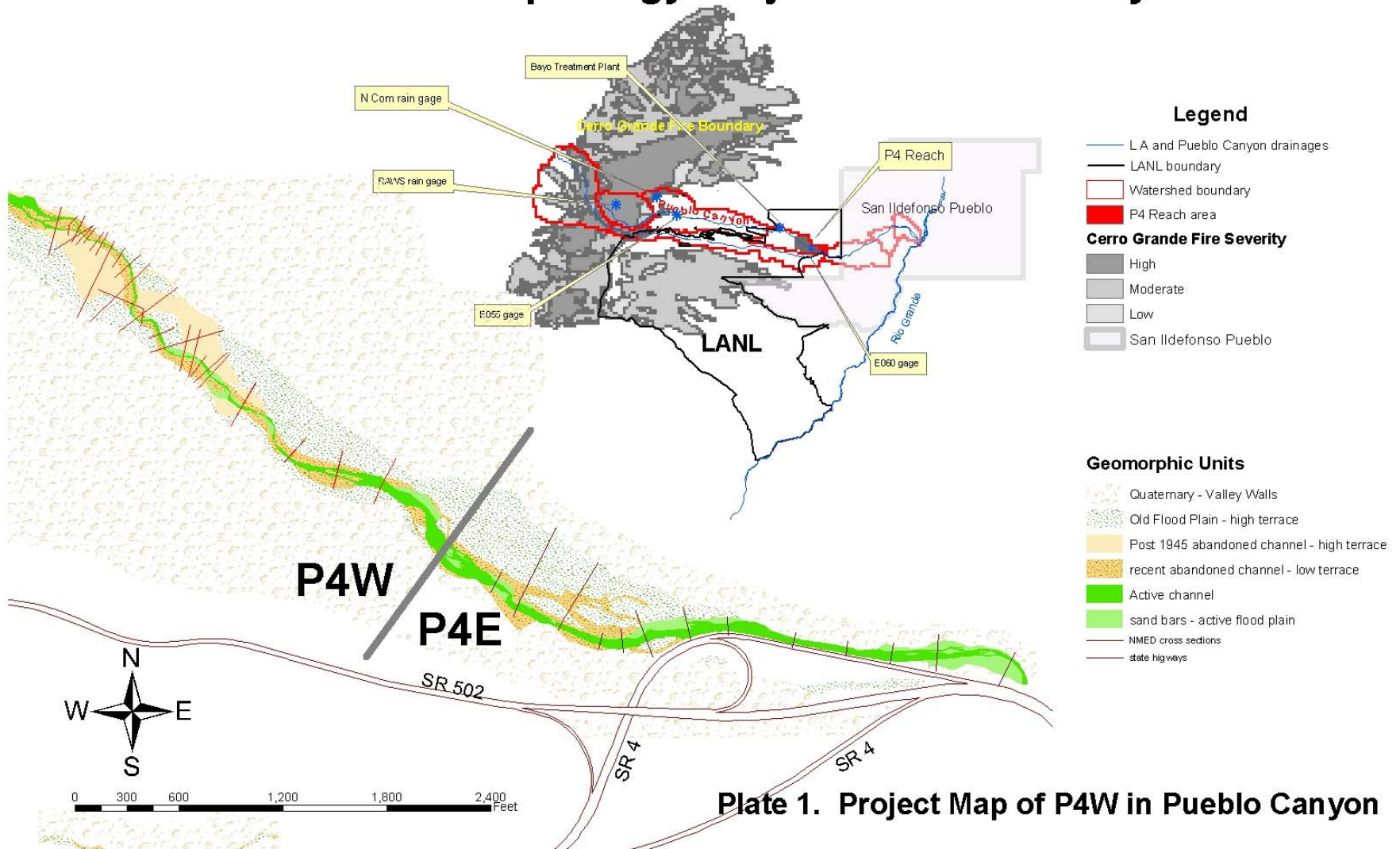


Plate 1. Project Map of P4W in Pueblo Canyon

In May 2000, the Cerro Grande fire burned 43,000 acres of land along the eastern flanks of the Jemez Mountains and on the Pajarito Plateau. Approximately 1,200 acres, nearly 80%, of the upper Pueblo Canyon watershed were subjected to a high intensity burn (BAER, 2000). A complete loss of vegetative cover (overstory, understory, and ground cover) and intense heat created conditions that reduced the soil's ability to absorb moisture, thereby increasing runoff. These conditions led to a greater frequency and magnitude of storm water flows in the canyons on the Pajarito Plateau. Investigations by Veenhuis (2002) of 2 forest fires in the region led us to believe that channels subjected to this flooding would adjust to these flows and contribute increasing amounts of sediments to storm water runoff.

These sediments contain legacy contaminants as well as fallout contaminants from nuclear atmospheric testing and potential LANL operational emissions. Forest biomass takes up the contaminants, as well as naturally occurring elements, as nutrients. The contaminants are then concentrated when forest materials are reduced to ash in fires.

We found plutonium-239/240 concentrations in ash to be 20 to 30 times that seen in reference soils. Investigations by the Oversight Bureau found that the mean concentration of plutonium-239/240 in Cerro Grande ash was 0.24 pCi/g (NMED report in progress), an order of magnitude greater than the upper limit of the background concentration in soil. According to the LANL Environmental Surveillance Report (LANL ESR, 2001), the LANL background reference value in soil is 0.019 pCi/g. This value is the mean of northern New Mexico regional values plus 2 standard deviations, and is intended to be the probable largest value of plutonium-239/240 in background soils.

The weighted mean concentration of plutonium-239/240 in storm water suspended sediments is 4.5 pCi/g., 20 times greater than the average value we measured for the Cerro Grande ash. We found that the legacy component of plutonium 239/240 in storm water greatly exceeds the contributions to contaminant transport from background soils or ash. Because of the magnitudes of differences between the background, ash, and legacy components of plutonium-239/240 in sediments being transported by storm waters; and because we found ash was removed from the watershed within the 3 year period of this study and that legacy plutonium-239/240 continues to be transported at increasing rates, we did not differentiate between the fallout, ash, or legacy plutonium transport yield in this study.

Additional discussions of contaminant transport in ash are found in Appendix A.

Despite some successful watershed rehabilitation, storm water runoff and sediment yield increased significantly after the Cerro Grande fire. This is consistent with results after the 1977 La Mesa fire and the 1996 Dome fire as discussed by Veenhuis (2002), who found that peak discharge increased over 100 times in the first two years compared to pre-fire conditions, and decreased rapidly after that to 3-5 times pre-fire flows. Before the Cerro Grande fire, lower Pueblo Canyon geomorphic characteristics were the result of

the adjustment of its boundaries to the pre-Cerro Grande fire flow and sediment regime. Pre-fire historic aggradation-degradation cycles have been documented and are discussed in Reneau and McDonald (1996) and Reneau et al. (1996, 1998, 2003). Since the fire, the channel changes have accelerated to compensate for increases in discharge and sediment yield. The channel changes are leading to transitional stream classifications and display a state of disequilibrium, instability, or departure from the channel's potential form and function.

A stable stream channel is able to maintain its plan form, channel dimensions, slope, and bed features while consistently transporting its sediment load without aggrading or degrading the channel form. If the stream equilibrium is impaired, or forces that formed its character are unbalanced, it moves into a state of adjustment striving to achieve equilibrium.

In order to evaluate the channel characteristics of Pueblo Canyon reach P-4 West, we measured channel dimensions at 27 cross sections along a 3000-foot section of this reach. We surveyed the stream channel thalweg, the water surface, and the lowest bank feature along this section producing a channel profile. We mapped the stream pattern by recording the thalweg and bed feature positions with global positioning and geographic information system tools. We then used stream classification methodologies developed by Rosgen (1996, 1994) to categorize the stream channel at each cross section. Stream features were finally compared to geomorphic mapping completed by LANL's Environmental Restoration Project, Canyons Focus Area. LANL's Environmental Restoration group is now part of the Risk Reduction and Environmental Stewardship division (RRES), and renamed the Remediation Services program (RS), or RRES-RS.

To evaluate sediment and associated contaminant transport we deployed portable Isco[®] programmable liquid samplers in Pueblo Canyon and sampled storm water runoff. We programmed the Isco[®] samplers to collect an array of samples that represents the changing characteristics of a storm runoff event. Samples were collected on the rising leg of the storm hydrograph, and then at 45 or 60-minute time intervals along the falling leg. Commercial analytical laboratories analyzed the samples for suspended sediment concentration, dissolved plutonium-239/240 concentration in water, total plutonium-239/240 concentration in water, and plutonium-239/240 concentration in sediment.

In this report, the term plutonium will be used synonymously with plutonium-230/240. Analytical methods we used for this study are not able to distinguish between the -239 and -240 plutonium isotopes and plutonium-238 was consistently measured near or below the analytical detection limits and therefore not included in the transport evaluation. Additional discussion regarding analytical methods is included under the Methodology section.

Setting

Pueblo Canyon is a 10-mile long, narrow canyon that crosses Santa Fe National Forest, Los Alamos town site, and LANL. The watershed area is approximately 5,400 acres (8

square miles). The upper third of the watershed, 1,450 acres, in Pueblo Canyon was severely burned during the Cerro Grande fire and is above the Los Alamos town site on the eastern flanks of the Jemez Mountains. Ash from the fire contains residual fallout contaminants and Pueblo Canyon sediments contain LANL legacy contaminants that are susceptible to transport.

Our study site in reach P-4 West is in lower Pueblo Canyon, approximately 900 feet west of the original P-4 East study site, and 5.5 miles downstream of the watershed area burned during the Cerro Grande fire. Plate 1 shows the varying intensities of the burn in shades of gray. The reach is near LANL's eastern property boundary and almost 1 mile above the Pueblo Canyon confluence with Los Alamos Canyon. San Ildefonso Pueblo is adjacent to LANL's eastern border and the Rio Grande is approximately 5 miles downstream.

The Los Alamos town site wastewater treatment plant, the Bayo plant, is approximately one-half mile above the P-4 West reach and 2 miles above the Pueblo-Los Alamos Canyon confluence. The plant's discharge flows through P-4 West and P-4 East to the Los Alamos Canyon confluence. LANL maintains a rain gage in the Los Alamos town site, North Community. It is in the upper Pueblo Canyon watershed. They also maintain 2 stream gages, gage E055 in upper and gage E060 in lower Pueblo Canyon. The Western Regional Climate Center installed a Regional Automated Weather Station, referred to as the Pueblo RAWs gage, in the burned watershed area in 2000.

The elevation of the Pueblo canyon channel ranges from 9100 to 6300 feet. The stream slope diminishes from approximately 10% in the upper watershed area on the mountain flanks, to 4% through the town site, to less than 2% at the P-4 reaches above its confluence with Los Alamos Canyon. Pueblo Canyon generates a well-developed floodplain in its lower reach associated with the smaller gradient and wider valley floor.

Mixed conifer forests had covered the mountain slopes in the National Forest before the fire. As the elevation declines eastward in the canyon, dominating ponderosa pine forests change to mixed ponderosa and juniper-piñon woodlands at the lower elevations. During the initial recovery stages of the burned forest, aspen and oak trees, forbs, and grasses are replacing the burned mixed conifer forest. Success of this recovery has been limited by a drought being experienced in the United States Southwest. The greatest recoveries are on the north slopes and in the canyon bottoms. The south facing mountain and canyon sides and steep slopes are experiencing limited regrowth. The ponderosa and piñon forests are presently experiencing severe impacts from the drought. More than 85% of the piñon forest has died from a pine bark beetle infestation, exacerbated by the drought.

Steep valley walls, colored light stippled brown on Plate 1, confine the alluvial filled canyon bottom in Pueblo Canyon. The valley walls are made up of Quaternary ignimbrite and pumice deposits of the Bandelier Tuff. Welded tuff units are comprised of the Tshirege and Otowi Members, the Tshirege Member being the youngest and more densely welded cliff-forming unit. Air fall ash deposits within the Bandelier Tuff include the Tsankawi and Guaje Pumice Beds. These rocks form vertical-ledge mesa tops and

steep colluvial slopes above the canyon bottom and are sparsely to densely covered by juniper and piñon forests. In some areas of the P-4 West and East reaches, stream channels have incised through the alluvial fill and into conglomerate units of the Puye Formation. The Puye Formation is more resistant to erosion and forms grade controls in the channel where incision to bedrock occurs.

Prior to the fire, LANL studies in Pueblo Canyon indicated contaminants were distributed throughout the canyon floor sediments. The primary source was radioactive wastewater discharge from TA-45, active from 1944 to 1964. Throughout the report we refer to legacy waste or legacy contaminants as those discharged from 1944 to 1964 into Acid Canyon and subsequently redistributed in Pueblo Canyon.

Contaminants found in the sediments include americium-241, cesium-137, plutonium-238 and -239/240, strontium-90, uranium-234, -235, and -238, polychlorinated biphenyls (PCBs), and other semi volatile organics, antimony, barium, cadmium, copper, lead, mercury, silver, and thallium above background and some above LANL screening action limits. Screening action limits are defined concentrations in samples, that if exceeded require further action.

A risk assessment in Pueblo Canyon (Reneau, et al, 1998), before the Cerro Grande fire, indicated the conditions in Pueblo Canyon posed acceptable human health risks and did not require immediate remedial actions. This assessment included possible warranted remedial actions following additional sampling and assessments, and presumed that contaminants in sediments carried by floods are stable or have been declining for decades, and that redistribution of contaminated sediments will not result in future increases in contaminant concentrations in downstream areas. Since the fire, sediments that required additional sampling and assessment have been eroded and transported downstream, contaminant transport rates have increased, and contaminants are being redistributed downstream onto San Ildefonso Pueblo lands and into the Rio Grande.

Reach P-4 has the largest estimated inventory of plutonium of any of the Pueblo Canyon reaches, due to an exceptionally large volume of mid-1940's and mid-1960's sediments with relatively high plutonium concentrations. The LANL RRES-RS group estimated a plutonium inventory of 158.5 mCi in P-4 West, of which 9% is stored in active channel units and 91% stored in older over bank and abandoned channel units. The highest concentrations were found in older post-1942 abandoned channel units, and in over bank units.

The active channel floodplain in reach P-4, colored light green on Plate 1, is covered in most areas by thick marsh grass sustained by an almost daily discharge of effluent water from the Bayo wastewater treatment plant. Older post-1942 channels that have been abandoned and subsequently sediment filled are colored shades of brown on Plate 1. Sagebrush, forbs, and sparse grasses cover these geomorphic units. The banks that confine the existing floodplain were formed as the active channel incised into these post-1942 units. Pre-1942 channel units, colored stippled green on Plate 1, are terrace forming and have been covered with post-1942 flood deposits. Ponderosa, piñon and juniper

woodlands cover these older units. Since the Cerro Grande fire, accelerated channel adjustments are occurring within the active channel; banks formed in post-1942 sediment units, exposed to high floodwater stages, are eroding; and sediments and debris are again being deposited on terraces.

The LANL RRES-RS established unit classifications, used in this report, describing the sediment geomorphic units in Pueblo Canyon. Labels consisting of “c” depict active and post-1942 abandoned channel units. Labels consisting of “f” depict post-1942 floodplain deposits. Quaternary and terrace deposits formed prior to the establishment of the Laboratory are labeled “Q” and “Qt”. Further classifications are designated by numerical suffixes. For example, the label “c1” designates the present active channel. Older channels, often abandoned and sediment filled have sequentially larger numbers. In this report the “c6” units reflect the oldest post-1942 channel units. They form terrace and stream bank units derived from active channels abandoned and subsequently filled during 1935 to 1954.

More than 1 curie of plutonium remains stored in Pueblo Canyon sediments from the original LANL wastewater discharges that occurred during the early days of operations. A total inventory of those discharges is unknown. Before the fire, LANL estimated that approximately 394 mCi, 38% of the plutonium inventory was in the active channel and most susceptible to remobilization (Reneau, et al, 1998)

Methodology

We evaluated the hydrology, channel characteristics, and sediment and contaminant transport using the methods and data sources described in the following sections.

Hydrological Evaluation

We evaluated the available storm water discharge data (rates, volumes, and frequency) from the LANL E060 gage located in Lower Pueblo Canyon. LANL publishes these data in annual water reports such as the Surface Water Data at Los Alamos National Laboratory: 2000, 2001, 2002 Water Year publications and at the LANL web site: <http://wqdbworld.lanl.gov/>. The LANL Water Quality and Hydrology program (RRES-WQH) installed the gage in Lower Pueblo Canyon in 1992 (Shaull, et. al., 2001). It is located in the lower Pueblo Canyon P-4 East reach, along New Mexico State Road 502. The gage station is northeast of the State Highway Department’s maintenance yard, 4.2 miles east of Los Alamos town site (latitude 35° 52’ 50” N, longitude 106° 13’ 1” W,

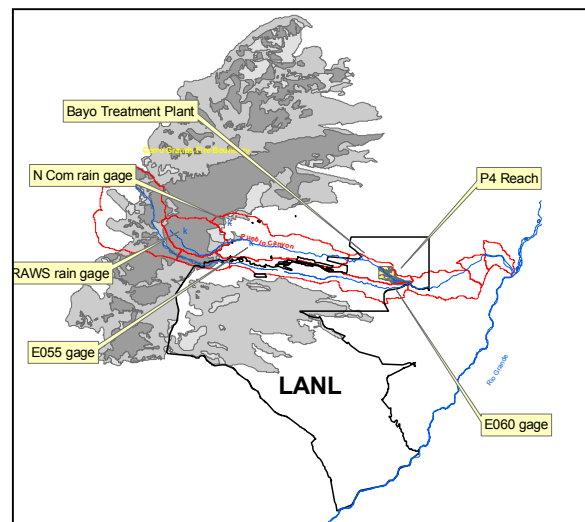


Figure 1. Stream and rain gages in Pueblo Canyon

elevation 6356 feet). Flow data was not evaluated at the E055 gage in Upper Pueblo Canyon, although it was used as a storm water sampling location.

We evaluated precipitation data from LANL's North Community meteorological station and the Western Regional Climate Center's regional automated weather station referred to as RAWS. These databases are on the following web sites: <http://weather.lanl.gov/> and <http://www.wrcc.dri.edu/losalamos/>. The gages are located in Pueblo Canyon's upper watershed; the North Community station is in a western Los Alamos residential area (latitude 35° 54' 2" N, longitude 106° 19' 17" W, elevation 7421 feet), the RAWS location is in the burned watershed area (latitude 35° 53' 41" N, longitude 106° 20' 38" W, elevation 8500 feet). Precipitation summaries were also found in the LANL document "Precipitation Events and Storm Water Runoff Events at Los Alamos National Laboratory after the Cerro Grande Fire" (Koch, 2001).

Field Morphologic Measurements

We used basic survey equipment and methods described by Harrleson (1994) to measure the dimensions and features in the P-4 West channel. We measured horizontal and vertical distances of channel features along 27 cross sections and a longitudinal profile. All cross sections were located perpendicular to the channel, and deposition, terrace, and vegetation features were noted. A longitudinal profile of more than 3,000 feet was measured through reach P-4 West. The longitudinal profile included measurements of the thalweg, the active channel bank, and when present, the water surface and abandoned floodplain banks developed by incising channels. The linear and vertical measurements for each cross section and longitudinal profile are compiled in Appendix B.

Treatment of Data

We used a Microsoft Excel spreadsheet developed by Dan Mecklenburg (© 1999 River4m, Ltd) to evaluate our field data. The program generates cross section and longitudinal profile figures. It also calculates the dimensional and hydraulic parameters listed throughout this report and summarized in Appendix C.

Global Positioning System (GPS) Use

We used a Trimble™ GeoExplorer III hand-held Global Positioning System (GPS) unit to determine the coordinates of the ends of each cross section and patterns of the thalweg and terrace features. We transferred these map features as well as theme coverages from LANL's Geographical Information Laboratory (GISLab) into ESRI Arcview 8.3® Geographic Information System. The LANL RRES-RS group's geomorphic mapping of Pueblo Canyon is an example of the thematic coverage provided by LANL GISLab. These tools were instrumental in preparing figures for this report and evaluating the geomorphology and channel meander geometry in the P-4 West reach. The coordinates for the cross section end points are listed in Appendix D.

Comparison of the features we mapped to those mapped by RRES-RS before the fire places the cross sections, current stream pattern, and stream and terrace bank features in context with conditions before the fire. This provides insight into the stability of the geomorphic units in Pueblo Canyon containing legacy contaminant inventories.

Stream Classification

We used the measured channel dimensions, longitudinal profile of the valley and stream, and the mapped plan view of the channel in lower Pueblo Canyon to classify the P-4 reach. We used a stream classification system, described by Rosgen (1996, 1994), to classify the channel at each cross section, predict changes in the reach, and establish references for future monitoring of stream conditions in lower Pueblo Canyon. The system uses measurable morphological features and their relationships to provide consistent and reproducible descriptions and assessments.

This system uses dimensionless ratios of basic morphological measurements to classify stream courses into eight basic morphological stream types (A, B, C, D, DA, E, F, or G). These measurements and ratios are listed below and classification criteria is shown in Table 1:

- Entrenchment Ratio (W_{fpa} / W_{bkf}) = Flood Prone Area Width / Bankfull Area Width
- Width / Depth Ratio (W_{bkf} / D_{bkf}) = Bankfull Area Width / Bankfull Mean Depth
- Sinuosity = Stream Length / Valley Distance
- Slope (%) = Stream Elevation Change / Stream Length

Table 1. Classification Key for streams (Rosgen 1996)

Stream Type	Entrenchment Ratio	W / D Ratio	Sinuosity	Slope
A	<1.4	<12	1.0 to 1.2	0.04 to 0.10
B	1.4 to 2.2	>12	1.0 to 1.2	0.02 to 0.039
C	>2.2	>12	>1.2	<0.02
D	N/A	>40	N/A	<0.04
DA	>2.2	Highly variable	Highly variable	<0.005
E	>2.2	<12	>1.5	<0.02
F	<1.4	>12	>1.2	<0.02
G	<1.4	<12	<1.2	0.02 to 0.039

Values of Entrenchment and Sinuosity ratios can vary by +/- 0.2 units, while Width/Depth ratios can vary by +/- 2.0 units (Rosgen, 1996). When application of these variances resulted in a possible change of classification, we noted both Rosgen classifications, and noted the possible transition of the stream section.

Determination of Bankfull Discharge

The stage of bankfull discharge is the single most important parameter used in this level of classification. The correct field identification of bankfull discharge indicators is necessary to identify the channel width, which is required to estimate the entrenchment and width to depth ratios, and is related to the channel pattern. By identifying these morphological indicators, we were able to estimate the discharge that formed it.

Bankfull discharge is the dominant or effective flow rate primarily responsible for forming and maintaining the stream channel, and transports the bulk of the available sediment over time. The bankfull stage corresponds to the discharge at which channel maintenance is the most effective and results in the average morphologic characteristics of channels. A correlation also exists between bankfull discharge, its channel dimensions and pattern, and watershed size. Additional references from Rosgen (1996) describing bankfull, dominant, frequent, or effective discharge, include Wolman and Miller (1960), Andrews (1980), Leopold et al. (1964), and Dunne and Leopold (1978).

Northern Arizona University (NAU) conducted a systematic study on the geomorphology of 75 reaches of streams and rivers in New Mexico. Their study showed a strong correlation ($R^2 = 0.90$) between watershed size and bankfull channel cross section area (Knight et al., 1999). The area of Pueblo Canyon watershed upstream from the P-4 reach is approximately 8 mi². According to the New Mexico regional curves in the NAU study, the predicted cross section area for streams with an 8 mi² watershed size is 13.8 ft², the 95% confidence interval ranges from 7 ft² to 28 ft². Figure 2, from the NAU study, demonstrates the relationship of watershed size and channel cross sectional area in this New Mexico study.

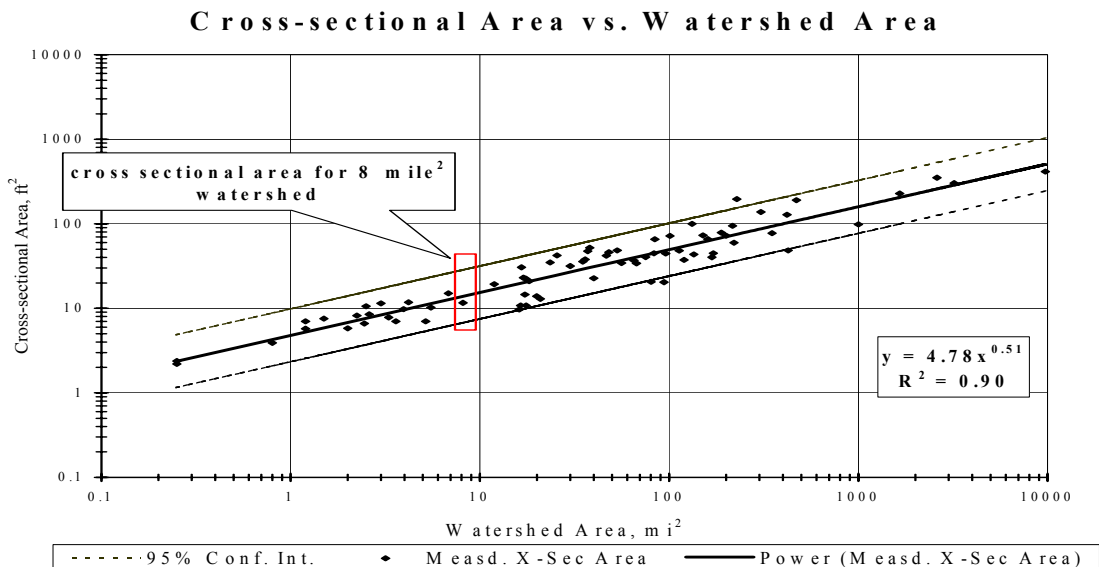


Figure 2. Bankfull Cross-Sectional Area as a Function of Watershed Area, All New Mexico Sites, (Knight et al., 1999)

Cerro Grande fire impacts to the upper watershed area have changed the flow regime in Pueblo Canyon. This changing flow regime complicated bankfull determinations. The maximum peak flow since the fire is 144 times greater than any recorded before May of 2000, and the average of all peak flows is about 11 times those measured before the fire. These increasing flows have altered, obscured, or abandoned pre-fire bankfull indicators. Abrupt bank slope breaks, change in vegetation, water staining, and scour marks are examples of bankfull field indications. In most cases, the stream channel was already adjusting to this new flow regime before we began this study.

We made linear and elevation measurements of all deposition and erosion features found at each cross section. We plotted these measurements, developing cross section charts that are presented in Appendix E, and used the channel dimensions and relationships in our classifications. The bankfull features resulted in cross section areas ranging from 7 to 34 ft². Initial estimates of bankfull discharge, based on these cross section areas, specific slopes of the reach, and an estimated roughness coefficient resulted in discharges ranging from 28 to 303 cfs. In areas that demonstrated the least impact to the changing flow regime, the estimated mean bankfull discharge was 49.5 cfs. Figure 3, from the NAU study, indicates that the bankfull discharge for an 8 mi² watershed is 56.5 cfs, the 95% confidence interval ranges from 15 to 150 cfs (Knight et al., 1999).

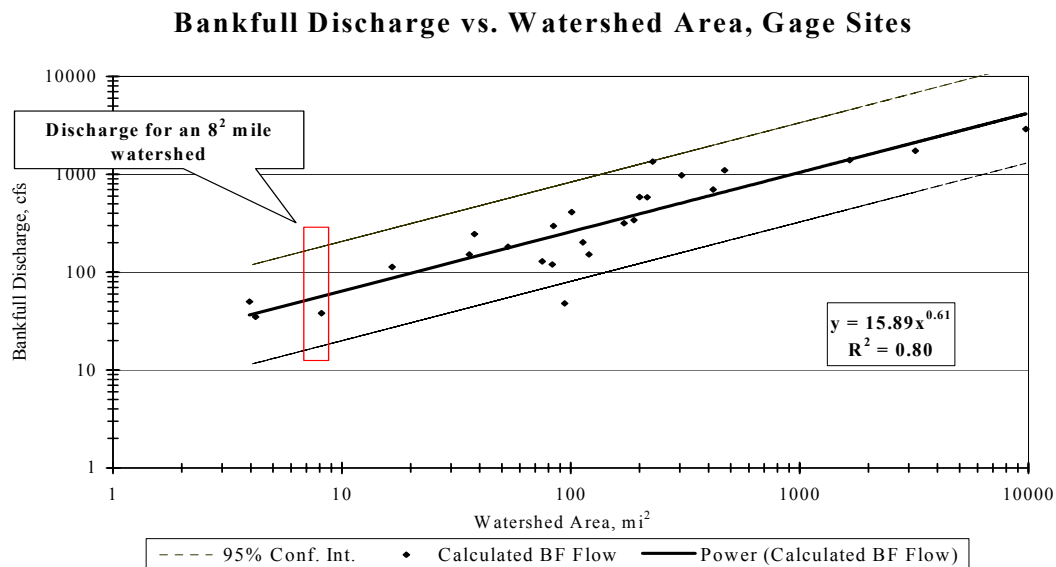


Figure 3. Bankfull Discharge as a Function of Watershed Area, New Mexico Gage Sites, (Knight et al., 1999)

Because of the variability in our initial flow estimates, and the expected channel adjustments, we re-selected bankfull channel features at each cross section that generated a 50 cfs effective discharge. For any given storm water runoff event, we assumed that its peak flow and flood duration should be nearly constant throughout the reach due to its relative shortness and lack of major tributaries. We also noted that when we subtracted the highest peak flows from 2001 and 2002 (1440 and 583 cfs), the average peak

discharge rate of the remaining 35 flows was 48 cfs. Many bankfull indicators at most cross sections in P-4 West were already correlating to this flow. This resulted in a reduction in the cross section average to 17 ft² in areas where braided stream patterns and wetland conditions prevail. The cross section area dropped to an average 11 ft² in areas where single-thread channel patterns and probable channel incision exists. These values are close to the 13.8 ft² value predicted by the cross sectional area versus watershed size regional curves generated by the NAU study.

The changes in the Pueblo Canyon watershed have increased the flow and sediment regimes, which are influencing its channel morphology. Rapid stream adjustments to increasing flow and sediment transport currently recognized in the canyon include deepening and widening of the channels, straightening of the stream pattern, and increasing the channel slope. Slower responses not yet recognized include lateral extension and redevelopment of new floodplains at the new lower base elevations. Figure 4 demonstrates an example the changing shape of the channel in Pueblo Canyon.

Cross Section 10 in Figure 4 demonstrates an example of the initial deepening and widening stages of the channel evolution in Pueblo Canyon. Cross Section 10 was measured in the mid sub-reach section of P-4 West and further details will be described in a later section. In this example, we identified channel features formed in response to 3 different flow regimes, at 300, 50, and at 10 cfs. The 300 cfs flow was modeled from bankfull features along the original floodplain. The floodplain was formerly well armored by marsh grasses. High magnitude and frequent floods are currently eroding the floodplain banks and the bank armor is no longer able to preserve the original channel form. Currently the banks are unstable, commonly undercut, and sloughing into the channel. The original channel at the floodplain elevation was probably similar in cross sectional area to the 10 cfs channel at the bottom of the 300 cfs channel.

The small capacity channel formed within the larger, is temporary and developed in response to daily wastewater treatment plant discharges that approximate 10 cfs flows. The banks are very fragile and storm flows regularly obliterate these features. The 50 cfs capacity channel is more stable and has developed in response to the probable dominant bank forming flows. These flows are the most frequent or of longer duration than others seen since the fire.

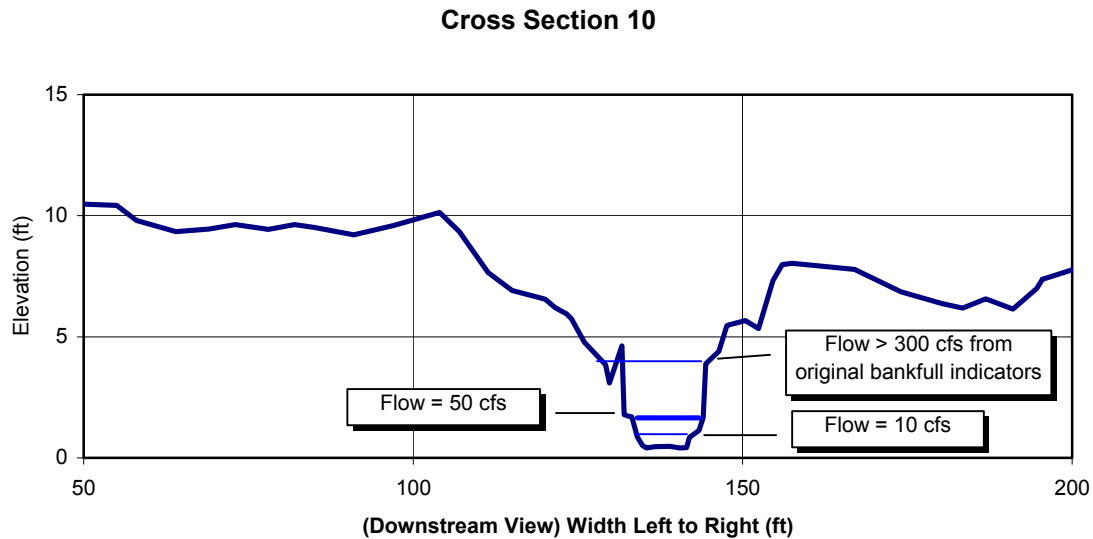


Figure 4. Cross Section 10 demonstrating the water level stage heights for 3 discharge rates.

Initially, the channel rapidly incised and widened in response to increased flows. The bankfull width to depth ratio increased and the entrenchment relationship diminished. Entrenchment is the width of the flood prone area relationship to the bankfull area width. In this case, the width of the flood prone area decreased in relation to the width of the bankfull area reflecting a deepening channel and abandonment of the original floodplain.

As the burned watershed recovers, we expect the flow regime to diminish and stabilize. A new state of equilibrium, responding to this smaller flow regime, will eventually be achieved. Lateral extension of the banks will continue until new floodplain areas are established. Renewed sediment deposition will develop a new series of point bars increasing the sinuosity. These features will allow the channel width to depth and entrenchment relationships to develop that are capable of sustaining the new flow regime. Although the channel morphology will gradually achieve stream morphology similar to that before the fire, advancement of the tributary drainage network will continue far into the future to compensate for the new base level that now exists at the lower elevation.

Storm Water Monitoring

Shortly after the Cerro Grande fire, we began a Laboratory wide storm water monitoring program to evaluate transport of contaminants associated with the forest fire. Unexpectedly high plutonium values were recognized in the Pueblo and Los Alamos drainages and we began to focus our storm water monitoring in Pueblo Canyon.

From 2000 to 2002, we collected 66 storm water samples from 12 runoff events in Pueblo Canyon to evaluate plutonium-239/240 and sediment transport in the canyon. Commercial analytical laboratories analyzed the samples for a variety of chemical suites,

including semi-volatile organics, metals, radionuclides, general water chemistry, and physical parameters such as suspended sediments and particle size distributions. By 2002 we were concentrating our measurements primarily on total plutonium-238, and -239/240 in water and in suspended sediment, total suspended sediment concentration, and sediment particle size distributions in storm water, though we continued to analyze a subset of samples for metals and other radionuclides.

Polychlorinated biphenyls, mercury, selenium and gross alpha were detected above New Mexico's livestock watering and wildlife habitat water quality standards. Our evaluation of metals and other radionuclides (e.g., gross alpha, gross beta) in storm water runoff suggest that elevated levels of these constituents in burned forest materials (ash) and eroding upland soils were significantly reduced due to sediment deposition in wetland areas of the middle and lower portions of Pueblo Canyon. In contrast, total plutonium in water and in the suspended sediment fraction increased as storm water passed through Pueblo Canyon leading us to focus our monitoring program on plutonium transport in Pueblo Canyon.

We evaluated the contribution of fallout plutonium and plutonium contributed by the ash produced from the Cerro Grande fire and found them to be a relatively small component of the total plutonium inventory transported from Pueblo Canyon. Our evaluation also suggests the contaminant inventories in ash available for transport was removed during the 3 year period of this study. (see discussion in Appendix A).

Commercial analytical laboratories performed plutonium-238 and plutonium-239/240 isotope measurements on our storm water and suspended sediment samples. Plutonium-238 levels were consistently low and are not included in further discussions except that legacy plutonium could be identified by consistent plutonium-239/240 to plutonium-238 isotope ratio differences seen between background and LANL derived plutonium. Legacy plutonium-239/240 concentrations are consistently 2 orders of magnitude greater than plutonium-238, while background concentrations of plutonium-239/240 are consistently one order of magnitude greater than plutonium 238 concentrations. Plutonium-239/240 isotopes are indistinguishable using alpha spectroscopy and the term plutonium is used in this report to reference the -239 and -240 isotope combination of plutonium.

We evaluated 3 different forms of plutonium in storm water: dissolved plutonium, plutonium adhered to sediment particles in storm water, and the total component of plutonium in storm water. In 2000 only dissolved plutonium was measured. In 2001 total plutonium, plutonium in suspended sediments, and dissolved plutonium measurements were made. In 2002 only total plutonium and plutonium in sediments were measured. Plutonium is relatively insoluble and we found that total plutonium was measured at levels consistently 3 to 4 orders of magnitude greater than its dissolved phase.

In all, 15 measurements of dissolved plutonium, 51 measurements of total plutonium, and 49 measurements of plutonium associated with suspended sediments were made. In

addition, 50 total suspended sediment measurements were made during 2001 and 2002. In 2002, 20 particle size distribution analyses of sediments were included.

We evaluated transport conditions in Pueblo Canyon by grouping our samples into reference reaches above and below the confluence of Acid and Pueblo Canyons and in Acid Canyon. Ten samples were collected in Acid Canyon and the south fork of Acid Canyon, below an area that received LANL legacy waste materials during the first 20 years of Laboratory operations. Fifteen samples were collected above the Acid and Pueblo Canyon confluence reflecting background conditions. The remaining 41 samples were collected below the canyon confluence to evaluate contaminant transport in Pueblo Canyon. Thirty-five of those samples were collected in lower Pueblo Canyon at the E060 storm water gage to evaluate transport of plutonium and sediments beyond Pueblo Canyon. See Appendix F for tables of analytical data used in this evaluation and Figure F1 for sample locations.

Our sample collection techniques included grab samples and automated sample collection methods and follow procedures described in the DOE OB Standard Operating Procedures for Sampling and Analytical Activities (Englert, 1996). Seventeen grab samples were collected. Grab sample methods consist of submerging appropriate sample containers into the storm water flow. Forty-nine samples were collected by automated Isco[®] devices.

We deployed portable Isco[®] programmable liquid samplers in 2 Pueblo Canyon locations, at LANL gage stations E055 and E060. Another sampler was installed in lower Acid Canyon just above the confluence with Pueblo Canyon. Single Isco[®] sampling units are capable of collecting 24 discrete 1-liter samples in varying programmable arrays. The samplers can be programmed to begin a sampling routine based on storm water stage height and the sample collection intervals can be based on elapsed time or flow.

We programmed the Isco[®] samplers to collect an array of samples that represent the changing characteristics of a storm runoff event. Samples were collected on the rising leg, near the peak of the storm hydrograph, sometimes referred to as the first flush or flood bore, and then at varying time intervals; for example, 45 or 60 minutes, along the falling leg. Two to four 6-liter samples were collected for each storm event. Isco[®] Model 3210 Flow Meters activated the sample routines based on water level rise. When the water level reached a height we predicted as storm flow, the flow meter enabled the sampler and started the sampling routine. The flow meters also recorded a hydrograph and sample history. The sample histories include the time and flow rate associated with each sample. We verified and correlated our sample collection history and hydrograph to LANL's rated gage stations.

The U.S. Geological Survey (USGS) recommends using equal-width-increment (EWI) sampling methods for producing the most representative stream flow samples. These methods create water quality cross sections across a stream. Automatic pumping samplers with a single-fixed intake, like Isco[®] samplers, are sometimes used to collect samples at remote sites or small streams with flashy hydrologic responses (Shelton,

1994). Samples collected with automatic pumping samplers can introduce an unknown bias and should be compared to EWI coefficients. These coefficients should be developed to determine the relation between the constituent concentrations at the single fixed-intake location and their respective mean concentrations in the EWI cross section. For the purpose of this report, EWI procedures were not followed and some unknown bias may exist.

Plutonium Analytical Measurements

Commercial analytical laboratories analyzed the storm water samples for total plutonium concentrations, dissolved plutonium concentrations, plutonium concentrations in sediment, and total suspended sediment in water. Plutonium is measured by alpha spectroscopy after a whole water, filtered water, or residual sediment sample is digested, chemically separated, purified, and fixed onto a planchet. The procedures used by our analytical laboratory are similar to DOE/EML 4.5.2.1 and meet or exceed the requirements referenced in EPA Procedures 907.0 and 908.0 (Paragon Confidential Standard Operating Procedure 714 Revision 5, 1999). Suspended sediment concentration is measured by centrifugation methodologies and is equivalent to ASTM method D 39777-97. Plutonium and suspended concentration data are compiled in Appendix F.

Radionuclide isotopes emit alpha particles at discrete energy groups. Analytical laboratories use the energy level of these emissions to identify individual isotopes, and the rate of the alpha interactions quantifies the concentration in a sample. Plutonium-239 and plutonium-240 alpha emissions occur at approximately 5,155 keV (keV = 1,000 electron volts), and plutonium-238 emissions occur at 5,499 keV (Knoll G. F. 1979). The resolution achieved by alpha spectroscopy methods is not adequate to resolve between plutonium-239 and -240 isotopes and plutonium-238 is consistently found at a small fraction of plutonium-239/240. In this report we refer to plutonium as synonymous with plutonium-239/240.

The types of analytical plutonium measurements we made on storm water samples collected during this study period included total plutonium in whole water samples, dissolved plutonium in water samples filtered through a 0.45 micron filter, and plutonium adhered to sediments separated from the sampled waters. Total plutonium concentrations are essentially the combination of the plutonium in its dissolved phase and the plutonium in the solid phase of a sample. Plutonium is fairly insoluble and dissolved plutonium measurements were not commonly made after the 2001 storm water season. Those measurements of dissolved plutonium were very close to, or below laboratory detection levels.

We evaluated plutonium mass transport in storm water from the total plutonium measurements. Plutonium measurements in suspended sediments provided a method to evaluate the variability in the plutonium inventory transport. It provided information regarding other variables associated with plutonium transport, for example the source of sediments and plutonium transport associated with different particle sizes of sediment. It also provided part of the quality assurance evaluation for each measurement. The

insolubility of plutonium provides a very close relationship of total plutonium in water and plutonium in suspended sediments. If the suspended sediment concentration and a value for total plutonium in water or plutonium in sediments is known, the alternate plutonium value can be calculated for a cross reference.

Mass Transport Calculation Methods

We calculated plutonium mass transport for individual, sampled runoff events using relationships between total plutonium concentrations in water and flow rates, and estimated transport for events not sampled using peak flow and mass transport relationships. Sediment transport was determined using similar relationships and methods, except the suspended sediment concentrations were used in place of plutonium concentrations.

Plutonium mass transport calculations for individual runoff events were based on regression equations that described the relation between the paired concentration and flow values for multiple samples collected during the event. The linear, power, logarithmic, or exponential equation that described the best fitting trend line (equation producing the best coefficient of determination (R^2)), was used to calculate the plutonium concentrations for 5 minute intervals throughout the event hydrograph. The storm water gages operated by the LANL RRES-WQH program, automatically records flow rates in 5 minute intervals. Integrating plutonium concentrations with associated water volumes provided the mass transport value for each interval. Reiterations of the calculation can be totaled for any time interval during the event to calculate the plutonium mass transported.

We saw relationships demonstrating increasing concentrations of total plutonium in water and suspended sediment as flow rates grew. Strong linear and nonlinear relationships developed, represented by the coefficient of determination (R^2). This value describes the percent of variation that can be described by the regression equation. Nonlinear relationships were represented by power or logarithmic equations. These type relationships suggest the rates of concentration increases were not uniform. The value 1, for the R^2 coefficient, indicates the regression line can explain 100% of the variation. We also found many of the non-linear relationships (i.e., exponential) are close to linear, indicated by the exponent approaching one.

To determine these relationships, we developed scatter or x-y plots for the paired data of each event that we sampled, where x is the independent flow variable, and y is the independent concentration variable. We used Microsoft Excel to fit trend lines through those data points to develop the regression equation that best described the data relationship. Predictions of concentration values for the remaining flows recorded during a runoff event can then be made using this equation.

For example, the power equation, $y = 44 * x^{0.74}$, $R^2 = 0.99$, did the best job expressing the relationship between suspended sediment concentrations and the paired flow values for samples collected during a runoff event that occurred June 22, 2002. The dependant y variable represents the suspended sediment concentration of a storm water sample, and

the independent x variable reflects the flow in liters, that existed while the sample was being collected.

The coefficient, 44, describes the rate of suspended sediment increase relative to increasing flow rates. For each unit rise in flow there is approximately 44 times the SSC unit (to the 0.74 power) rise in suspended sediment concentration. The 0.74 exponent describes the degree of linearity, where values close to 1 describes strong linearity. The coefficient of determination, $R^2 = 0.99$, describes the adequacy of the regression curve in expressing the relationship of suspended sediment concentrations and flow rates for the samples collected during the June 22, 2002 runoff event, where values close to 1 describes strong correlations. Therefore, we can say the relationship is nonlinear, expressed by the power exponent 0.74, has a strong correlation, expressed by $R^2 = 0.99$, and for every 1 L/s (to the 0.74 power) increase in flow, we would expect an approximate 44 mg/L increase in the suspended sediment concentration. Although the power exponent, 0.74, suggests this relationship is fairly linear, it also indicates the suspended sediment concentration rate of increase decreases as the flow rate increases.

After the concentrations were derived for flows recorded throughout the runoff event, using the regression equation, we calculated the inventory mass associated with each time interval. The mass inventory was calculated by integrating the flow rate, time, and concentration. First, we converted flow rates for each specified 5 minute time period into water volume. For example, by multiplying 100 cubic feet of water per second flow rate (cfs) by a 5 minute time interval (300 seconds), a 30,000 cubic feet of water volume is calculated (100 cfs x 300 seconds = 30,000 cf over a 5 minute interval).

We then converted water volume in cubic feet to liters, by using the conversion factor 28.32 L/cf (30,000 cf * 28.32 L/cf = 849,600 L). This volume of water is multiplied by its suspended sediment or plutonium concentration to determine the mass transported within the specified time interval (100 pCi plutonium per liter x 849,600 liters = 84,960,000 pCi or 0.085 mCi of plutonium transported in 5 minutes).

Reiterations of this process would then provide an inventory mass transport value for each 5 minute time interval during the duration of the runoff. A mass transport value can be derived for any time period during the runoff by summing the values derived for each 5 minute interval.

We developed sediment and plutonium rating curves to estimate offsite transport during runoff events not sampled. Rating curves are x-y plots of plutonium or suspended sediment mass transport values plotted against the peak flow rates of floods they were collected from. We used the methods just described to determine the relationship between the total mass transport and peak flows for the runoff events we sampled. We then applied the regression equations that describe these relationships to the remaining peak flow measurements for runoff events that were not sampled. From these calculations we derived mass transport estimates for each event. We then summed the mass transport estimates for all events to determine the seasonal and total mass transport values for plutonium and sediment.

Almost all environmental data contains variability. This variability is comprised of random measurement error and natural environmental dispersion. Controlling measurement error allows us to understand and reflect environmental variability. We measured this data variability by calculating standard error values for each estimator (i.e. plutonium concentrations derived from peak flow regressions, where plutonium is the dependant variable y, and flow is the independent variable x) using the following equation. We then established 95% confidence intervals for our data and discussed potential error sources in the report text.

$$\text{Standard Error (SE)} = t * s * \sqrt{\frac{1}{n} + \frac{(x - \bar{x})^2}{S_{xx}}}$$

Where:

t = critical value for 95% confidence

y = dependent variable

(standard deviation) $s = \sqrt{\frac{S_{yy} - \beta_1 * S_{xy}}{n - 2}}$

$S_{xx} = \sum x_i^2 - \frac{(\sum x_i)^2}{n}$

n = number of values

$S_{yy} = \sum y_i^2 - \frac{(\sum y_i)^2}{n}$

x = independent value

$S_{xy} = \sum x_i y_i - \frac{\sum x_i \sum y_i}{n}$

\bar{x} = mean of independent values

β_1 = slope from regression equation

and the standard error is used to determine a 95% confidence interval:

$$y - SE < y < y + SE.$$

Hydrologic Data

In this section we use the term peak flow to describe the maximum flow rate that storm floodwaters achieve. In these semi-arid ephemeral stream channels, storm water flows are of relatively short duration, demonstrated by a quick rise to a hydrograph peak and then a slow decline to a level representing base flow. During long, low intensity rainfall the rise and fall of the hydrograph limbs increase in duration.

The Cerro Grande fire has exacerbated the water runoff conditions that previously formed and maintained the channel systems on the Pajarito Plateau. The runoff conditions vary, dependant on the degree and extent of the fire in each watershed, the size of the watershed, and structures in the canyons. For example the Los Alamos Reservoir in upper Los Alamos Canyon and a water retention structure built later in lower Los Alamos Canyon modulated the runoff through the canyon. Before the fire, flow rates in Pueblo Canyon rarely exceeded 10 cfs. Since the fire, the magnitude and frequency of peak flows have increased, while during the same period, precipitation rates have declined.

The number of peak flow rates that exceeded 10 cfs in Pueblo Canyon since the fire was 6 in 2000, 17 in 2001, and 14 in 2002. Average peak flows for these years were 64, 147, and 77 cfs; median peak flows were 50, 25, and 20 cfs. A maximum peak flow of 1,440 cfs occurred July 2, 2001. Figure 5 demonstrates the increased magnitude and frequency of storm water peak flows since the Cerro Grande fire.

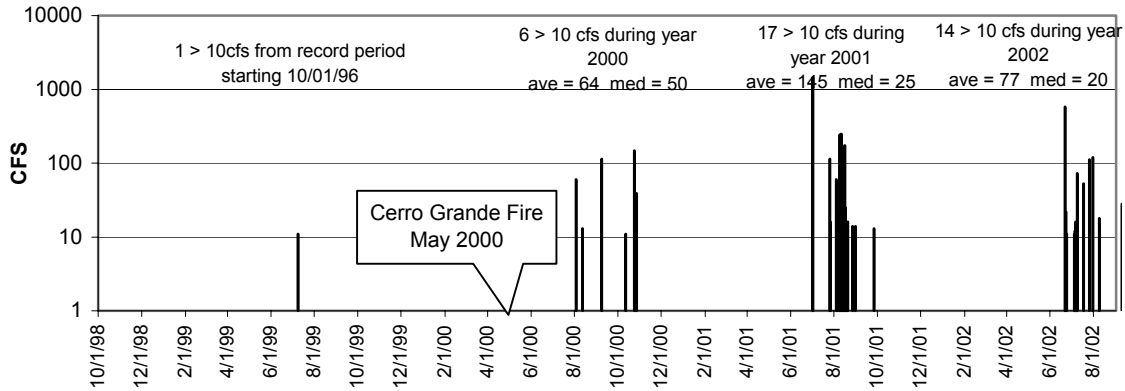


Figure 5. Magnitude and frequency of storm water flows greater than 10 cfs at LANL gage E060 in lower Pueblo Canyon

Peak flows, total discharge, and sediment yield have increased as well as the subsequent flooding and flood impacts. In Pueblo Canyon peak flows have increased about 144 times and average about 11 times pre-fire flow conditions. From 1992 to the fire, only one flow exceeded 10 cfs at the LANL gage station, E060, in lower Pueblo Canyon. Since the fire and up to the end of 2002, 37 flows have exceeded 10 cfs. The average peak flow value is 107 cfs, including the July 2 1,440 cfs flow (Shaull, et al, 2002). Twenty-three of the 37 runoff events were less than 50 cfs.

The peak flows in these contexts reflects the changing flow regime on the Pajarito Plateau. The effective bank forming channel flow is related to the frequency and duration of the total flow regime. Field observations of newly formed bankfull indicators suggest that the effective bank forming channel flow is around 50 cfs, increased from a pre-fire effective bank flow that was probably less than 10 cfs.

Other recent fires have burned forests in the Jemez Mountains near this area. The 1977 La Mesa fire burned forests in and around Frijoles Canyon. This area is southwest and adjacent to the Cerro Grande fire area. In 1996, the Saint Peters Dome fire impacted Capulin Canyon, immediately southwest and adjacent to the La Mesa Fire northeast boundary. The U.S. Geological Survey in cooperation with the National Park Service monitored wildfire effects on stream flow in Frijoles and Capulin Canyons. Peak flows increased about 160 times the maximum recorded flood prior to the fires. They receded to about 3 to 5 times the pre-fire maximum peaks within three years. In the 22 years since the La Mesa wildfire, flood magnitudes have not completely returned to pre-fire size (Veenhuis, 2002).

The Pueblo Canyon channel is ephemeral through most of the canyon, responding primarily to occasional summer rainstorms and spring snow melt. The lower Pueblo Canyon stream is intermittent, maintained artificially by almost daily discharges from the Bayo wastewater treatment plant. For part of each day, the average flow from the plant discharge is approximately 6 cfs. The flow is not maintained throughout the day, and occasionally, the effluent discharge is diminished even more when it is diverted for city irrigation. In addition, the Bayo wastewater treatment plant discharges up to 10 CFS on a weekly basis when the operators back flush the trickling filters.

The Cerro Grande fire reduced the water infiltration rates and storage capacity of soil, thereby increasing storm water runoff. Rainfall storage capacity in soils in a forest setting is a function of precipitation captured by overstory interception and water infiltration into the soil matrix. In areas of intense burn, the fire eliminated the overstory, understory, and groundcover, including the duff. During periods of rain, water quickly runs off the unprotected slopes and accumulates as floods in channels draining the watershed. These conditions will remain until the burned forest has rehabilitated.

Most of the rain occurs as localized, heavy downpours during the summer, between June and September. The maximum hourly rainfall rate measured at the RAWs station in 2002 was 0.8 inches per hour. It occurred June 21 and produced the maximum daily accumulation for that year, 1.38 inches, and a 583 cfs peak flow in Pueblo Canyon. The maximum hourly rate in 2001 was 0.7 inches per hour and occurred July 2. It produced the year's maximum 1.23 inches daily accumulation and the maximum flow measured in Pueblo Canyon of 1440 cfs.

In 2000, the maximum rate at the RAWs gage station was 0.77 inches per hour on July 9, although at the North Community gage the rainfall accumulation was only 0.13 inches. This rainfall did not produce significant runoff. The first storm water flow greater than 10 cfs in Pueblo Canyon was 60 cfs measured August 3, and it was associated with minimal recorded rainfall; the daily accumulation was only 0.02 inches at a maximum rate of 0.01 inches / hour. This may demonstrate the difficulty in predicting flood parameters in Pueblo Canyon because of the non-uniform rainfall over the watershed area (the localized nature of summer downpours, gage placement relationships to rain, and dissimilar runoff source areas such as urban or forests areas). Figure 6 demonstrates the daily precipitation accumulation measured at the LANL North Community gage and the peak flow measurements at lower Pueblo Canyon E060 water gage from January 1998 to September 2002.

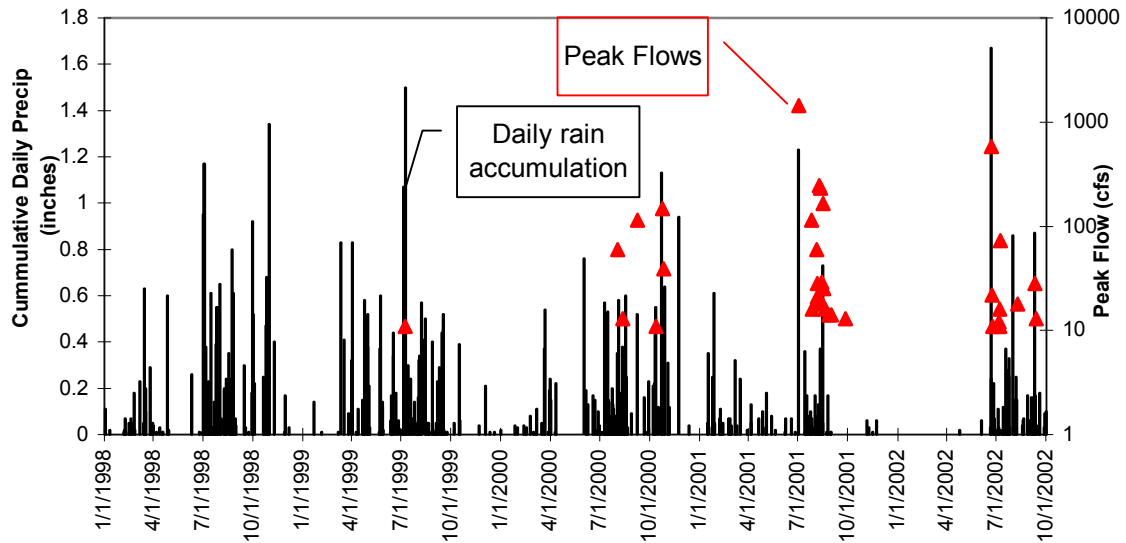


Figure 6. Daily cumulative precipitation at North Community rain gage in upper Pueblo Canyon correlated to runoff events greater than 10 cfs in lower Pueblo Canyon. Snowfall is measured in equivalent rainfall units.

Due to the increased number and magnitude of peak flows and the duration of the floods, the total water volume from Pueblo Canyon has increased relative to the precipitation in the area. The normal average annual precipitation at Los Alamos is 18.95 inches per year, although that amount has diminished in recent years. Currently the southwest United States is experiencing a drought. Average annual rainfalls at the North Community rain gage have ranged from 94% to 41% of the 20 year long term average since 1999. Annual rainfalls were 94%, 81%, 41%, and 60% of the long term average value during the years 1999, 2000, 2001, and 2002, respectively.

Although precipitation has diminished, relative total volume of discharge in Pueblo Canyon has increased. The ratio of annual total flow to annual cumulative precipitation has increased from about 14 to 36. In 1998 and 1999, the flow to precipitation ratio equaled 15 and 13, respectively; in 2000, 2001 and 2002, the ratio increased to 38, 37, and 31, respectively. Precipitation includes snowfall in inches of water and total flow includes the discharge from the Bayo plant. The annual rainfall accumulation in inches and total flow or discharge volume in acre feet relationship is shown in Figure 7.

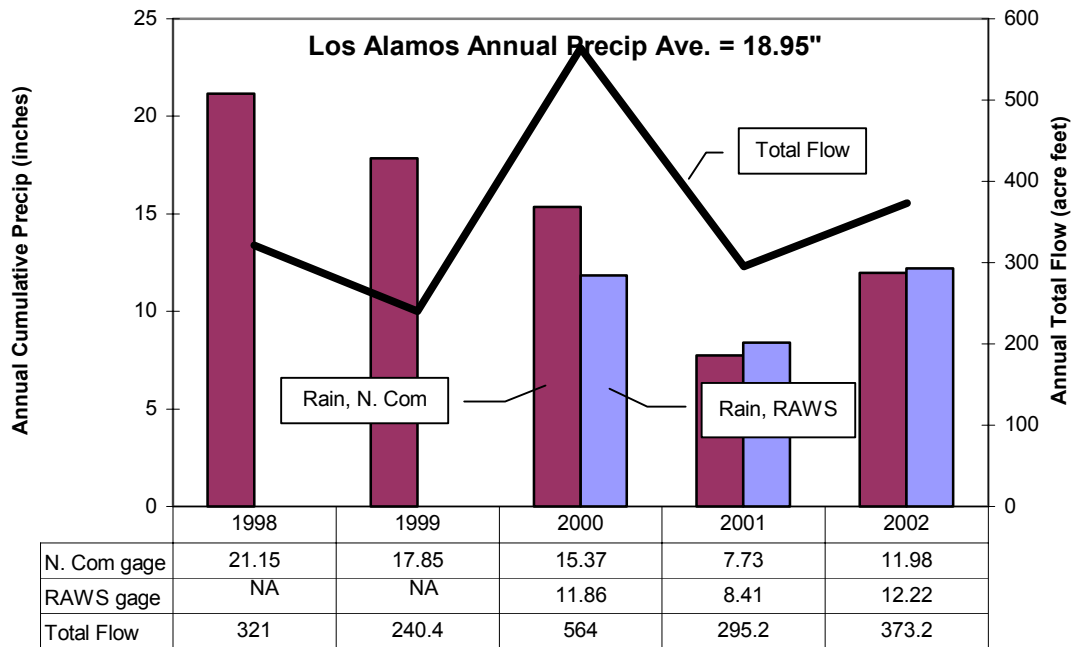


Figure 7. Annual cumulative precipitation and total flow relationship at lower Pueblo Canyon.

The total precipitation and total runoff relationship can be used to predict storm runoff and determine recovery rates of the burned watershed, although these evaluations are complex since rainfall over the Pajarito Plateau is non-uniform. Rainfall variables that were examined include rainfall location, intensity, and accumulation. Storm flow variables that were examined include magnitude, duration, and total volume.

Examination of these variables provided direction to storm water monitoring decisions we made. Daily rain accumulation, maximum hourly rate, peak flows, travel time of flood bore to the E060 gage, as well as the hydrographs for the storm runoff events we evaluated are included in Appendix F. Evaluation of the recovery rates of the burned watershed areas would be useful in predicting future channel adjustments in Pueblo Canyon, but is beyond the scope of this report.

Channel Characteristics and Discussion

The channels in P-4 West are comprised of 2 distinct types: a multiple, braided channel system that developed on a wide floodplain, confined by low terrace banks, and a single thread channel system that developed on a narrow floodplain confined by high, steep confining banks. The floodplains consist of recent post-1943 alluvial deposits. They are covered by thick marsh grasses, and are deeper in the multiple braided systems than the single thread channel reach. The confining terrace banks consist of older post-1943 deposits and are relatively bare of armoring riparian plants.

The P-4 West reach in Pueblo Canyon is experiencing impacts from the increasing flow regime since the Cerro Grande fire. The channels are incising and widening. A single channel is developing in the braided section and threatens to capture most of the water flow, abandoning the remaining channels and exacerbating the destabilized conditions

within the floodplain. Much of the floodplain materials within the single channel reach have been eroded and transported from the area, and the confining banks are experiencing increasing erosion.

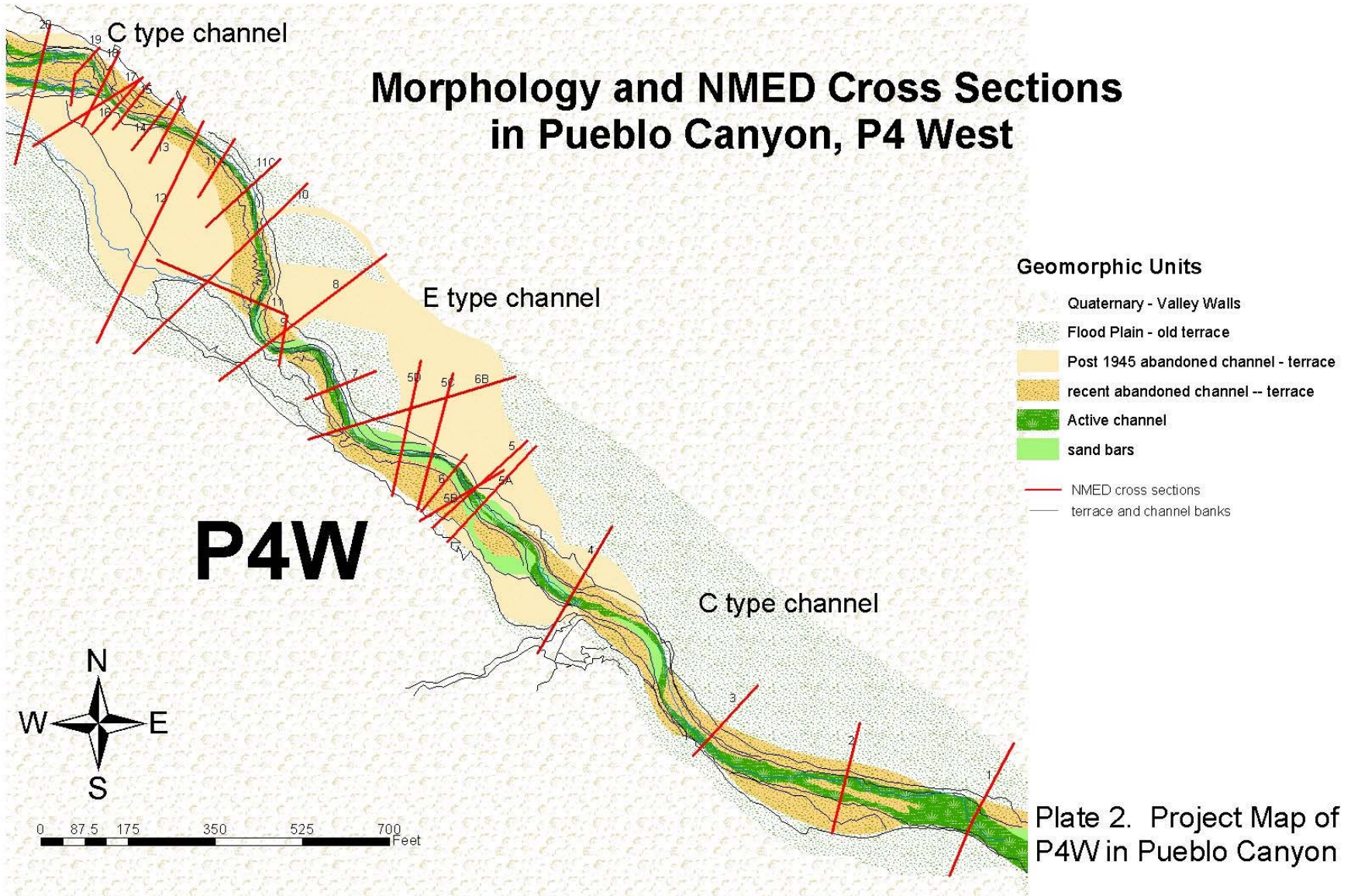
Stream types described in this document are classifications based on channel dimensions and their relationships, such as width, depth, sinuosity, and slope. Stream classifications may change in response to impacts from changing flow or sediment yield regimes. Degradation or deepening and widening of a channel by scour, or aggradation caused by deposition are changes that reflect evolution of a stream to an alternate type and function. Our field measurements for the cross sections, longitudinal profile, and bank and thalweg delineations, are intended to capture the existing dimensions of the channel in P-4 West. Plate 2 illustrates the locations of our field measurements, and their relation to the channel morphology described by the LANL RRES-RS group. The cross section charts, dimension summaries, and remarks are found in Appendix D.

LANL's geomorphic evaluation and chemical analysis of sediment samples in Pueblo Canyon indicate contamination exists from post-1942 LANL operations. Reach P-4 has the largest estimated inventory of plutonium of any of the Pueblo Canyon reaches, due to an exceptionally large volume of mid-1940's and mid-1960's sediments with relatively large plutonium concentrations. The LANL RRES-RS group estimated a plutonium inventory of 158.5 mCi in P-4 West, of which 9% is stored in active c1 and c2 channel units and 91% stored in older post-1943 over bank and abandoned channel c4 through c6 units. The highest concentrations were found in c4 and c5 abandoned channel units, and in c6 over bank units. LANL RRES-RS has estimated that over 1 curie of plutonium has been distributed throughout the Pueblo Canyon stream sediments below Acid Canyon.

The sediment unit classification system used above uses the letter c to label channel depositional units and f to label floodplain units. The numbers that follow the letters denote relative age of post-1942 units. A brief description of the sediment unit classification system is found in the Setting Section of this report. A more detailed description can be found in LANL's report, "Evaluation of Sediment Contamination in Pueblo Canyon Reaches P-1, P-2, P-3 and P-4" (Reneau, et al, 1998).

Prior to the Cerro Grande fire, the stream dimensions in Pueblo Canyon P-4 West reach reflected conditions that evolved from effective bank forming flows of less than 10 cfs. The post-fire increases of flow and sediment yields are changing the channel dimensions and function in Pueblo Canyon. A wide variability of flows developed after the fire, ranging from 1440 cfs to regular flows from the Bayo treatment plant of less than 10 cfs. The flows vary in magnitude and duration, but appear to be developing an effective bank forming flow of approximately 50 cfs. Functional changes include erosion and transport of sediments contaminated with waste discharged into Pueblo Canyon during the first 20 years of LANL operations. Forest rehabilitation, bank stabilization, and sediment control efforts could reduce off site transport of LANL legacy wastes.

Morphology and NMED Cross Sections in Pueblo Canyon, P4 West



Stream type characteristics and the dimensions that classify them are summarized in Table 2. The stream section in P-4 West was divided into three areas; the upper and lower sections are dominated by the C type channels, whereas the middle section is dominated by E type stream channels.

Table 2. Summary table of cross section classifications and stream dimensions

Cross Section	Distance on longitude (beginning of profile is upstream of x-sec 20)	Entrenchment ratio	W/d ratio	Slope	Sinuosity (braided)*	Classification
P4W-1	2935.0	1.2	160.2	0.012	Multi chan*	(DA) F
P4W-2	2627.0	4.0	50.4	0.011	Multi chan*	(DA) C
P4W-3	2318.0	6.1	7.8	0.018	Multi chan*	(DA) E
P4W-4	1882.0	6.0	13.1	0.017	Multi chan*	(DA) C
P4W-5a	1604.0	9.1	5.5	0.011	1.03	E
P4W-5	1568.0	6.3	10.9	0.003	1.12	E
P4W-5b	1563.0	7.2	4.5	0.010	1.12	E
P4W-6	1503.0	2.1	32.3	0.014	1.13	(E) Bc
P4W-5c	1445.0	3.2	15.7	0.011	1.14	C
P4W-5d	1385.0	13.1	2.0	0.013	1.01	E
P4W-6b	1260.0	5.0	11.8	0.013	1.15	E
P4W-7	1175.0	5.1	7.8	0.019	1.15	E
P4W-9	997.0	3.5	3.1	0.008	1.11	E
P4W-8	965.0	8.0	1.6	0.014	1.38	E
P4W-11	871.0	2.1	5.6	0.014	1.10	E?
P4W-10	718.0	1.2	8.6	0.016	1.03	G
P4W-11c	618.0	4.1	3.6	0.023	1.08	Eb
P4W-11a	537.0	2.8	20.3	0.018	1.05	C
P4W-12	465.0	3.3	3.5	0.012	1.07	E
P4W-13	405.0	15.7	0.9	0.016	1.06	E
P4W-14	367.0	3.2	18.7	0.017	oblique x-sec	C?
P4W-15	302.0	2.0	7.0	0.022	1.14	Eb?
P4W-16	277.0	2.7	3.7	0.020	1.04	E-Eb?
P4W-17	255.0	1.9	7.0	0.030	1.04	B? Eb?
P4W-18	233.0	1.3	13.2	0.092	Falls	F
P4W-19	208.0	8.7	21.1	0.092	Multi chan*	(DA) C
P4W-20	60.0	23.7	23.9	0.026	Multi chan*	(DA) C
Mean		5.7	17.2	0.021	1.11	
Median		4.0	7.8	0.016	1.10	
Std Deviation		5.1	30.6	0.021	0.08	
Minimum		1.2	0.9	0.003	1.01	
Maximum		23.7	160.2	0.092	1.38	

* Multiple braided channels

The upper and lower stream sections in P-4 West demonstrate characteristics that reflect C type channels with some variations. They may have transitioned from DA stream types that had anastomotic or multiple, interconnected, and well armored channels with highly variable sinuosity and width to depth ratios.

The channels in the western section of P-4 East were classified as E type streams based on pre-fire 10 cfs flows. They are similar to the P-4 West upper and lower sections but are more entrenched with slightly less width to depth ratios. These sections may also have evolved from DA stream types.

From above Cross Section 20, probably as far upstream as the Bayo treatment plant, to Cross Section 19, and below Cross Section 4 to P-4 East, the channel is slightly entrenched (ratio $> 2.2 \pm 0.2$), moderate to highly sinuous, and has moderate to high width to depth ratios ($> 12 \pm 2$). Cross Section 20 displayed in Figure 8 is typical. It exhibits slight entrenchment (bkf W / fpa W) and a large width to depth ratio (bkf W / mean D). The cross section also displays the original anastomotic (braided and interconnected) channels from 125 to 160 and at 225 feet, and the low confining bank, where high water stages flow onto the c6 terrace at 230 feet. Based on the dimensions at this cross section, runoff events greater than 200 cfs would crest the banks, flowing over the c6 terrace in this area. Lower banks and developing channels on the terrace exist and smaller flows may encroach onto the terrace.

NMED 20, 8/29/02 Riffle ---

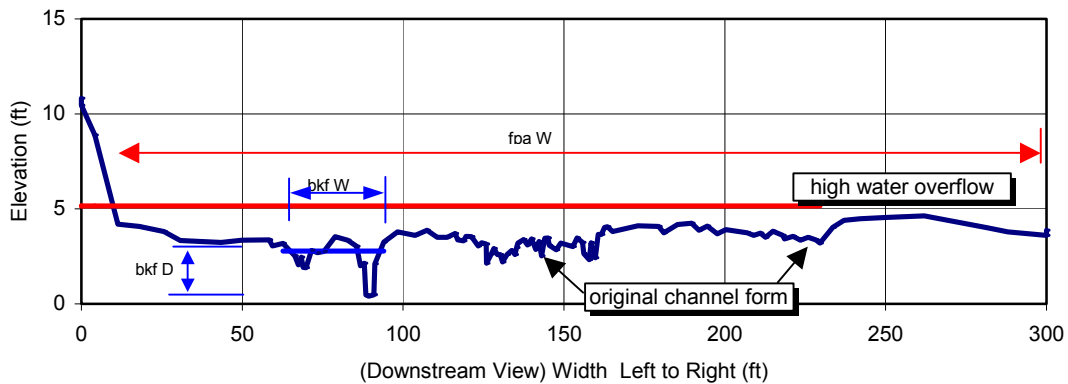


Figure 8. Cross Section 20, most upstream measurement, and representative of the upper and lower stream sections at P-4 West.

The area from approximately 30 feet in the chart to 225 feet is the floodplain area covered by thick reed canary grass. Steep banks on the north, or left, side of the valley, and low banks, comprised of post-1943 deposits to the south, effectively confine this area. The grasses covering the floodplain act as an effective filter. They diminish flood energies and retain sediments. The channel developing at 80 feet is beginning to capture most flows across the floodplain, focusing the runoff energies into a single channel. The remaining channels are abandoned, and erosion impacts are exacerbated within the single

incising channel. The water table is also lowered, abandoning the marsh grasses on the floodplain, further destabilizing the channel.

The mid stream section in P-4 West, Cross Sections 16 to 5a, demonstrates mostly E type characteristics with some alterations already evident along this 1,500 foot stretch. This section is also slightly entrenched but has a very low width to depth ratio (< 12 +/- 2). The banks of an old channel incised into older post-1942 LANL sediment deposits confine the sinuosity of the active channel. Reneau, and others (1998) indicate this incision occurred during the 1960s, before the Cerro Grande fire. These terrace banks are high, unarmored sediment units exposed to large flood stage heights. During floods this area contributes sediments that contain higher concentrations of plutonium to runoff.

Figure 9 demonstrates the typical dimensions of the mid section channel and its relationship with the confining post-1942 bank forming deposits. Cross Section 10 demonstrates entrenchment and a low width to depth ratio. It also exhibits confinement of the stream by steep, 7 to 10 feet high banks, formed by an earlier channel incision. The channels at 185, 265 and at 395 feet convey the floodwaters that flow onto the c6 terrace further upstream.

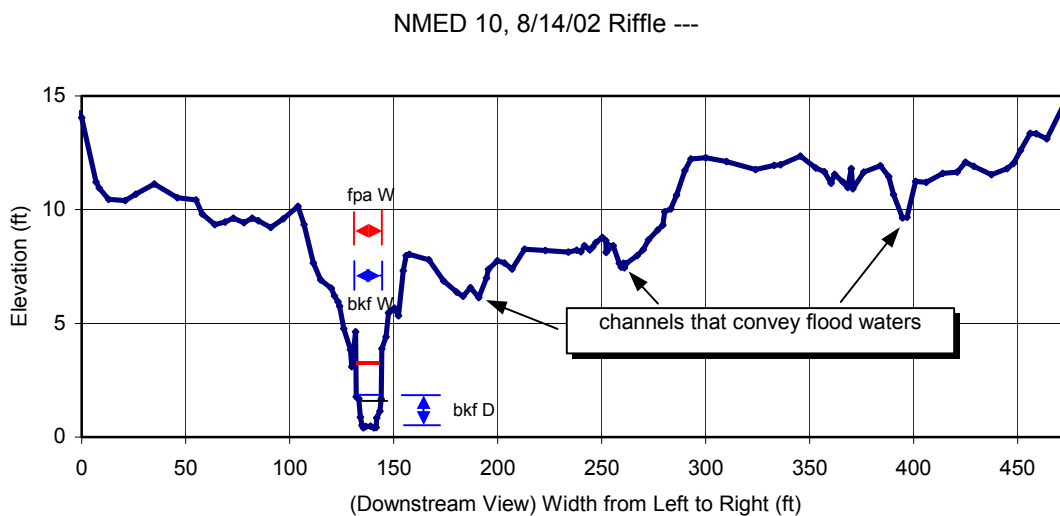


Figure 9. Cross Section 10, representative of the channel within the mid section of P-4 West.

The area on this cross section, from 10 to 450 feet, reflects the older post-1943 deposits incised by the channel formed during the 1960's between 110 to 160 feet. The high steep banks effectively confine floods except during extraordinary events, and re-entry of over bank flow to the main channel is creating large head cuts in the banks. Floodplain materials in the existing channel are heavily impacted and being eroded and removed from the area.

At the upper end of this mid section the slope and entrenchment increases, and the width to depth ratio decreases, culminating at a large head cut (waterfall) at Cross Section 18, approximate location of a bedrock nickpoint. Head cuts develop when surface runoff is concentrated at a nickpoint where there is an abrupt change of elevation and slope

gradient and a lack of protective vegetation. The fall of water over this nickpoint causes it to be undermined and to migrate up-canyon. In P4 East, downstream from P4 West, one head cut migrated 50 feet in 2002, and over 400 feet during one event in 2003. Downstream, at Cross Sections 10 through 11c, the slope, width to depth ratios, and entrenchment generally increases. Lower in this mid section, at 5c and 6, the entrenchment and width to depth ratios also increase. The longitudinal profile in Figure 10 demonstrates the stream relationships along the entire stretch of P-4 West.

Our evaluations indicate the stream is adjusting to the increased storm water discharges and sediment yields. The upper and lower stream sections in reach P-4 West, are classified as predominantly C type streams, evolved from a DA type. According to Rosgen (1994), C type streams are very highly sensitive to stream flow and sediment increases, contribute high to very high sediment supplies, and have a high to very high stream bank erosion potential. In the mid section, the stream classification is predominantly an E type stream, and according to Rosgen (1994), demonstrates a very high sensitivity to stream flow and sediment increases, a low to moderate sediment supply contribution, and very high stream bank erosion potential. Channel classification differences exist in areas around Cross Sections 10, 5c, and upstream of 15 to the waterfall. These differences indicate the instability, and sensitivity to flow and sediment supply, and erosion potential is increasing at greater rates in these areas.

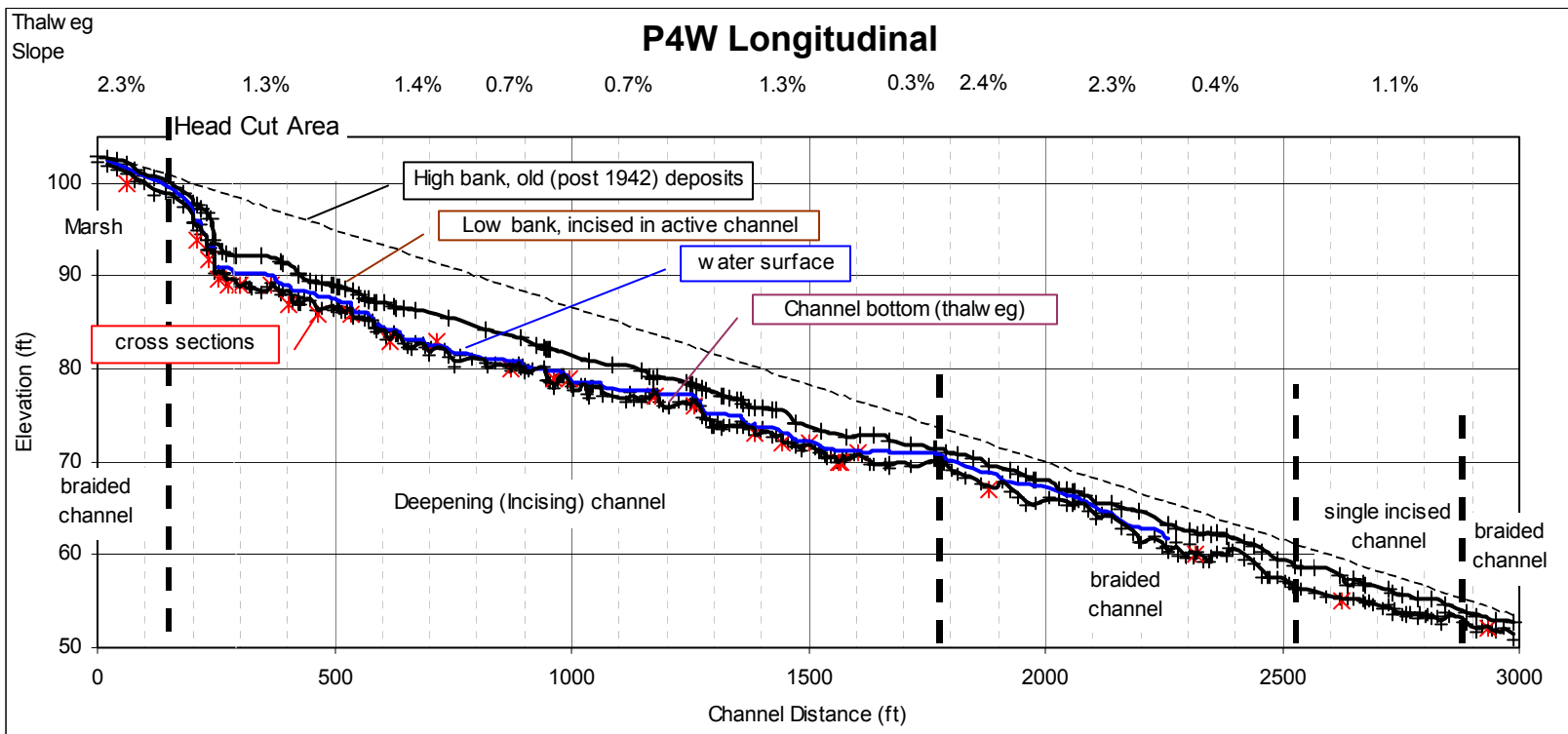


Figure 10. Longitudinal profile of P-4 West.

Sediment and Plutonium-239/240 Transport

Since the Cerro Grande fire in 2000 through the summer of 2002, 37 storm runoff events greater than 10 cfs have occurred. We sampled 8 of 31 storm events during 2001 and 2002 at the E060 storm water gage, and commercial analytical laboratories measured the samples for suspended sediment and plutonium concentrations. Only 6 of those events had recoverable flow data. This section demonstrates the methods we used to calculate the plutonium and sediment mass transported beyond lower Pueblo Canyon in individual events and the total masses transported since the fire to the end of the 2002 storm runoff season.

The earlier parts of this section demonstrate the relationship of storm water flow to suspended sediment and plutonium concentrations, and methods for evaluating sediment and plutonium mass transport for individual storm water. The later parts demonstrate the techniques used to predict and evaluate mass transport for runoff events not sampled, and provides estimates of plutonium and sediment transport during the 2000 to 2002 storm water seasons. The last parts provide additional support showing that the plutonium concentration in storm water is dependant on the mass of suspended sediment in water and the plutonium concentration in suspended sediments.

Recall from the Methods section in this report that plutonium-239/240 isotopes are indistinguishable using alpha spectroscopy analytical methods, and that plutonium-238 was measured at a small fraction of plutonium-239/240. In this section plutonium is used synonymously for plutonium-239/240. Also recall that three distinctly different plutonium measurements were made for our storm water samples: dissolved plutonium in storm water, total plutonium in storm water, and plutonium in sediments separated from storm water.

We generally find that suspended sediment and plutonium concentrations increase as storm water flow rates increase. The sediment is derived from eroding stream banks as the channel adjusts to increasing flow, and from material dislodged by rainfall on exposed mountain and channel slopes. Increasing total plutonium concentrations in water are associated with the rising concentration of suspended sediments containing plutonium. The plutonium is derived from legacy contaminants discharged into Pueblo Canyon and stored in bank and bed sediments.

Other plutonium sources exist, but are a small component of the total plutonium mass being transported from Pueblo Canyon. Storm water transported a small plutonium contribution from atmospheric nuclear testing fallout as well as plutonium in ash from the Cerro Grande fire. Fallout materials naturally absorbed by the forest biota were concentrated in ash as the fire reduced the biomass. The concentration of legacy plutonium, approximately 4 pCi/g in suspended sediments, overwhelmed any input from fallout materials in soils or ash and we did not try to differentiate between them. We found the average concentration of plutonium-239/240 in 15 suspended sediment samples collected at locations upstream from Acid Canyon was 0.049 pCi/g which fell below the range of background values for soils and canyon sediment (0.054 – 0.068 pCi/g

respectively) determined by the LANL RRES-ES group. Plutonium levels in the environment derived from atmospheric testing, are referred to as background.

Shortly after the Cerro Grande fire, NMED collected 27 ash samples in and around the burned forest to determine whether or at what levels contaminants exist. The plutonium 239/240 levels in ash ranged from 0.02 pCi/g to 0.60 pCi/g and averaged 0.23 pCi/g. Storm water monitoring and observations of the burned forest areas suggest most of the ash has been transported beyond Pueblo Canyon. Additional discussion of plutonium in background fallout and ash is found in Appendix A.

The plutonium derived from background was not differentiated from legacy plutonium in the transport estimates based on the magnitude of differences between plutonium levels in background, in ash, and in sediments contaminated with LANL legacy wastes. Concentrations of plutonium in suspended sediment were 2 orders of magnitude greater than background levels and an order of magnitude greater than levels seen in the ash generated during the Cerro Grande fire. Plutonium in suspended sediments is consistently measured around 4 pCi/g, in Cerro Grande ash it was 0.23 pCi/g, and in background soils it is less than 0.054 pCi/g.

The following discussion describes the plutonium, suspended sediment, and flow relationships for an individual runoff event. Figures 11 and 12 present those relationships and the associated text summarizes the sediment and plutonium mass transport calculations for a runoff event that occurred June 22, 2002. Figure 11 presents sediment mass transport and the Figure 12 presents plutonium mass transport. These relationships are similar in the other 5 events that we evaluated and are presented in Appendix G.

LANL gage E060 was inoperable in the later half of August 2002, and flow data had to be recovered from stage heights recorded by our flow meters. The stage heights were applied to discharge rating curves developed for the gage to develop complete hydrographs for 2 August events. One occurred August 18 and another August 26. Flows were not available for 2 events collected in October and November of 2002 and could not be evaluated.

Using the methods described in the Storm Water Monitoring Methodology section of this report, we evaluated mass transport of sediment and plutonium for a flood event on June 22, 2002. We found approximately 3,045 tons of suspended sediment was transported in the first 5 hours of the event. An additional 91 tons were carried beyond the lower Pueblo Canyon gage station during the following 5 hours of flow. Plutonium transport during the first 5 hour period is equal to approximately 14.06 mCi, 98% of the total 14.34 mCi transported during a 10 hour period of the runoff event. Although the duration of the floods vary, we observed that the major proportion of transport occurred during the early part of each event. To provide continuity in our comparisons we evaluated the first 10 hours of each event.

The suspended sediment concentration (SSC) relationship to flow is characterized by Figure 11. It reflects a maximum SSC measurement of 84,500 mg/L at 106 cfs on the

rising leg of the hydrograph, and a peak flow of 583 cfs shortly after the first sample was collected. The flow and SSC diminish during the following 1 hour and 50 minutes to our last measurements of 19,500 mg/l at 127 cfs. We calculate that 2,715 tons, 87 percent, of the sediment was transported within this 2 hour and 15 minute time period. The flow continued to diminish until it reached probable base flow of approximately 9 cfs from the treatment plant almost 8 hours later.

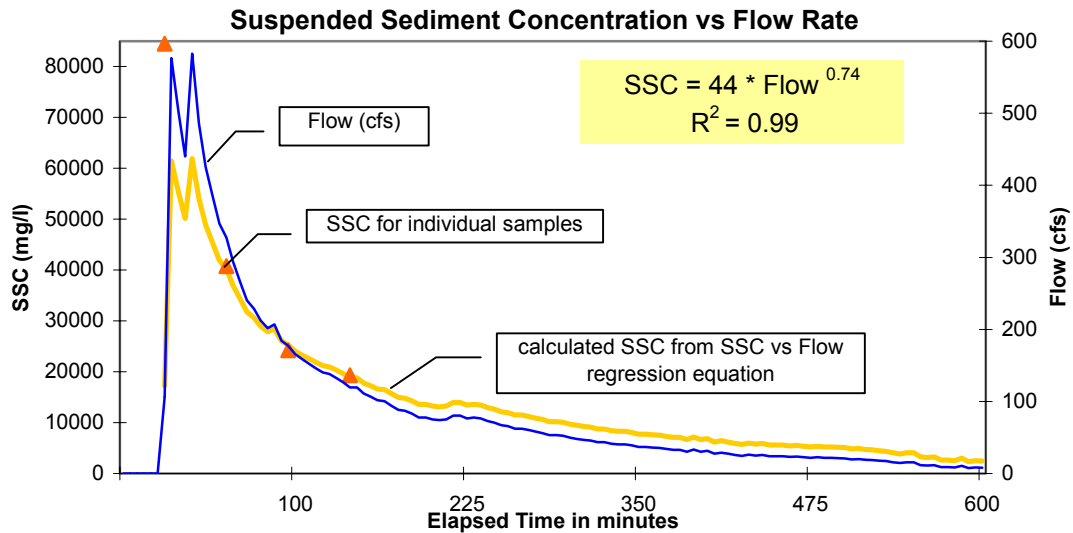


Figure 11. June 22, 2002 hydrograph and associated suspended sediment concentrations

Refer to the Mass Transport Calculation Methods section for the evaluation techniques used to determine sediment mass transported during each event. The regression equation describing the relationship between the paired suspended sediment concentrations and flows were used to calculate suspended sediment concentration for the remaining flow measurements. Integrating the sediment concentration and the associated water volume resulted in the suspended sediment mass transported for each 5 minute time interval. The total mass transport for any period during the event can be determined by summing all reiterations during the time frame of interest.

A power regression equation, $y = 41 * x^{0.74}$, does the best job expressing the relationship between the suspended sediment concentration and flow for this event. Suspended sediment concentration is the y variable and flow is the x variable. The first measurement was collected on the rising leg of the hydrograph rather than at peak flow and was not used to determine the regression analysis. The coefficient of determination, R^2 , is equal to 0.99, suggesting that almost 100% of the variation in suspended sediment concentrations can be described by the equation.

Figure 12 characterizes the total plutonium concentration and flow relationship in the runoff event. We calculate that 84 percent, 12.03 mCi of the 14.34 mCi plutonium inventory transported in this event occurred within the initial 2 hours and 15 minutes of this runoff event. The figure reflects a maximum plutonium measurement of 197 pCi/L

at 347 cfs within 45 minutes from the start of the flow event and a potential value of 239 pCi/l at peak flow. The plutonium concentration for the first sample, collected 5 minutes from the start of the event on the rising leg of the hydrograph, was 161 pCi/L. The 583 cfs maximum flow occurred 20 minutes later. The flow and plutonium concentrations diminish during the following 1 hour and 50 minutes to our last plutonium measurement of 123 pCi/L. We predict that these concentrations continued to diminish until they reached the probable treatment plant base flow of approximately 9 cfs almost 8 hours later.

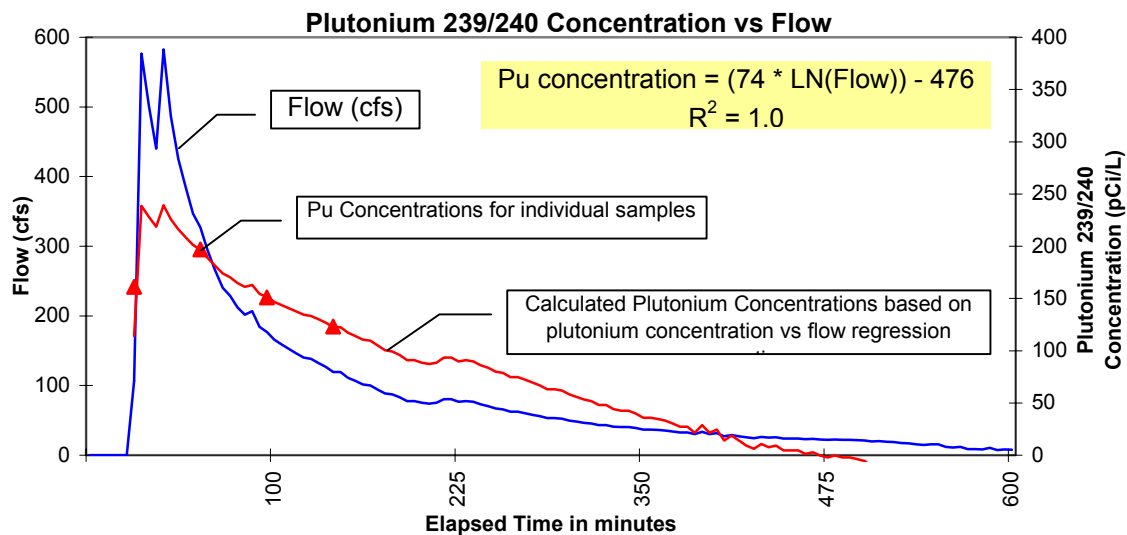


Figure 12. June 22, 2002 hydrograph and associated plutonium-239/240 concentrations

The plutonium transport evaluation methods are the same as those used to evaluate sediment transport and are described in the Mass Transport Calculation Methods section, except plutonium concentrations rather than suspended sediment concentrations are correlated to flow rates. The logarithmic equation, $y = (74 * \text{LN}(x)) - 476$, does the best job expressing the relationship between the paired total plutonium concentrations and flow measurements. Total plutonium concentration is the y variable and flow is the x variable. The first measurement was collected on the rising leg of the hydrograph rather than at peak flow and not used to determine the regression analysis. The coefficient of determination, R^2 , is equal to 1.0, suggesting that 100% of the variation in plutonium concentrations can be described by the equation.

The differences seen in plutonium concentration and suspended sediment concentration between the first and second samples reflect the variability in the environment and difficulty in collecting a sample at peak flow. The first measurements were associated with the start of the runoff event at a 106 cfs flow, on the rising leg of the hydrograph. They resulted in the maximum SSC and a plutonium measurement that was not the maximum level. This first SSC was largest at 84,500 mg/L, and the plutonium concentration of 161 pCi/L was less than the second sample collected 50 minutes later that was measured at 197 pCi/L.

This inconsistency is explained by the plutonium measurements made in the suspended sediments. The suspended sediments were separated from the June 22, 2002 storm water samples and the plutonium concentrations measured. Figure 13 presents total plutonium in water relative to plutonium in sediments. Recall that total plutonium measurements are made on a whole storm water sample and include the dissolved fraction of plutonium as well as the solid plutonium phase associated with sediments. The plutonium in sediments ranges from 1.67 to 5.63 pCi/g, although they appear consistent and average 5.32 pCi/g after the first value. On the other hand, after the plutonium measurements in sediment stabilized, total plutonium concentrations in water declined from 197 pCi/L to 123 pCi/L concurrent with diminishing SSC as well as flow. Suspended sediment concentrations declined from the first measurement of 84,500 mg/L. This also demonstrates the obvious relationship of total plutonium in water to SSC, but it also shows that varying plutonium concentrations in sediments introduces variability to storm water concentrations of plutonium.

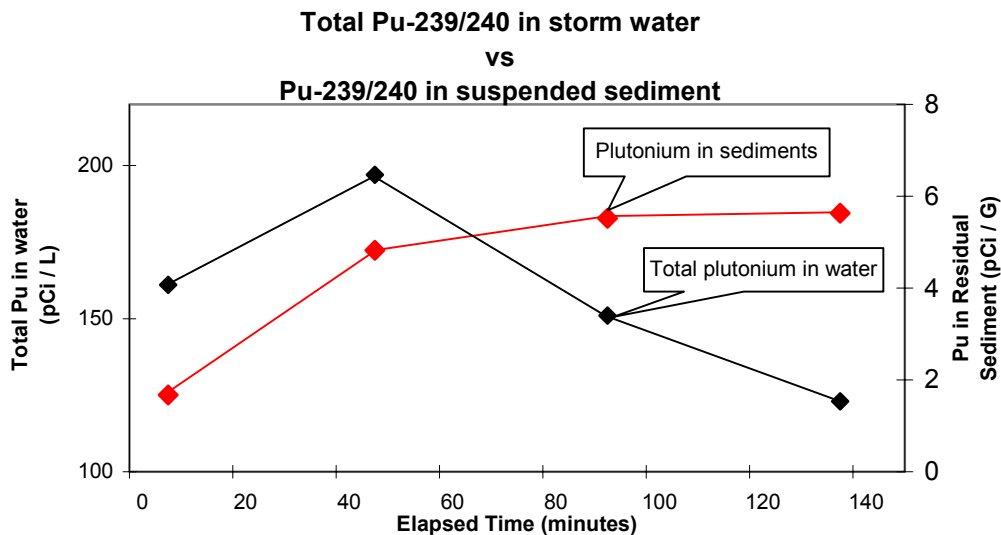


Figure 13. Total plutonium-239/240 in water compared to plutonium-239/240 in residual sediments.

This variability in plutonium measurements (1.67 to 5.63 pCi/g) in suspended sediments may result from the sediment source area; for example an influx of sediments with smaller plutonium concentrations would dilute the sample concentration. It may also be related to the suspended sediment matrix, coarser grained sediments tend to have smaller concentrations of contaminants associated with them.

The first sediment measurement, 1.67 pCi/g plutonium, may be related to source of the sediment load or to larger grain size sediments that reflect bed load material. The initial wave front of a flood, or flood bore, often carries a greater proportion of coarse-grained bed load sediments, which diminish as the flow recedes. In this case, it appears the variability comes from the sediment source area. The grain size distribution measurements were fairly consistent in the 4 samples collected during the June 22 runoff event. The grain size analysis showed the sand, silt, and clay fraction were consistently

around 72%, 27%, and 1%, respectively; and no relationships could be established between grain size, suspended sediment concentration, or plutonium concentrations in sediment.

Many contaminants have an affinity for small grain size sediments, which is related to the larger surface area and increased ion exchange capacity of the silt and clay particles as compared to the sands. At higher flow rates a greater portion of bed load may be suspended in the water column. This would increase the concentration of suspended coarse sands, increasing the particle size in the sample and diminish the total concentration of a contaminant in samples of equal SSC. Our evaluation of plutonium in suspended sediments and particle size does not explain the variability observed in the plutonium measurements. The coarse to fine sand fraction in our samples ranged from 0 to 6% by weight, silt comprised 44% to 77% of the sample weight, and the clay fractions ranged from 22% to 59%. The plutonium, suspended sediment, and grain size distribution correlations are slight and inconsistent for individual storm sample sets as well as the entire data set.

An observation that provided additional insight into the Pueblo Canyon fluvial system and sediment transport was that the sand fraction became smaller and the clay fraction larger in the lower Pueblo reaches. The upper reaches are steeper and the valley narrower than in lower Pueblo Canyon. Also, in the lower reach, below the Bayo treatment plant, marsh grasses in the active channel areas and on floodplains increase the channel roughness, which reduces flow velocities, and promotes sediment deposition.

A small percentage of the variability may have been explained by grain size but it was overwhelmed by other uncertainties. Environmental uncertainties may be due to the suspended sediment source, total organic carbon content, or other unknown variability, but could also include technical uncertainties associated with sampling and analytical methods and techniques.

The most probable source of this variation comes from the sediment sources. Influx of sediments from areas with low plutonium concentrations dilutes the total plutonium concentration in storm water. Sediment and plutonium vary in provenance, which contributes varying proportions of plutonium and sediment mass. These proportions determine the plutonium and suspended sediment concentrations in storm water. They come from within the active channel, old bank forming channel deposits, and the upper watershed areas, and have different stream lengths, slopes, and susceptibilities to erosion or deposition. Each area provides varying degrees of plutonium concentrations in suspended sediments. These concentrations could vary from LANL sediment background levels of less than 0.068 pCi/g (Ryti et al, 1998) to values greater than 502 pCi/g, an upstream Pueblo Canyon overbank measurement reported by RRES-RS.

South Fork Acid Canyon, an area that received the original radioactive water waste discharges, continues to contribute sediments with elevated plutonium concentrations. Fortunately, the relative suspended sediment contribution to Pueblo Canyon is small sustaining a small overall contribution to plutonium transport inventories. Two storm

water samples collected there in 2000 contained plutonium concentrations in sediments that ranged from 38 pCi/g to 107 pCi/g. Acid Canyon, below the South Fork, contributed diluted plutonium concentrations in sediments that ranged from 0.1 pCi/g to 22 pCi/g. Only 6 SSC measurements, containing relatively small concentrations, were made in this area. The values ranged from 12 mg/L to 320 mg/L. These relationships produced relatively small total plutonium concentrations in water ranging from <0.2 pCi/L to 16.4 pCi/L. The watershed area is small and it appears that runoff periods are brief and carry relatively small quantities of sediment, although Acid Canyon does receive urban runoff from the Los Alamos town site. Reducing this storm water source could further improve conditions in Pueblo Canyon.

The active channel bed sediments could be a primary source for suspended sediments in storm water and have been monitored by LANL RRES-WQH since the 1970s. Plutonium concentrations in the active channel bed are demonstrated in Figure 14. It shows 10-year concentration averages at 6 surveillance stations in Pueblo Canyon by the RRES-WQH (ESP 1991 through ESP 2000). The annual samples are collected from within the Pueblo channel at an upstream location just above Acid Canyon, downstream to State Road 4. These samples reflect bed load and are coarser grained materials than would be expected in suspended sediments. The sediments are readily available for transport and further mixing, and the average concentrations range from 0.2 pCi/g to 6 pCi/g.

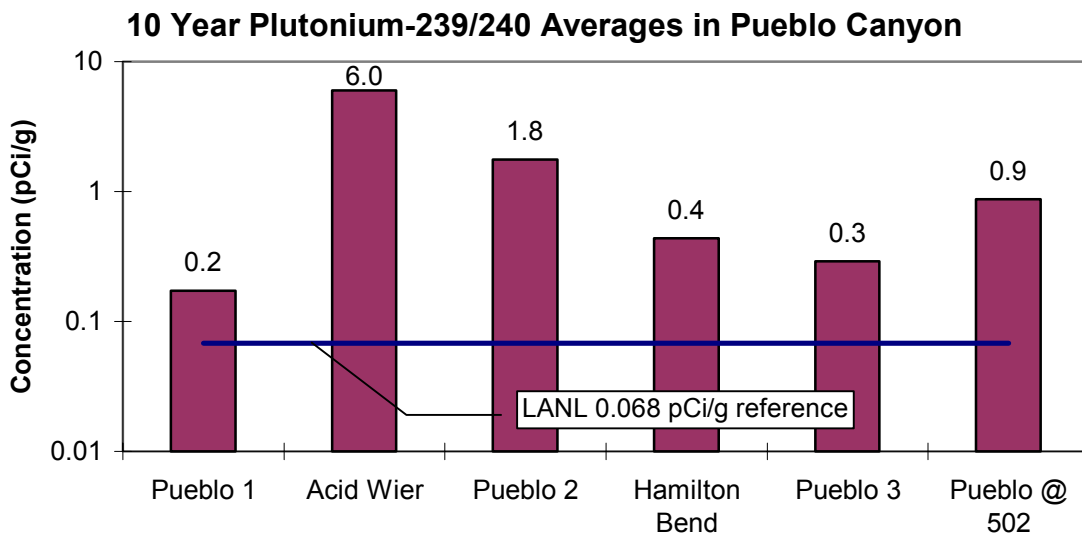


Figure 14. Ten year averages of plutonium-239/240 in bed load within the Pueblo Canyon channel
 Below the Acid Weir, LANL RRES-WQH 's annual surveillance samples ranged in plutonium concentrations from 11.8 to 0.003 pCi/g, averaging 6.0 at the Weir to 0.3 pCi/g at Pueblo 3, which correlates to P-4 West Cross Section 1. Above Acid Weir at Pueblo 1, most of the values are consistent with the LANL 0.068 pCi/g background reference value although some exceptional high values exist.

LANL RRES-RS undertook additional active channel evaluations and estimated plutonium in younger active channel sediment deposits in P-4 West average 1.3 pCi/g, ranging from 0.120 to 3.180 pCi/g. RRES-RS measurements in channel deposits throughout Pueblo Canyon vary from 12.6 pCi/g in Acid Canyon to less than background (Reneau, et al, 1998). They have estimated over 1 curie plutonium is distributed throughout the Pueblo Canyon alluvial sediments of which 38% or 383 mCi was estimated as susceptible to redistribution.

Besides the active channel source, other areas contribute sediments containing plutonium, including channel banks, floodplains, and terraces, which are currently impacted by the increased storm water flows. LANL RRES-RS average estimates of plutonium in the older, post-1942, bank-forming geomorphic units in P-4 West range from 1.27 to 37.8 pCi/g. Individual measurements range from background levels to 170.5 pCi/g. These include geomorphic channel and overbank units exposed above and along the Pueblo channel. Channel deposits are generally coarse grained sands with lower contaminant levels; overbank and floodplain units consist of fine grained materials, including clay to fine grained sand, and commonly contain higher contaminant concentrations. They are exposed at greater heights above the active channel, and to erosion from higher flood stages.

Our evaluations of the remaining 5 runoff events indicate 24 mCi of plutonium in 6,672 tons of sediment were transported beyond the E060 gage station during the storm flows we sampled. These events represent 6 of the 37 runoffs that occurred since the Cerro Grande fire to the end of 2002. Using the relationships between the peak flows and plutonium and sediment transport inventories, we estimated the transport inventories for the remaining 31 runoff events. Plutonium and sediment mass transported during these 6 events are compiled in Table 3. The following text describes the technique we used to estimate the plutonium and sediment mass transported during the storm runoff events described in this report.

Table 3. Plutonium-239/240 and sediment inventory transported beyond E060 during 6 of 37 storm water flows during 2000, 2001, and 2002

Runoff Date	Peak Flow (cfs)	Plutonium Inventory			Sediment Inventory		
		Transported during first hour (mCi)	Transported over 5 hours (mCi)	Transported over 10 hours (mCi)	Transported during first hour (tons)	Transported over 5 hours (tons)	Transported over 10 hours (tons)
8/11/2001	248	0.91	1.6	1.74	1223	1621	1650
8/16/2001	174	2.04	3.36	3.93	373	673	818
6/22/2002	583	8.66	14.06	14.34	2109	3045	3136
7/18/2002	53	0.73	1.07	1.59	115	248	312
7/26/2002	94	0.91	1.86	2.26	297	601	724
9/10/2002	29	0.01	0.09	0.11	2	27	32
Total inventory for 6 of 29 flows during 2001 and 2002		13.3	22.0	24.0	4119	6215	6672

We estimate 87.1 mCi plutonium in 21,980 tons of sediment were transported beyond the E060 gage during 2000 through 2002. This estimate is based on the relationships that were observed between the peak flows and the plutonium and sediment mass transport inventories of the events we sampled. Rating curves were developed based on the paired peak flow measurements and sediment and plutonium mass transport values we derived. Applying the regression equations describing these relationships to the remaining peak flows provided an estimate of the sediment and plutonium mass transport for each event. Summing the results for all flows provided an estimate of the sum total discharges of sediment and plutonium. By calculating the 95% confidence interval for each event and summing the upper and lower limits of these estimates, we found that that as much as 189 mCi and as little as 34 mCi of plutonium could have been transported. Correlations of plutonium and sediment inventories to peak flows are shown in Figures 15 and 16. Runoff dates, peak flows, plutonium and sediment transport estimates, and summations are listed in Table 4.

The following graphs in Figures 15 and 16 depict the plutonium and sediment mass transport relationships to peak flows from the 6 storm events listed in Table 3, and the estimated values for the remaining flows. The solid diamonds on the chart represent the plutonium values derived from the events we sampled. The smaller hollow squares represent the plutonium values we estimated based on the regression equation that reflects the plutonium mass and flow relationship. This relationship is presented in Figure 15, and described by the linear equation, $y = 0.022x$, where the y variable is equal to the plutonium inventory in mCi, and x is equal to the peak flow measured in cubic feet per second. A close relationship is implied by $R^2 = 0.88$.

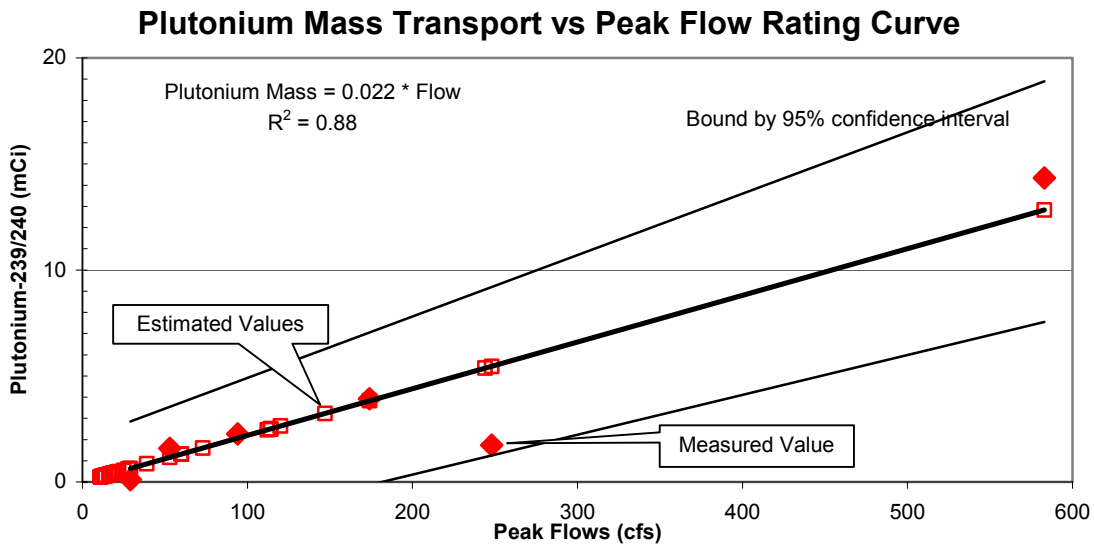


Figure 15. Plutonium-239/240 inventory transport correlation to peak flows

An example of this estimation method is illustrated for a 60 cfs peak flow that occurred August 8, 2000. Using the regression equation $y = 0.22 x$, we find that 1.3 mCi of plutonium was transported during this event. The plutonium inventory was calculated by

multiplying the flow, x , by 0.022 from the regression equation. This suggests that for every unit of peak flow increase, there is an associated 0.022 times the plutonium unit increase.

The sediment yield versus flow relationship in Figure 16 is described by $y = 5.55x$, where the y variable is equal to tons of sediment and x is flow. A close relationship also exists, where $R^2 = 0.97$. The y intercepts were set at 0, assuming there can be no transport at 0 flow. The 60 cfs flow used as an example above yielded 333 tons of sediment, based on the regression equation ($60 \text{ cfs} * 5.55 = 333 \text{ tons of sediment}$). The solid diamonds represent the values we derived from measured samples, and the square outlines represent the values estimated using the regression equation that describes the sediment mass transport to peak flow relationship.

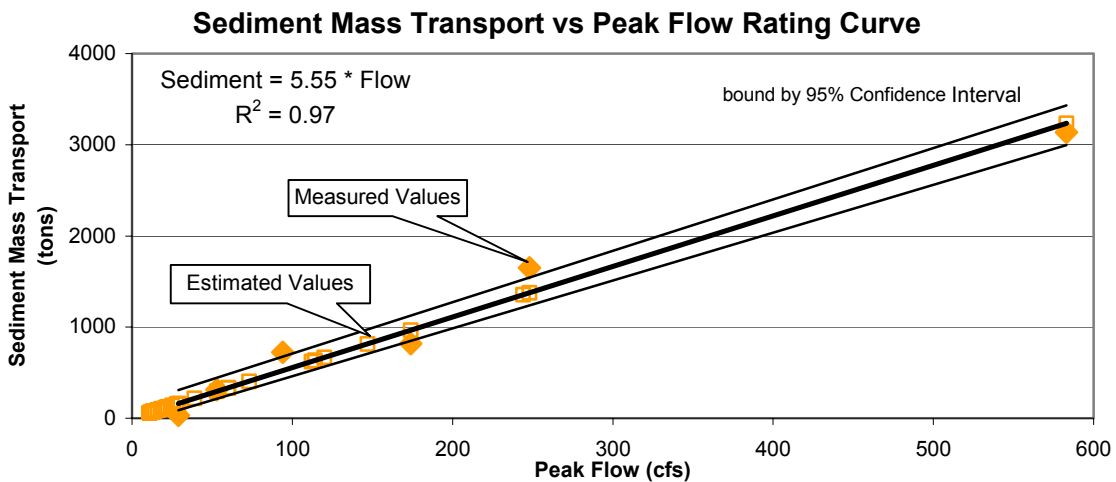


Figure 16. Sediment yield correlation to peak flows

Additional monitoring of all the storm events would have been required to fully characterize the total discharges of sediment and plutonium, but interpolating data obtained from the six events to the remaining 31 provided a transport estimate. Plutonium and sediment mass transport estimates might also be made for future discharges using the sediment, plutonium, and flow rating curves demonstrated by Figures 15 and 16.

In addition to the 87.1 mCi plutonium in 21,980 tons of sediment transported during 2000 through 2002, we characterized transport for individual flow regimes as well as annual sum totals. Runoff dates, peak flows, plutonium and sediment transport estimates, and summations are listed in Table 4. During 2000, we estimate 8.4 mCi of legacy plutonium in 2,131 tons of sediment were transported beyond Pueblo Canyon during 6 runoff events. In 2001, 54.8 mCi plutonium in 13,838 tons sediment were transported in 17 runoff events. In 2002, 23.8 mCi plutonium in 6,011 tons sediment were transported in 14 runoff events. In both 2001 and in 2002 over half of the plutonium and sediment masses that were transported were removed in single events. The 1440 cfs, July 2, 2001

Table 4. Runoff Dates, peak flows, plutonium and sediment transport estimates, and summations

Runoff Event	Peak Flow	Average and Median Flows	Plutonium Mass Transport	Total Plutonium Mass Transport and Average per event	Sediment Mass Transport	Total Sediment Mass Transport and Average per event
8/3/2000	60	Year 2000 64 49.5	1.3	Year 2000 8.4 1.4	333	Year 2000 2131 355
8/12/2000	13		0.3		72	
9/8/2000	114		2.5		633	
10/12/2000	11		0.2		61	
10/24/2000	147		3.2		816	
10/27/2000	39		0.9		216	
7/2/2001	1440	Year 2001 147 25	31.7	Year 2001 54.8 3.2	7993	Year 2001 13838 814
7/26/2001	114		2.5		633	
7/27/2001	16		0.4		89	
8/4/2001	60		1.3		333	
8/5/2001	28		0.6		155	
8/6/2001	21		0.5		117	
8/9/2001	244		5.4		1354	
8/10/2001	18		0.4		100	
8/11/2001	248		5.5		1377	
8/13/2001	19		0.4		105	
8/14/2001	29		0.6		161	
8/16/2001	174		3.8		966	
8/17/2001	25		0.6		139	
8/20/2001	16		0.4		89	
8/27/2001	14		0.3		78	
8/31/2001	14		0.3		78	
9/26/2001	13	0.3	72			
6/22/2002	583	Year 2002 77 20	12.8	Year 2002 23.8 1.7	3236	Year 2002 6011 429
6/23/2002	22		0.5		122	
6/24/2002	11		0.2		61	
7/5/2002	11		0.2		61	
7/6/2002	12		0.3		67	
7/7/2002	16		0.4		89	
7/8/2002	11		0.2		61	
7/9/2002	73		1.6		405	
7/18/2002	53		1.2		294	
7/26/2002	112		2.5		622	
7/31/2002	120		2.6		666	
8/9/2002	18		0.4		100	
9/10/2002	28		0.6		155	
9/13/2002	13	0.3	72			
Average Peak Flow	107	Total Mass Plutonium Transported	87.1	Total Sediment Mass Transported	21980	

event carried 31.7 mCi of plutonium and 7,993 tons of sediment beyond the E060 gage. In 2002, the June 22, 583 cfs event removed 12.8 mCi of plutonium in 3,236 tons of sediment.

Less than 1 mCi plutonium and 245 tons of sediment transport would be expected in flows less than 44 cfs. Twenty-three runoff event flows were less than 44 cfs, similar to the 50 cfs value we suggest is the post Cerro Grande fire, dominant bank forming discharge rate.

Plutonium and sediment transport rates have not been this high since the 1950's and 1960's. A study by William Graff (Graff, 1993) showed plutonium transport from the Los Alamos Canyon into the Rio Grande as great as 44 mCi in 1957. During 1951, 52, 55, 57, and 58, he estimated 17, 18, 9, 44, and 7 mCi of plutonium transport, respectively. He estimated 10 mCi of plutonium was transported in each of these years, in 1963, 65, and 67, and 22 mCi in 1968.

His estimates were based on flow measurements and samples collected at a gage station in lower Los Alamos Canyon that is no longer operational. The samples were described as bed load in runoff in his report, and analytical techniques may have been different than those used in this study. Interestingly, plutonium concentrations in sediments were similar as well as regression equations that reflect the correlation of plutonium transport mass to peak flow. The plutonium values that we derived from his data ranged from 7.03 pCi/g to 0 pCi/g. The average of those values was 3.4 pCi/g without using pre-1950 and post-1981 values, which reflected very low values. Our average plutonium measurement in suspended sediments from all E060 samples was 3.5 pCi/g. The regression equation describing Graff's plutonium to flow data was; Plutonium Mass = 0.029 * peak flow, and $R^2 = 0.62$. The regression equation describing the plutonium to peak flow correlation in this report is; Plutonium Mass = 0.022 * peak flow, and $R^2 = 0.88$.

The last part of this section describes the relationships we observed from all of our samples. They include relationships between all of our plutonium and suspended sediment values vs their paired flow measurement, and relationships that are independent of flow, such as plutonium in water vs suspended sediment. These are different from the preceding evaluations in that those relationships were based on individual events and used to derive transport masses from peak flow values. Observations of the following relationships provided insight into the variability we saw in our measurements, whether it came from natural environmental conditions or error in the technical measurements required for these assessments.

The graph in Figure 17 depicts the strong correlation between plutonium concentration and SSC, where total plutonium in water increases as the suspended sediments increase. It was derived from 31 storm samples collected in lower Pueblo Canyon at E060. They include multiple samples per storm event, collected from 8 events during 2001 and 2002. A minimum 0.11 pCi/L plutonium concentration was measured with a 19 mg/L SSC. A maximum 253 pCi/L plutonium concentration was measured with a SSC of 39,400 mg/L. This relationship is described by the equation, $y = 0.004x^{0.99}$, where the y variable is

equal to the plutonium concentration in pCi/L, and x is equal to SSC in mg/L. A close relationship is implied by $R^2 = 0.94$, and the exponent 0.99 describes a strong degree of linearity.

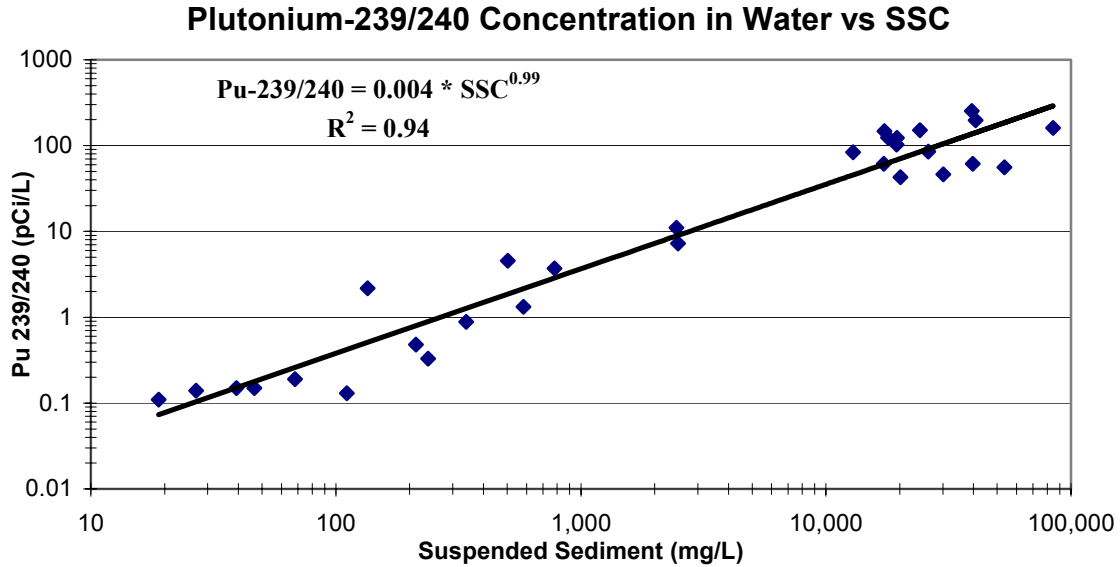


Figure 17. Suspended sediments concentration and plutonium-239/240 concentration relationship

The dispersion that is evident comes from the variability of plutonium concentration in sediments. The minimum, maximum, mean, and median plutonium concentrations in sediments from samples collected at E060 were 1.05 pCi/g, 5.88 pCi/g, 3.48 pCi/g, and 3.42 pCi/g, respectively. These measurements of total plutonium and suspended sediments range in almost 4 orders of magnitude. The total plutonium and suspended sediment relationship is not impaired by the small differences of plutonium in sediments at E060.

The graph in Figure 18 describes a fairly strong relationship of plutonium concentrations in water to storm water flow. It demonstrates that total plutonium increases as storm water flow increases. The graph correlates the plutonium and flow measurements from 18 storm samples collected in lower Pueblo Canyon at E060. They include multiple samples per storm event, sampled from 4 of the 17 flows during 2002 and 2 events during 2001. Flow measurements for 2 of these events were recovered from our flow gages and used for these correlations. Flows for events collected in October and November of 2002 were not available. A minimum 3.70 pCi/L plutonium concentration was measured with a 4 cfs flow. A maximum 253 pCi/L plutonium concentration was measured with a 174 cfs flow.

It presents a strong linear correlation, $y = 0.94 * x^{1.02}$, $R^2 = 0.70$. This equation suggests that for every cfs unit increase in flow there is an associated 0.94 pCi/L increase in plutonium concentration.

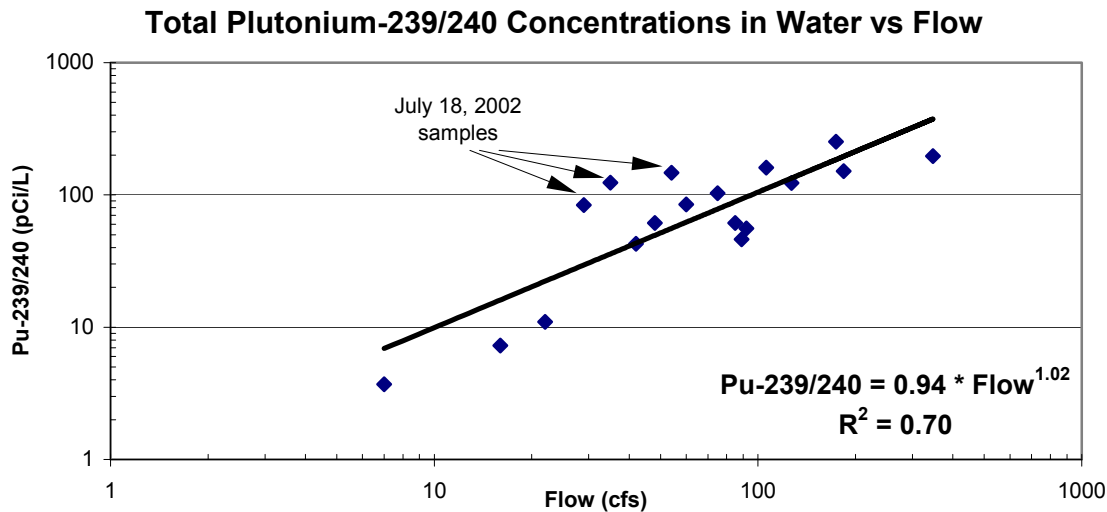


Figure 18. Plutonium-239/240 concentration correlation to flow rate.

Three measurements from a runoff event collected on July 18, 2002 had larger residual errors, the difference between the predicted values and measured values, than the majority of the samples. These errors may be from a natural environmental dispersion or from measurement error. For example, the total plutonium measurements range from 84 pCi/L to 147 pCi/L for these samples; the predicted values range from 29 pCi/L to 55 pCi/L and the differences reflect a variation incurred by natural environmental variability or analytical measurement error.

The July 18, 2002 plutonium concentrations in the suspended sediments are slightly higher but not extraordinary, averaging 5.08 pCi/g relative to a 3.58 pCi/g average for the remaining samples. They contained a larger percent of clay than the other samples, 42% to 55% relative to an average 35%, possibly producing a larger plutonium concentration. Plutonium, as well as other contaminants, has the tendency to adsorb to finer materials increasing in concentration as the percent of fine grain size materials increase. Another source of variability, or in this case error, may be the analytical measurement. As a cross reference, we calculated the total concentration of plutonium in water using the concentration of plutonium in sediment and the suspended sediment concentration for each sample using the following equation:

$$[(X \text{ pCi/g} * Y \text{ mg/L}) / 1000 \text{ mg/g} = \text{pCi/L}]$$

Where:

X = concentration of plutonium in suspended sediments as pCi/g

Y = concentration suspended sediments as mg/L

1000 mg/g = conversion factor to reduce milligrams to grams

We found the relative percent differences of the actual measured values and calculated values in the July 18th samples ranged from 10% to 34%. The average relative percent difference for all samples, excluding the July 18th samples, was 16%. We found these

measurements acceptable based on the relative percent differences comparison and larger clay content in the July 18th samples.

The most probable source of the error may have developed from the flow measurements. As noted before, the E060 gage was inoperable during the last part of August, and the flows were recovered from our stage heights and discharge rating curves. The difference between the flow measurements that ranged from 29 cfs to 54 cfs, used above, and an inverse prediction from the chart in Figure 18 might suggest that the flows could be 81 cfs to 141 cfs. Adjustments or removal of these values did not substantially improve the relationships we found, and they were retained in these assessments.

Figure 19 describes the relationship of suspended sediment concentrations to storm water flow. It represents the same 18 samples described above. A minimum SSC of 781 mg/L was measured with a 4 cfs flow. A maximum SSC of 84,500 was measured with a 106 cfs flow. It represents a strong linear relationship, $y = 221.9 * x^{1.06}$, $R^2 = 0.71$.

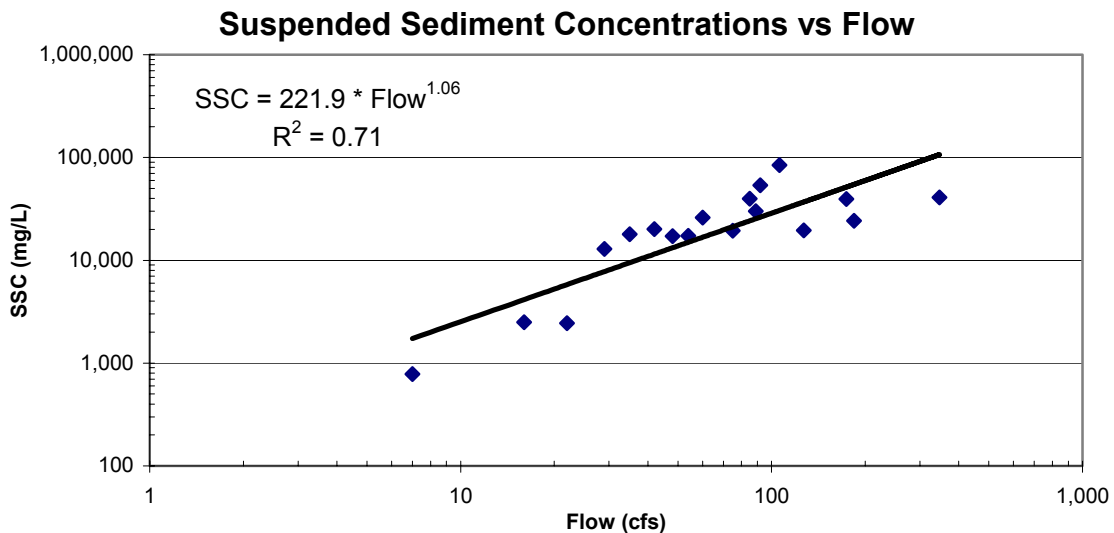


Figure 19. Suspended Sediment Concentrations correlated with flow.

The relationship supports the conceptual model that suspended sediment concentrations increase as flow increases. In this case the relationship is linear and the suspended sediment concentration increases at a rate of approximately 222 times with each unit of flow increase.

Our last figure, Figure 20, is similar to the rating curve developed in Figure 13, which reflects the plutonium mass transport inventory relationship with peak flows. That figure contained plutonium mass and peak flow values from evaluations of the 6 storm flow events that we measured. In Figure 20, we tried to improve the relationship by including a derived mass transport for each sample collected during the 6 events, increasing the number of correlations to 18. We achieved this by summing the mass transport inventory from the time of collection to the end of the flow event, and correlating that value to its paired flow measurement.

This correlation substantiated our prior assessment by reproducing a relationship very similar to the original rating curve. The regression produced the equation $y = 0.022x$, and a coefficient of determination, R^2 , that was equal to 0.87. The original equation developed in Figure 13 is $y = 0.022x$, and $R^2 = 0.88$.

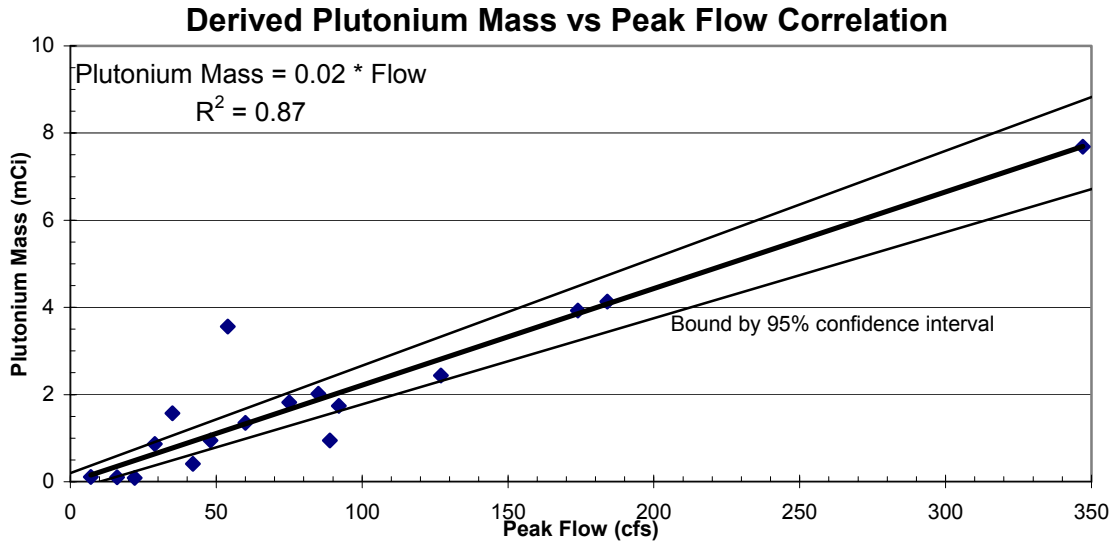


Figure 20. Derived plutonium transport inventory and peak flow estimates from all samples collected during sampled storm events

Summary

In July and August of 2002, and later in 2003, the Department of Energy Oversight Bureau of the New Mexico Environment Department measured physical variables of reach P-4 West in Pueblo Canyon. We measured channel dimensions, stream pattern, stream profile, and bed features to assess channel stability and establish benchmarks for monitoring future stream adjustments. We also collected and evaluated storm water samples for sediment and plutonium-239/240 transport during the summer months after the Cerro Grande fire. Reneau and others (1998) described this reach as having exceptionally large deposits of early post-1942 sediment dating to the time of peak contamination from TA-45. The sediment volume, and plutonium concentration and inventory are greater relative to other reaches in Pueblo Canyon and are downstream of an area burned during the fire.

The May, 2000 Cerro Grande fire burned 1,200 acres, nearly 80%, of the upper Pueblo Canyon watershed (BAER, 2000). A complete loss of vegetative cover and intense heat reduced the ability of soil to absorb moisture leading to 37 storm water runoff events greater than any measured previously at the lower Pueblo Canyon stream gage. Average flows for years 2000, 2001, and 2002 were 64, 145, and 67 cfs; median flows were 50, 25, and 15 cfs, and flows ranged from 11 to 1440 cfs.

To evaluate sediment and associated contaminant transport we deployed an automated sampler in Pueblo Canyon and sampled 8 of the 37 storm water runoff events since the

fire. Commercial analytical laboratories analyzed the samples for suspended sediment, total plutonium-239/240 concentrations in water, and plutonium-239/240 concentrations in sediment.

We estimated 87.1 mCi of plutonium-239/240 in 21,980 tons of sediment were transported beyond the E060 gage in lower Pueblo Canyon. In addition, the reach extending from the E060 gage to the Los Alamos Canyon confluence has contributed a large amount of contaminated sediments to off-site transport. This reach has been severely eroded since our 2002 P4 East study was completed and most active channel deposits have been mobilized and redistributed downstream.

We established 27 cross sections, a longitudinal profile, and mapped the stream pattern and bed features along a 3,000-foot section of P-4 West to categorize channel reaches and compare their features to post-1942 sediment deposits containing legacy contaminants. The changes in fluvial processes have modified the stream form and function. Areas of recent alternating channel degradation and aggradation, accelerated bank erosion, vertical and lateral channel migration, and recent fine grained flood deposits on terraces as well as coarse grained deposits within the active channel areas demonstrate the changing stream condition.

Our evaluations of the channel's physical variables indicate the stream is adjusting to the increased storm water discharges and sediment yields. The upper and lower stream sections in reach P-4 West, are classified as predominantly C type streams. According to Rosgen (1964), C type streams are very highly sensitive to stream flow and sediment increases, contribute high to very high sediment supplies, and have a high to very high stream bank erosion potential. In the mid section, the stream classification is predominantly an E type stream. According to Rosgen (1964), E type streams demonstrate a very high sensitivity to stream flow and sediment increases, a low to moderate sediment supply contribution, and very high stream bank erosion potential. Channel classification variances exist in areas within the mid section, indicating the stream is in transition. These changes indicate instability, increasing sensitivity to stream flow and sediment supply, and increasing erosion potentials. This is demonstrated by deepening channels that resulted in localized lowering of the alluvial water table. The existing riparian vegetation nourished by the alluvial water then becomes stranded, and the bank armor provided by the vegetation is diminished. This has led to accelerated bank erosion, and development of head cuts.

LANL analytical measurements of samples from geomorphic units in Pueblo Canyon indicate contamination exists from post-1942 operations. Reach P-4 has the largest estimated inventory of plutonium-239/240 in Pueblo Canyon, due to the largest volume of mid-1940's and mid-1960's sediments with relatively larger plutonium concentrations than other reaches. The LANL RRES-RS group estimated a plutonium-239/240 inventory of 158.5 mCi in P-4 West, of which 9% is stored in active c1 and c2 channel units and 91% stored in abandoned c4 through c6 units. The highest concentrations and inventories were found in c4 and c5 abandoned channel units, and in c6 over bank units. Other contaminants, such as mercury, other inorganic, and semi-volatile contaminants were

discharged and dispersed into Pueblo Canyon. For simplicity, only plutonium-239/240 was evaluated to relate contaminant inventory, dispersion, and transport.

The c4 through c6 units containing the highest percentage of plutonium-239/240 in P-4 West are exposed predominantly in its mid-section reach, between Cross Sections 4 and 19, where bank erosion potential is great especially during high flood stages. The older units comprising the banks appear to be moderately eroded, except at areas of accelerated erosion along the banks between Cross Sections 19 and 14, 10 and 11, and 5d and 5c. During periods of moderate to high flood stage, over bank flow occurs above Cross Section 20 and flows over a c6 unit until it reenters the main channel upstream from Cross Sections 11 and below 6b. The highest plutonium-239/240 measurement, 170 pCi/g, by the RRES-RS group was made in this unit.

Aggradation is occurring in the lower section below Cross Section 4. Deposition of coarse-grained materials on the active grass-armored floodplain as well as fine materials in the channel is changing the course and function of the channel in this area.

In the c1 and c2 units, accelerated channel erosion is occurring above Cross Section 4. Deepening of the channel is resulting in localized lowering of the alluvial water table, stranding existing riparian vegetation, and accelerating bank erosion. This is leading to widening of the channel and contributes a large sediment supply. Geomorphic units most affected are the lower active-channel features generally containing a smaller overall percentage of contaminants.

We found that normal channel adjustments: degradation, aggradation and subsequent sediment mixing have accelerated since the Cerro Grande fire. Destabilized channel banks are mostly limited to the pre-fire active channel and lower floodplain banks, where legacy waste contaminant inventories are the smallest. In some areas, floodwaters have flowed over terraces, causing erosion, sediment mixing, and net deposition on them. Where the floodwaters return to the main channel, bank erosion of older sediment units that contain larger plutonium concentrations and inventories is common. The channel and functional changes include erosion and transport of sediments contaminated with waste from Pueblo Canyon onto private and public lands. The changes are mostly limited to the pre-fire active channel where contaminant inventories are the smallest. Although in some areas, floods have flowed over terraces, depositing new sediments on them, and causing bank erosion of the older sediment units that contain larger plutonium concentrations and inventories.

Recommendations

We recommend that Los Alamos County develop and implement urban runoff controls in the Los Alamos town site to reduce the peak flows delivered to Pueblo Canyon and tributaries. Impervious surfaces in urban landscapes contribute large water volume very quickly to drainages below a city. We commend the Pajarito Plateau Watershed Partnership (of which Los Alamos County is a member) efforts to implement the group's watershed restoration strategy.

Stabilization measures should be implemented in Pueblo canyon.

- Vegetation should be established on stream banks. Miles of stream banks are without vegetation due to a combination of factors. Banks that are comprised of C3 – C6 units are often sandy, with a southern exposure, and have little or no grass cover. These should be seeded with xeric grasses, mulched with straw, and jute-matted to hold the straw in place until the grass germinates.
- Many sections of stream bank have been eroded producing vertical, steep, exposed faces, and should be treated in a similar fashion. In some cases, these vertical banks should be contoured to reduce the steepness of the banks prior to stabilizing with mulch, seed, and jute matting.
- Riparian woody vegetation should be established along the stream channel and banks to armor against high flows and stabilize eroding bare reaches.
- Grade controls should be strategically placed to prevent and control accelerated head cutting. In areas where head cutting has eroded the alluvial sediments to bedrock, grade control would be useful to reestablish the alluvial sediments and restore the lost alluvial water storage capacity. This newly available alluvial water would help to reestablish the riparian vegetation community.
- Wetland restoration: Shallow, multiple thread channels are reverting to single, deep and wide channels that are containing all but the highest flood flows. This channeled flow effectively bypasses the wetland and causes substantial erosion within the wetland itself. In some cases, the wetlands are contributing to the contaminant loading in Pueblo Canyon rather than mitigating the high sediment loads. Grade controls should be placed in wetland areas that are currently incising and widening to restore the wetland's ability to slow flow, trap sediments, and store alluvial waters.
- Los Alamos County should consider relocating their Bayo sewage treatment facility outfall upstream from their proposed new treatment plant. The wetland vegetation supported by the outfall for the lower two miles of the canyon have proven to be effective at reducing sediment transport. Concentrations of metals, radioisotopes (except plutonium), and suspended sediment have been reduced by two to four times through sedimentation once entering the wetlands. Moving the outfall upstream could potentially establish miles of new wetland areas and enhance the establishment of bank stabilizing woody vegetation, grasses, and forbs.

- Head cuts have formed in C3 – C6 bank forming sediments when overbank flood flows return to the main stream. These should be repaired to prevent further degradation and contaminant input to the system.
- Floodplains that are frequently inundated by overbank flows should be “roughened up” using straw wattles or logs to create a tortuous path for floodwaters enhancing sediment deposition.

Monitoring of stabilization measures and storm water quality must continue to verify the performance of the measures and document water quality improvements along the length of Pueblo Canyon. There are many measures of success to gauge the performance of the measures we are recommending. They range from counting successful woody vegetation starts to determining specific water quality parameter changes. The following are specific recommendations:

- Geomorphic investigations, such as those discussed in this report, should continue to determine channel morphology changes and to document the effectiveness of stabilization measures. This will require installing new cross sections at locations where measures have been implemented and the continued monitoring of a subset of the 40+ cross sections already in Pueblo Canyon. Cross sections placed across “roughened up” floodplains will be needed to measure net sediment deposition.
- Head cut repairs, grade stabilization measures, and wetland restoration grade controls should be monitored to assure effectiveness and that new erosion does not occur at those locations.
- Woody riparian vegetation starts and square feet of successful grass establishment will have be tallied and tracked.
- Storm water monitoring conducted for this report used primarily two sampling locations, upstream from Acid Canyon at LANL E055 and at the LANL E060 gages. While this provided insight into the water quality changes that occurred over a five-mile reach, the changes in contaminant flux occurring at various points in the system are not well understood. For example, in 2002, LANL RRES-RS sampled at multiple locations in Pueblo Canyon and found distinct changes in contaminant flux depending upon where in the canyon the samples were collected. We recommend that a minimum of two additional stations be located in the canyon to monitor changes in contaminant inventory and any improvements due to stabilization measures.
- Multiple samples should be collected during each flow event to show changes in contaminant concentrations due to changing flow regime throughout the hydrograph.
- While some samples should be analyzed to demonstrate compliance with water quality standards, the bulk of the analyses should be focused on understanding the changing concentrations of suspended sediment and bed load sediment, plutonium in water, plutonium in suspended sediments, and plutonium in bed load sediments.

References

Andrews, E.D., 1980, Effective and Bankfull Discharges of Streams In the Yampa River Basin, Colorado and Wyoming. *Journal of Hydrology* 46, p 311-330, in Rosgen (1996)

ASTM, 1999, D 3977-97, Standard Test Method for Determining Sediment Concentration in Water Samples, *Annual Book of Standards, Water and Environmental Technology*, 1999, Volume 11.02, p 389-394

BAER, 2000, Cerro Grande Fire, Burned Area Emergency Rehabilitation (BAER) Plan; report by Interagency Burned Area Emergency Rehabilitation Team.

Dunne, T. and L.B. Leopold, 1978, *Water in Environmental Planning*. W.H. Freeman and Co. San Francisco, CA. 818 pp. In Rosgen (1996)

Ford-Schmid, R., D. Englert, 2003, Post Cerro Grande Fire Stream Channel Morphology In Lower Pueblo Canyon, Reach P-4 East, New Mexico Environment Department, Department of Energy Oversight Bureau, September 2003

Graff, W.L., 1993, Geomorphology of Plutonium in the Northern Rio Grande, Department of Geography, Arizona State University, Tempe, Arizona 85287-0104, for Environmental Surveillance Group, Los Alamos National Laboratory, LA-UR-93-1963, March 1993

Harrelson, C.C., C.L. Rawlins, J. P. Potyondy, 1994, Stream Channel Reference Sites: an Illustrated Guide to Field Technique. General Technical Report RM-245, Fort Collins, CO; U.S. Department of Agriculture, Forest Service, Rocky Mountain National Forest and Range Experiment Station. 61 p.

Knight, K., T. Moody., W. Odem., M. Wirtanen M., 1999. Stream Channel Morphology in New Mexico: Regional Relationships. Northern Arizona University, College of Engineering and Technology, Department of Civil and Environmental Engineering, Water Resources Engineering Laboratory, December 1999

Koch, R.J., D.A. Shaull, B.M. Gallaher, 2003, Storm Runoff at Los Alamos National Laboratory in 2002. Los Alamos National Laboratory report LA-14080, September 2003

Koch, R.J., D.A. Shaull, B.M. Gallaher, M.R. Alexander, 2001, Precipitation Events and Storm Water Runoff Events at Los Alamos National Laboratory after the Cerro Grande Fire, Los Alamos National Laboratory report LA-13849-MS, July 2001

LANL Environmental Surveillance Program, 1993, Environmental Surveillance at Los Alamos during 1991. Los Alamos National Laboratory report LA-12572-ENV, August 1993

LANL Environmental Surveillance Program, 1994, Environmental Surveillance at Los Alamos during 1992. Los Alamos National Laboratory report LA-12764-ENV, July 1994

LANL Environmental Surveillance Program, 1995, Environmental Surveillance at Los Alamos during 1993. Los Alamos National Laboratory report LA-12973-ENV, October 1995

LANL Environmental Surveillance Program, 1996, Environmental Surveillance at Los Alamos during 1994. Los Alamos National Laboratory report LA-13047-ENV, July 1996

LANL Environmental Surveillance Program, 1996, Environmental Surveillance at Los Alamos during 1995. Los Alamos National Laboratory report LA-13210-ENV, October 1996

LANL Environmental Surveillance Program, 1997, Environmental Surveillance at Los Alamos during 1996. Los Alamos National Laboratory report LA-13343-ENV, September 1997

LANL Environmental Surveillance Program, 1998, Environmental Surveillance at Los Alamos during 1997. Los Alamos National Laboratory report LA-13487-ENV, September 1998

LANL Environmental Surveillance Program, 1999, Environmental Surveillance at Los Alamos during 1998. Los Alamos National Laboratory report LA-13633-ENV, September 1999

LANL Environmental Surveillance Program, 2000, Environmental Surveillance at Los Alamos during 1999. Los Alamos National Laboratory report LA-13775-ENV, December 2000

LANL Environmental Surveillance Program, 2001, Environmental Surveillance at Los Alamos during 2000. Los Alamos National Laboratory report LA-13861-ENV, October 2001

LANL Environmental Surveillance Program, 2002, Environmental Surveillance at Los Alamos during 2001. Los Alamos National Laboratory report LA-13979-ENV, September 2002

Leopold, L.B., M.G. Wolman and J.P. Miller, 1964, Fluvial Processes In Geomorphology. Freeman, San Francisco, CA. 522 pp, in Rosgen (1964)

Moody, T., M. Wirtanen, and S.N. Yard, 2003, Regional Relationships for Bankfull Stage in Natural Channels of the Arid Southwest, Natural Channel Design, Inc., Flagstaff AZ, March 2003

Rosgen, D.L., 1994. A Classification of Natural Rivers. CATENA, Journal of the International Society of Soil Science. Vol. 22, No. 3, pp 169-199, Elsevier Science B.V., June 1994

Rosgen, D.L., 1996. Applied River Morphology. Wildland Hydrology, Pagosa Springs, Colorado.

Reneau, S.L., E.V. McDonald, 1996, Landscape History and Processes On the Pajarito Plateau, Northern New Mexico: Rocky Mountain Cell, Friends of the Pleistocene, Field Trip Guidebook, Los Alamos National Laboratory report LA-UR-03-1654, March 2003

Reneau, S., R. Rytty, M. Tardiff, J. Linn, 1998. Evaluation of Sediment Contamination in Pueblo Canyon; Reaches P-1, P-2, P-3, and P-4. Environmental Restoration Project, Canyons Focus Area, Los Alamos National Laboratory report LA-UR-98-3324, September 1998

Rytty, R.T., P.A. Longmire, D.E. Broxton, S.L. Reneau, and E.V. McDonald, 1998, Inorganic and Radionuclide Background Data for Soils, Canyon Sediments, and Bandelier Tuff at Los Alamos National Laboratory, "Los Alamos National Laboratory document LA-UR-98-4847, September 1998

Shaull, D.A., M.R. Alexander, R.P. Reynolds, R.P. Romero, E.T. Riebsomer, C.T. McLean, 2001, Surface Water Data at Los Alamos National Laboratory: 2000 Water Year, Los Alamos National Laboratory report LA-13814-PR, June 2001

Shaull, D.A., D. Ortiz, M.R. Alexander, R.P. Romero, E.T. Riebsomer, 2001, Surface Water Data at Los Alamos National Laboratory: 2001 Water Year, Los Alamos National Laboratory report LA-13905-PR, April 2002

Shaull, D.A., D. Ortiz, M.R. Alexander, R.P. Romero, 2003, Surface Water Data at Los Alamos National Laboratory: 2002 Water Year, Los Alamos National Laboratory report LA-14019-PR, March 2003

Shelton, L.R., 1994, Field Guide for Collecting and Processing Stream-Water Samples for the National Water-Quality Assessment Program: U.S. Geological Survey Open-File Report 94-455, 1994

Wolman, M.G. and J.P. Miller, 1960, Magnitude and Frequency of Forces in Geomorphic Processes. Journal of Geology 68, p 54-74, in Rosgen (1996)

Veenhuis, J.E., 2002, Effects of Wildfire on the Hydrology of Capulin and Rito De Los Frijoles Canyons, Bandelier National Monument, New Mexico, U.S. Department of the Interior, U.S. Geologic Survey, Water-Resources Report 02-4152, prepared in cooperation with the National Park Service, 2002

Appendix A. Historical Perspective

After the Cerro Grande fire, we expected increased runoff from watersheds impacted during the fire. We expanded our storm water monitoring efforts to monitor potential changes in hydrology, suspended sediment yield, and contaminant transport rates from the Pajarito plateau. The contaminants we were concerned with included fallout materials concentrated in the burned forest biomass and LANL legacy wastes distributed in areas around the Laboratory. During a three year period, we observed elevated plutonium 239/240 concentrations in Pueblo Canyon storm water and began to focus our storm water monitoring there. Concentrations of strontium-90 and cesium-137 associated with forest fire ash diminished each year as the ash was flushed from the mountain slopes.

We compared our measurements to a number of reference values in order to understand changes in the environment. The LANL regional background level for plutonium-239/240 in northern New Mexico soils is 0.02 pCi/g (mean plus 2 standard deviations), and the background level in river sediments is 0.01 pCi/g (mean plus 2 standard deviations). These reference levels and the methodology used to develop them are described in LANL Environmental Surveillance reports. Their references were derived from soil or sediment samples measured over a period of years from samples collected well beyond the potential influence of the Laboratory, and include a mean of those values plus a measurement of variability. Those numbers reflect an upper tolerance level at the 95% confidence level, the mean plus 2 standard deviations. They reflect the most probable largest value that might be measured in areas beyond potential impact by the Laboratory. During 1999 we began a soil background study in the Jemez mountains and established a similar reference level of 0.04 pCi/g for plutonium 239/240 in soils.

LANL ER established additional reference values for soils and sediments at the Laboratory (Ryti, 1998). They used environmental samples from ES regional stations, as well as LANL perimeter and on-site locations collected from 1992 through 1995. The statistical treatment used to establish the upper 95% confidence tolerance level was also slightly different. We included these reference values in Table A-1.

After the fire, we collected ash that represented materials burned during the fire, including overstory and understory components of the forest. The upper tolerance level, or value that we developed to reflect probable largest values of plutonium 239/240 in ash was 0.6 pCi/g. We also studied plutonium 239/240 measurements in ash laden sediments in stream channels and on channel banks. The sediments were collected from the upper burned watershed areas downstream to the banks of the Rio Grande. Those measurements indicated the plutonium concentrations were diminishing with time and distance from the areas impacted during the fire. The plutonium in ash became diluted as the ash mixes with clean soils and sediments.

Twenty two ash and ash laden sediment samples collected soon after the Cerro Grande fire from the burned forest floor area and in drainages near the burned forest were used to develop the 0.6 pCi/g ash reference. This group did not include 15 ash laden bank

deposits near or along the Rio Grande. The bank samples near the Rio Grande demonstrated significant dilution and the average value, 0.06 pCi/g, was near our 0.04 pCi/g background level.

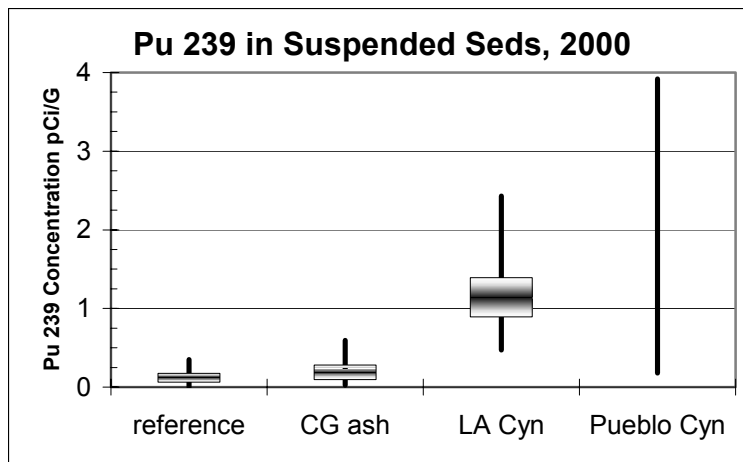
During the first storm water season after the Cerro Grande fire, we established a storm water monitoring program to study contaminant transport associated with ash. Storm water samples were collected based on opportunity and included 30 samples from several of the canyons impacted by the fire. We observed plutonium 239/240 measurements in Los Alamos and Pueblo canyons substantially greater than the 0.6 pCi/g reference value we established for the Cerro Grande ash. Over the following 2 years, we began to focus our monitoring in these areas, particularly Pueblo Canyon. These reference values and measurements made for plutonium in storm water suspended sediments are summarized in Table A-1.

Table A-1. Plutonium-239/240 reference values and concentrations measured in storm water suspended sediments

Reference Values		pCi/g
LANL Regional Background Soils (ES)	UTL ^a mean + 2sd	0.02
LANL Perimeter Soils Reference (ER)	Linear interpolation	0.054
LANL On-site Sediments Reference (ER)	Linear interpolation	0.068
NMED Jemez Mountain Soils	UTL ^a mean + 2sd	0.04
Cerro Grande Ash	UTL ^a mean + 2sd	0.6
Plutonium 239/240 in Suspended Sediments		
2000 – 2002 Pajarito Plateau Storm water (w/o Pueblo, LA.)	Mean	0.1
2000 – 2002 Pueblo Canyon Storm Water	Mean	3.4

^a Upper Tolerance Level = the sample population mean plus 2 times its standard deviation

The following charts represent the values we observed from 2000 to 2002. Figure A-1 demonstrates the plutonium 239/240 differences in Cerro Grande ash and storm water suspended sediments from 3 canyon groups during 2000. They include reference



canyons dissecting the Pajarito Plateau, mid Los Alamos Canyon, and lower Pueblo Canyon. It reflects much larger plutonium concentrations in Los Alamos and Pueblo Canyons.

The reference values shown in the chart represent plutonium 239/240 in suspended sediments from 28 storm water samples collected in drainages

Figure A-1. 2000 Plutonium-239/240 in ash from the Cerro Grande fire, and in storm water suspended sediment from reference canyons. Los Alamos Canyon, and Pueblo Canyon

below the burned forest area other than mid Los Alamos and lower Pueblo Canyons. The minimum, 25th percentile, 75th percentile, and maximum values for these reference canyons are 0.001, 0.06, 0.18, and 0.4 pCi/g respectively. They include 5 samples in Pueblo and Acid Canyons above areas impacted by post-1943 TA-45 discharges, 3 in upper Los Alamos Canyon above the DP Canyon confluence, and 20 in other canyons in the Pajarito Plateau. The samples we collected in the other Pajarito Plateau canyons include 1 in Guaje, 6 in Pajarito, 5 in Water, 3 in Canon del Buey, and 5 storm water samples in the Rio Grande.

The second group in the chart reflects the values from 22 Cerro Grande ash and ash laden sediments in or near the burned forest area. They reflect the ash contribution of plutonium we expected in the solid phase of the storm water samples. The minimum, 25th and 75th percentiles, and maximum values are 0.03, 0.09, 0.28, and 0.60 pCi/g respectively. These values were retained in the following 2 charts for reference.

Six samples in mid Los Alamos Canyon demonstrate potential transport of legacy materials. The samples were collected at the LANL E050 storm water gage station below the retention structure at State Road 4, along the eastern boundary of the Laboratory. Those values ranged from 0.47 to 2.43 pCi/g.

Only two samples were collected in Pueblo canyon. They were collected in lower Pueblo Canyon just above the Bayo Wastewater Treatment Plant and were measured at 0.18 and 3.92 pCi/g. Two storm water samples were also collected in the South Fork of Acid Canyon with concentrations of 107 and 38.1 pCi/g, but are not represented on the chart.

From these data comparisons and increased magnitude and frequency of storm water runoff, we recognized that legacy contaminants from Acid Canyon, Pueblo Canyon, and Los Alamos Canyon were potentially being moved at greater rates than before the fire. We began to focus storm water monitoring in Pueblo and Los Alamos Canyons.

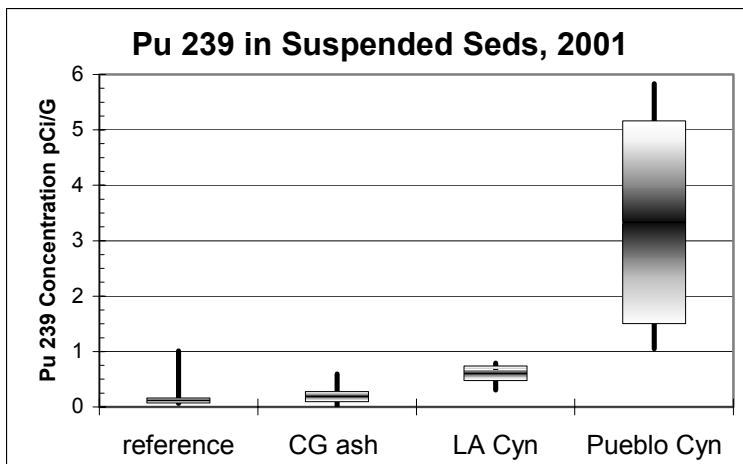


Figure A-2. 2001 Plutonium-239/240 in ash from the Cerro Grande fire, and in storm water suspended sediment from reference

Figure A-2 represents samples we collected in 2001. It also corroborates our observations made in 2000 that legacy plutonium transport rates in Pueblo Canyon were increasing. During 2001, we collected 8 samples to reflect reference storm water conditions. They were collected in drainages below the burned forest areas and include 3 samples in Pajarito Canyon and 5 in Water Canyon.

The minimum, 25th percentile, 75th percentile, and maximum values of plutonium-239/240 in suspended sediments are 0.06, 0.07, 0.16, and 1.01 pCi/g respectively.

The Cerro Grande ash reference is from the same samples described for 2000. They are the ash and ash-laden samples collected shortly after the fire from the forest floor and stream channels in close proximity to the burned watershed.

Four samples were collected from Los Alamos Canyon 5 miles upstream of the Pueblo confluence. The minimum, 25th percentile, 75th percentile, and maximum values are 0.31, 0.47, 0.74, and 0.79 pCi/g respectively. Most of the measurements are greater than the 0.6 pCi/g upper tolerance value used to describe plutonium in the Cerro Grande ash. These samples demonstrate potential transport of legacy contaminants, but at a smaller degree than in Pueblo Canyon.

Five samples were collected in lower Pueblo Canyon at storm water gage E060. The minimum, 25th percentile, 75th percentile, and maximum values are 1.05, 1.50, 5.16, and 5.83 pCi/g respectively. These values are up to 10 times greater than the Cerro Grande ash reference and reflect legacy contaminants.

Our evaluation indicated both Los Alamos and Pueblo Canyons were contributing legacy plutonium to offsite transport. Pueblo Canyon was contributing more sediment at higher plutonium concentrations than Los Alamos Canyon. We also observed a greater frequency of floods at greater flow rates at the lower Pueblo Canyon gage station, E060. We saw total plutonium-239/240 concentrations in water as high as 253 pCi/L. Storm water retention structures and lower plutonium concentrations in Los Alamos Canyon suspended sediments, as well as the lack of storm water controls and apparent greater runoff potential in Pueblo Canyon led us to focus additional monitoring efforts in Pueblo Canyon to more fully characterize the storm events.

Figure A-3 represents samples collected during 2002, and continue to corroborate our findings from previous years that plutonium transport from Pueblo Canyon has increased.

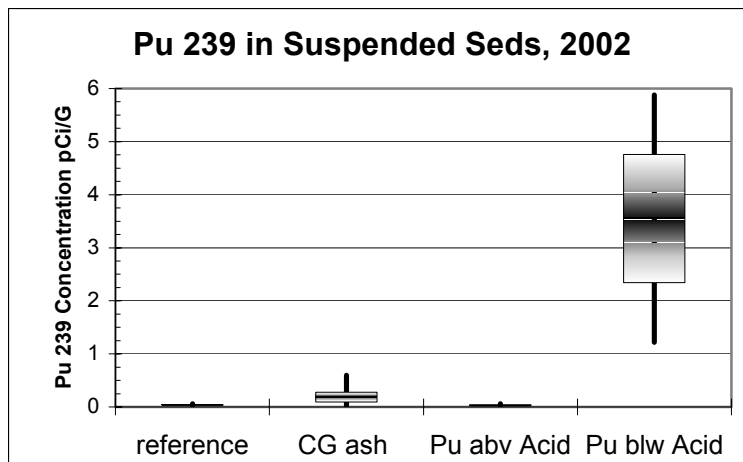


Figure A-3. 2002 Plutonium-239/240 concentrations in Cerro Grande ash, reference canyons, and Pueblo Canyon

An evaluation of plutonium concentrations in reference canyons and samples collected above Acid Canyon suggests that increases seen in storm water from ash had diminished.

The same Cerro Grande ash samples were used for reference. Ash did not appear to have a long-term affect on contaminant

transport from the Pajarito Plateau. Evaluations of other constituents, strontium-90, cesium-137 suggested the same.

A total of five reference samples were taken from Guaje, Canon del Buey, and Pajarito Canyons. The minimum, 25th percentile, 75th percentile, and maximum values are 0.01, 0.03, 0.04, and 0.06 pCi/g respectively. Twelve samples in Pueblo Canyon above Acid canyon also demonstrate reference conditions. The minimum, 25th percentile, 75th percentile, and maximum values are 0.02, 0.02, 0.04, and 0.06 pCi/g respectively.

Most of twenty samples that reflect plutonium transport from Pueblo Canyon were collected in the lower reaches of the canyon at E060. The minimum, 25th, 75th percentiles, and maximum concentrations from Pueblo Canyon storm water samples are 1.22, 2.34, 4.76, and 5.88 pCi/g respectively. An additional 2 samples in Acid Canyon, not represented in the chart, were measured at 9.1 and 22.3 pCi/g.

The plutonium concentrations measured in Pueblo Canyon storm water suspended sediments did not diminish during the three years described in this report. This observation also suggests an alternative source of plutonium in storm water rather than from the Cerro Grande ash.

Our evaluation of cesium-137 measurements in ash and storm water suspended sediments demonstrated similar conditions. Cesium-137, like plutonium-239/240, concentrates in ash after fire reduces the biomass of an organism. As time and distance increases from the source, in this case the burned forest areas, the ash mixes with clean soils and sediments, diluting the original concentrations. Figure A-4 shows cesium-137 concentrations diminish each year after the Cerro Grande fire until it approximates the LANL regional reference background level for soils at 0.51 pCi/g. The measurements in the Cerro Grande ash were more variable than seen in the Viveash ash. A storm event

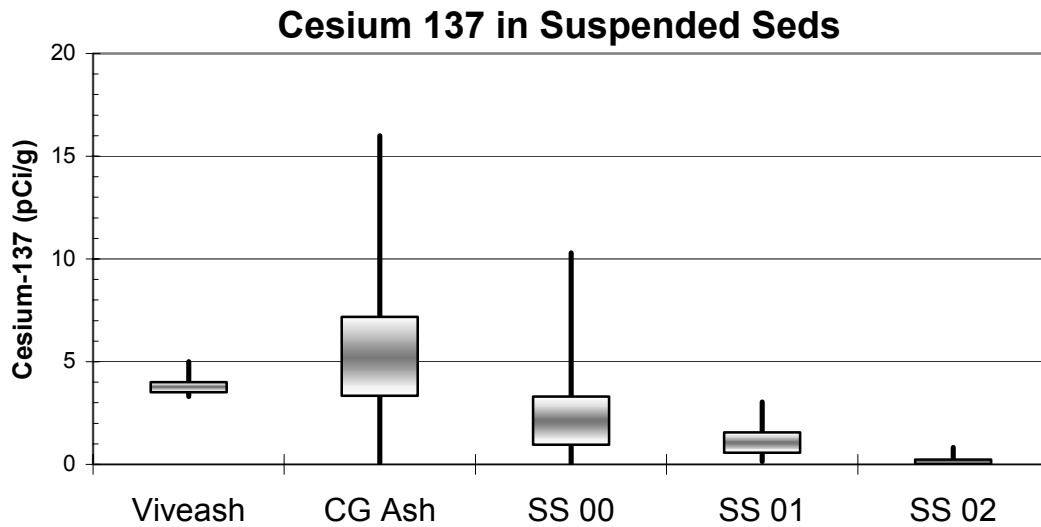


Figure A-4. Cesium-137 concentrations in Viveash and Cerro Grand ash, and in storm water suspended sediment samples collected in 2000, 2001, and 2002

occurred before the Viveash samples were collected, and mixing with the underlying soil may have modified the variation as seen in the Cerro Grande ash.

Five samples were collected from ash in the Viveash area, 45 miles east of the Cerro Grande fire. Twenty-eight ash and ash laden samples were collected and analyzed for cesium-137 in the Cerro Grande area. Twenty-eight samples were also collected from storm water runoff during 2000. In 2001 and 2002, 17 and 15 samples were collected from runoff, respectively. The cesium-137 concentrations in the Viveash, and Cerro Grande ash, and in the 2000, 2001, and 2002 storm water runoff ranged from 3.3 to 5 pCi/g, 0.06 to 16 pCi/g, 0.0 to 10.3 pCi/g, 0.14 to 3.04 pCi/g, and -0.34 to 0.82 pCi/g respectively. These values diminish at an approximate 50% rate from each preceding year. A Mortandad Canyon suspended sediment sample from 2000 was measured at 234 pCi/g and is not represented in this chart.

Figure A-5 demonstrates similar characteristics for strontium-90 concentrations in ash and suspended sediments, although strontium-90 concentrations reached background reference levels, 0.71 pCi/g, by 2001. The Viveash samples also were measured at levels near background. Strontium-90 is more soluble than plutonium-239/240 and cesium-137 and may have been removed more efficiently by the storm water runoff.

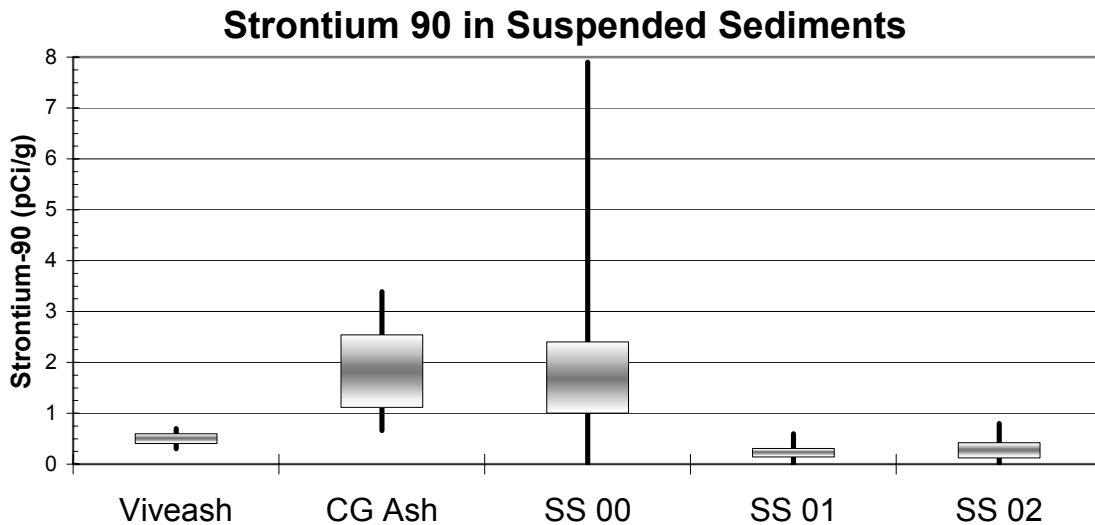


Figure A-5. Strontium-90 measurements in ash collected from the 2000 Viveash and Cerro Grande fires, and in suspended sediments collected from storm water in 200, 2001, and 2002

These measurements were made on the same samples described above for cesium-137. Five samples were collected from ash in the Viveash area, 28 ash and ash laden samples were in the Cerro Grande area. Twenty-eight samples were collected from storm water runoff during 2000, 17 samples in 2001, and 15 in 2002. The strontium-90 concentrations in the Viveash, and Cerro Grande ash, and in the 2000, 2001, and 2002 storm water runoff ranged from 0.3 to 0.7 pCi/g, 0.66 to 3.39 pCi/g, 0.0 to 7.9 pCi/g, -0.11 to 0.6 pCi/g, and 0.0 to 0.8 pCi/g respectively.

The legacy contaminants described in this report refers to the discharges from LANL during the first 20 years of operations there. LANL discharged untreated and treated radioactive industrial wastewater into Acid Canyon from 1943 to 1963. Early release estimates indicated 180 mCi of plutonium were discharged into the canyon (Stoker et al., 1981). Later inventory estimates of plutonium in Pueblo Canyon sediments indicated a larger release. In 1985, LANL estimated that 300 to 900 mCi of plutonium 239/240 existed in Pueblo Canyon, and up to 3 curies of plutonium could have been released into the canyon (J. L. Lane, 1985). By 2003 LANL estimated up to 1.3 curies existed in Pueblo Canyon from the Acid / Pueblo Canyon confluence downstream to the Pueblo/Los Alamos confluence (Reneau, 2003). Younger sediment deposits have replaced much of the older post-1943 more contaminated units. These younger units are comprised of cleaner background sediments mixed with those deposited during the main discharges from the Laboratory.

In 1993, William Graff estimated 188 mCi of plutonium was transported from Los Alamos Canyon into the Rio Grande by storm water runoff from 1944 to 1986. Graff suggested the contribution to the plutonium budget from Los Alamos is associated with relatively coarse sediment, which often behaves as bed load in the Rio Grande. Infusions of these materials into the main stream were largest in 1951, 1952, 1957, and 1968. Although the Los Alamos contribution to the entire plutonium budget was relatively small, in these four critical years it constituted 71-86 percent of the plutonium in bed load immediately downstream from Otowi (Graff, 1993).

Graff developed his estimates from previous researcher's calculations for the probable sediment yield from the canyon into the Rio Grande. They used data from an intermittent storm water gage record for the (Los Alamos) stream and precipitation records at nearby locations (Graff, 1983). His evaluation was for plutonium contribution to the Rio Grande at the confluence with Los Alamos Canyon. Pueblo Canyon is a tributary to Los Alamos Canyon 5 miles upstream from there and provides the majority of contaminants. Although other sources, including plutonium liquid waste discharges into DP Canyon from the plutonium processing facility at TA-21, exist in Los Alamos Canyon above the Pueblo confluence. Analytical methods may also have been different than those we used to evaluate suspended sediments in storm water.

A table summary of Graff's findings is provided below in Table A-2. We included additional information derived from the data in Graff's table. The average concentration of plutonium-239/240 was derived from plutonium mass transported per year measured in mCi, and the sediment yield per year measured in tons. The average suspended sediment concentration was derived from the water volume flow for each year measured in acre feet and the sediment yield per year measured in tons. We found these measurements similar to those measured in Pueblo Canyon storm water during 2000 to 2002.

Table A-2. Estimates of plutonium-239/240 and sediment transport into the Rio Grande at lower Los Alamos Canyon (Graff, 1983)

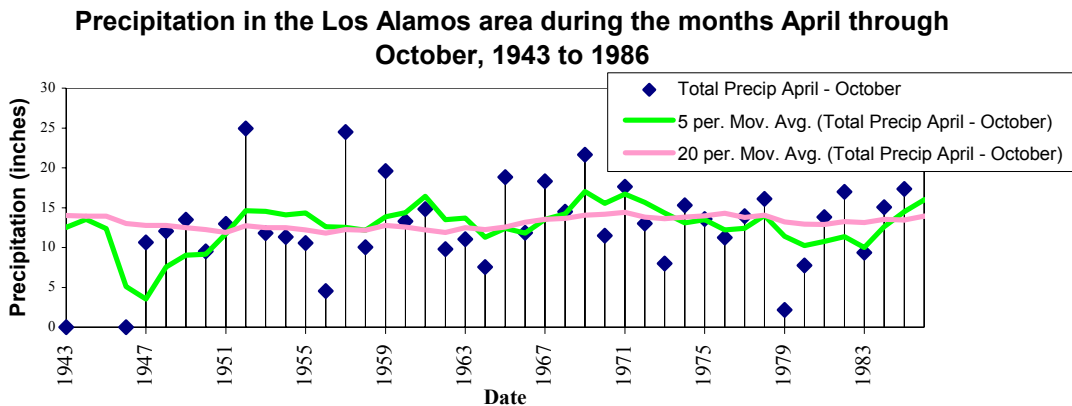
From W. L. Graff, (1993) Geomorphology of Plutonium in the Northern Rio Grande

Water, Sediment, and Plutonium Data for Los Alamos Canyon						Additional Calc from table	
Year	Water (ac ft)	Flood (cfs)	Sediment (tons)	Pu Sum (mCi)	Pu (Yr) (mCi)	Pu ave conc. in SS pCi/g	ave SSC mg / l
1943	22	66	466		0		15578
1944	198	631	8393	3	2.798	0.37	31175
1945	0	0	61	3	0.03	0.54	0
1946	28	80	611	3	0.32	0.58	16049
1947	1	2	65	3	0.05	0.85	47805
1948	0	0	61	3	0.04	0.72	0
1949	0	0	61	3	0.05	0.90	0
1950	6	20	77	3	0.06	0.86	9438
1951	236	687	9814	20	16.9	1.90	30584
1952	209	386	6316	38	17.61	3.07	22226
1953	2	4	12	38	0.03	2.76	4413
1954	40	129	1006	41	2.86	3.13	18497
1955	91	283	2783	50	8.83	3.50	22492
1956	0	0	0	50	0		0
1957	433	649	16470	94	43.95	2.94	27975
1958	63	203	2002	101	7.36	4.05	23371
1959	33	59	532	103	1.74	3.61	11857
1960	0	0	154	103	0.75	5.37	0
1961	18	53	443	106	2.4	5.97	18101
1962	0	1	138	107	0.88	7.03	0
1963	88	283	2772	117	10.07	4.00	23167
1964	0	0	0	117	0		0
1965	124	233	3163	127	9.88	3.44	18760
1966	10	32	165	127	0.53	3.54	12135
1967	129	351	4197	137	10.24	2.69	23928
1968	287	924	14120	159	21.82	1.70	36184
1969	124	149	2899	164	4.96	1.89	17194
1970	0	0	0	164	0	0.00	0
1971	16	42	247	165	0.42	1.87	11354
1972	0	0	0	165	0		0
1973	109	349	3955	173	8.2099	2.29	26686
1974	6	20	129	173	0.3301	2.82	15812
1975	4	6	99	173	0.3	3.34	18203
1976	6	20	77	174	0.23	3.29	9438
1977	1	4	8	174	0.0299	4.12	5884
1978	108	293	3198	180	6.0101	2.07	21778
1979	10	312	426	181	1.4899	3.86	31331
1980	0	0	183	182	0.8001	4.82	0
1981	0		0	182	0		
1982	0		0	182	0		
1983	43		24357	185	2.78	0.13	416597
1984	0		0	185	0	0.00	
1985	43		41461	187	2.08	0.06	709140
1986	3		2460	188	1.59	0.71	603079

Note: 1943-1980 data from calculation by J. L. Lane in support of Lane, Purtyman, and Becker (1985); 1981- 1986 data from Purtyman et. Al. (1990) using different techniques. The comparability of the two data sets is unknown.

Graff showed plutonium transport from Los Alamos Canyon into the Rio Grande as great as 44 mCi in 1957. Based on this table, 86% of the plutonium transport inventory during 1943 to 1986 occurred during the 50's and 60's. While approximately 15% was transported during the remaining periods of his study, the 40's, 70's and 80's. The 4 greatest mass transport rates occurred in 1957, 1968, 1952, and 1951, where 44, 22, 18, and 17 mCi of plutonium transport occurred respectively. Water volume that passed through lower Los Alamos during those years was 433, 287, 209 and 236 acre feet, associated with single maximum runoff rates of 649, 924, 386, and 687 cfs. These transport inventory, annual water volume, and single largest annual flow rate associations are demonstrated Figures A-6, A-7, and A-8.

We observed similarities in the measurements presented by Graff, values derived from those measurements, and our measurements from lower Pueblo Canyon. Plutonium in sediment values that we derived from his data ranged from 7.03 pCi/g to 0 pCi/g. The average plutonium concentration in sediments sampled from 1950 to 1981, is 3.4 pCi/g. The average sediment concentration in storm water for this period was calculated as 15,045 mg/L. The pre-1950 and post-1981 values reflected very low values and may suggest contaminant dispersion had not reached lower Los Alamos Canyon or storm flow rates were greatly diminished during these periods. Our average plutonium concentration in sediments and suspended sediment concentration, calculated from the total mass transport inventory of plutonium and suspended sediments estimated in this report, was 4.5 pCi/g plutonium in 13,133 mg/L sediments.



Data source: Bowen, 1990 and LANL Meteorological Monitoring Program

Figure A-6. Annual precipitation in Los Alamos area from 1943 to 1986

Figure A-6 demonstrates precipitation amounts for the years 1943 to 1986 during the months April through October. It also shows the long term 20 year average at 1986 to be 13.8 inches. The total long term average, including precipitation during November through March, was 18.6 inches. Precipitation during the 4 years of greatest plutonium transport inventory was 24 inches during 1957, 15 inches in 1968, 25 inches in 1952, and 13 inches in 1951. Northern New Mexico was demonstrating drought conditions during the 1950's and is often the case, rain fall that did occur, originated during infrequent but intense rainstorms.

New Mexico is currently experiencing a drought. During 2000, 2001, and 2002, the average annual precipitation between two rain gages in the upper Pueblo Canyon watershed was 13, 8, and 12 inches respectively. A similar relationship between lower Los Alamos Canyon during the years of highest inventory transport and currently in Pueblo Canyon is occurring. The ratio of total annual flow and precipitation in Pueblo Canyon doubled after the Cerro Grande fire, from 15 to 36. In lower Los Alamos Canyon the ratio between flow and precipitation was small, less than 1, during times of little transport. During the periods of greatest transport, the ratio increases ranged from 5 to as much as 15.

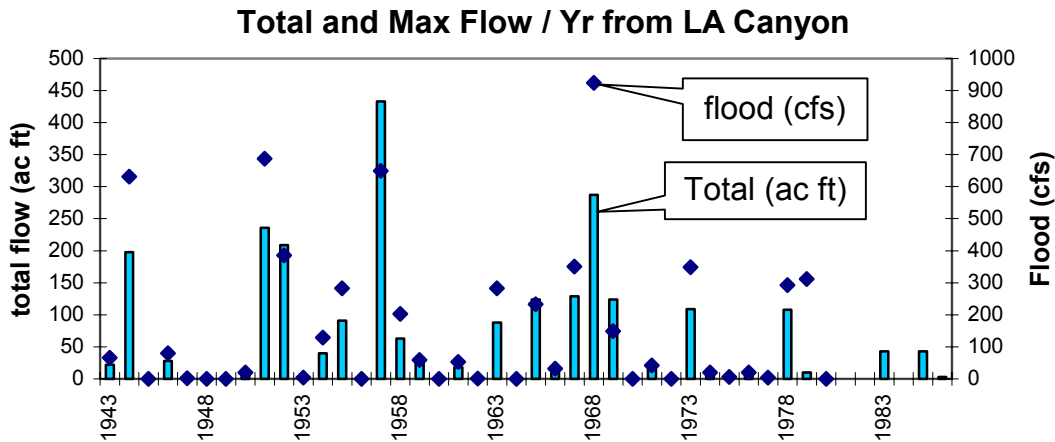


Figure A-7. Total annual flow in acre feet and the maximum flow for the single greatest runoff event per year in cfs.

In Figure A-7 the vertical bars demonstrate these relatively large flow volumes. For example in 1951, 1952, 1957, and 1968, relatively large flows occurred, 236, 209, 433, and 287 acre feet respectively. The flow volume to precipitation ratios described above, were 15, 7, 15, and 15 respectively. Flood flow rates were greatest in each of the years with greatest inventory transport. During 1951, 1952, 1957, and 1968, the annual single greatest flow rates were 687, 386, 649, and 924 cfs. In 1944 a large flow of 631 cfs occurred, although the plutonium transport rate was relatively small. This was probably due to plutonium not being thoroughly distributed in the canyon systems. It appears flows through lower Los Alamos canyon were nonexistent to infrequent after 1969.

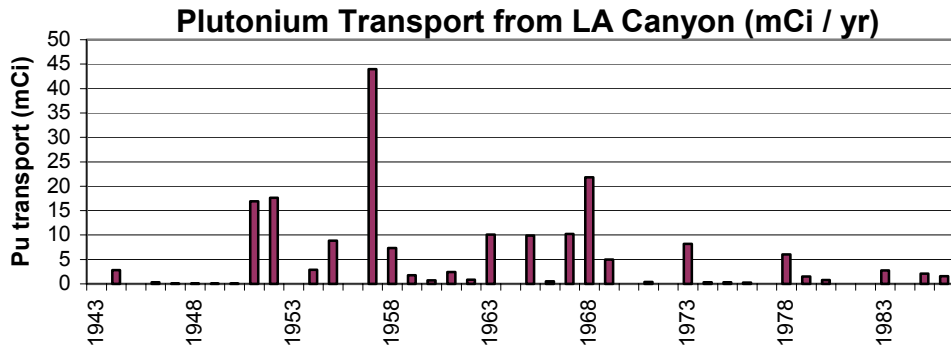


Figure A-8. Plutonium annual mass transport rates estimated by Graff

Figure A-8 demonstrates the annual mass transport rates of plutonium estimated by Graff. It shows the relative relationships of mass transport between years. For example, the greatest mass transport rate, 44 mCi per year, occurred in 1957, followed by 22 mCi in 1968, 18 and 17 mCi in 1952 and 1951. Several years of 10 mCi per year transport rates occurred. These were all associated with large annual flow volumes or flood flow rates. Plutonium transport rates as large as these have not been seen since the 1950's and 1960's until after the Cerro Grande fire. Since the fire, we estimate 55 mCi, 24 mCi, and 8 mCi of plutonium-239/240 was moved beyond the E060 gage in lower Pueblo Canyon during 2001, 2002, and 2000 respectively.

Appendix B. Linear and Vertical Field Measurements For Cross Sections and Longitudinal Profile

Cross Sections are listed from upstream, cross section 20, to downstream, cross section 1. The cross section identification, date of survey, and the height of survey instrument (HI) are found in the header. Instrument height elevation is arbitrary, not associated with a benchmark.

Linear measurements are listed in the first column and are in feet. They are measured to the nearest tenth of a foot along 300-foot field measuring tapes stretched horizontally from the left cross section end point to the right end point. The measurements are made from the left to the right bank. Left and right are determined while facing downstream. Turn points are made on cross sections that are greater than 300 feet or when obtrusions existed in line of site of the survey instrument and stadia rod.

Vertical measurements are listed in the second column as foresights (FS). They are made with a laser-level survey instrument and electronic receptors, read from survey stadia rods to the nearest hundreds of a foot. The elevations are relative to the height of the survey instrument. The foresight measurements of bankfull stage and top of bank are field determinations (see discussion of bankfull determination in text). Top of banks are channel banks well above the bankfull stage and may be terrace or floodplain banks. Widths of floodplains (W fpa) are linear measurements between banks at elevations that are twice the bankfull depth. The stream channel slopes are determined from the longitudinal profile at cross section intercepts. They are made along a reach approximately 20 to 30 bankfull channel widths at riffle-to-riffle characteristics in the channel. The Manning's "n" was estimated from particle size ranges established in the P-4 East report, references, and discussions with stream modelers and others familiar with stream characteristics on the Pajarito Plateau.

The tables summarizing the stream dimensions and hydraulics were derived from the dimensions measured at each cross section. These dimensions are used to determine the classifications discussed in this report. The hydraulic parameters were not discussed, although provided for references.

The dimensions of key features within a stream valley, their relationships, and variables for characterizing stream channels are outlined below. The ability to characterize and evaluate changes in stream channels can be useful as Los Alamos National Laboratory and the Bureau continue to monitor the effects of the Cerro Grande fire on Pajarito Plateau watersheds. The equations and definitions we used to evaluate our field data are in a Microsoft Excel spreadsheet developed by Dan Mecklenburg (Copyright © 1999 River4m, Ltd). The program generates cross section and longitudinal profile figures. It also calculates the dimensional and hydraulic parameters listed throughout this report.

The method of characterizing stream channels consists of establishing permanent, benchmarked, measurements of stream dimensions (cross sections and profiles) that can

be used to document adjustments to changes in stream flow and sediment supply. These measurements and descriptions are particularly useful in determining changes in stream stability and provide quantifiable information for determining whether the channels are down cutting, filling in, or eroding new channels. These features include the following:

Stream Dimensions

Cross Section

- Bankfull Width (W_{bkf})
- Bankfull Mean Depth (d_{bkf})
- Bankfull Cross Section Area (A_{bkf})
- Width / Depth Ratio (W_{bkf} / d_{bkf})
- Maximum Bankfull Depth (d_{mbkf})
- Width of Flood prone Area (W_{fpa})
- Flood prone Height ($2 \times d_{mbkf}$)
- Entrenchment Ratio (W_{fpa} / W_{bkf})
- Thalweg - deepest part of channel

Longitudinal Profile

- Stream Length
- Valley Length
- Bankfull Height
- Waters Edge Height
- Thalweg Height
- Terrace Height
- Sinuosity (Stream Length / Valley Distance)
- Water Surface Slope (Vertical Distance, Ft. / Linear Distance, Ft)

Physical Locations, measured with a Trimble Explorer III GPS unit

- Cross Section End Points
- Thalweg
- Terrace and Floodplain Banks

Stream Channel Cross-Section Dimensions

Height of Instrument (HI) is the elevation of the survey level. It is found by adding the back sight rod reading to the elevation of a benchmark or turning point.

If the relative elevation is unknown, an arbitrary elevation can be entered. (i.e. 100 feet).

Distance (ft) of the cross section is the measurement across the stream, from the endpoints of the cross section.

By convention, distance is measured from left to right when facing down stream.

Foresight (FS) rod readings are vertical distances measured from the level to the ground.

Elevation is found by subtracting the foresight rod reading from the height of the instrument.

Foresight at Bankfull is the rod reading at the top of the channel banks, which may be a terrace and well above bankfull. Bankfull elevation can then be calculated from this measurement.

Foresight at Top of Bank is the rod reading at the top of the channel banks, which may be a terrace and well above bankfull. Top of Bank elevation can then be calculated from this measurement.

Width of the Flood Prone Area (W_{fpa}) is the flooded width at a stage twice the maximum depth for bankfull stage in a riffle or straight reach. This value is not valid in pool cross sections.

Channel Slope (S) is the “rise over run” for a reach approximately 20 to 30 bankfull channel widths in length with the “riffle to riffle” surface slope representing the gradient at bankfull stage. Slope is determined from longitudinal profile data.

Manning’s Roughness Coefficient value “n” is based on channel materials and stream hydraulic velocities.

Bankfull Cross-Section Area (A_{bkf}) is the area of the stream channel cross section at bankfull stage in riffle sections of the stream.

Bankfull Width (W_{bkf}) is the width of the stream channel at bankfull stage in riffle sections of a stream.

Maximum Bankfull Depth (d_{mbkf}) is the maximum depth of flow at bankfull stage.

Flood Prone Height ($2 \times d_{mbkf}$) is flood stage height measured at twice the maximum depth in a riffle or straight stream section.

Bank Height is the height of the lowest bank, measured from the channel bed (thalweg) to the top of the bank.

Bank Height helps describe entrenchment. Over-bank flow begins at this stage defined by bank height.

Width of the flood prone area (W_{fpa}) is the flooded width at flood prone height.

It is used to define entrenchment and forms the entrenchment ratio when divided by the bankfull width.

Bankfull Mean Depth (d_{bkf}) = $(A_{bkf}) / (W_{bkf})$
 (A_{bkf}) = cross section area (square feet)
 (W_{bkf}) = width at bankfull stage (feet)

This is the area of the stream channel cross section at bankfull stage in a riffle cross-section.

Wetted Perimeter (P) (feet) is the perimeter of the channel cross section formed by the bed and banks.

Hydraulic Radius (R) (feet) = $(A_{bkf}) / P$
 (A_{bkf}) = cross section area (ft²)
P = wetted perimeter (ft)

Width to depth ratio Width / Depth Ratio (W_{bkf} / d_{bkf}) is the channel width at bankfull stage divided by the mean depth.

Entrenchment Ratio (W_{fpa} / W_{bkf}) is the flood prone width divided by the bankfull width.

Hydraulic Calculation Equations

Velocity (V) (ft / sec) = $(1.487 \times R^{2/3} \times (S / 100)^{1/2}) / n$
n = Mannings “n” coefficient

Discharge (Q) (cfs) = V (A_{bkf})

Shear Stress (pounds / ft²) = 62.4 x R x S
62.4 = density of water (lbs / ft³)

Shear Velocity = $(32.2 \times R \times S)^{1/2}$
32.2 = gravitational acceleration (ft / sec²)

Unit Stream Velocity = power / unit area = $(62.4 \times Q \times S) / W_{bkf}$
Power = density of water x flow x slope

Froude number = $V^2 / 32.2 \times \text{Maximum Bankfull Depth} (d_{mbkf})$

This is a dimensionless number expressing the ratio of inertial to gravitational forces. Values less than 1 are termed sub critical and are characteristic of relatively deep, slow stream flow. Values of 2q denote “critical” flow. Values greater than 1 are termed supercritical and are characteristic of shallow fast streams.

Friction Factor = V / shear velocity
Values vary from about 2 for rough streambeds to 16 for smooth.

Threshold grain size (mm) is the size particles predicted to be at “the threshold of motion” at the shear stress calculated. It is found from Shield’s curve, which is a plot of particle size against the critical shear stress or the shear stress required to initiate movement.

Table B-1. Measurements at Cross Sections 20 and 19

Cross-section P4West, NVED20 Date 8/29/2002 height of instrument (ft): 14.00								Cross-section P4West, NVED19 Date 8/27/2002 height of instrument (ft): 13.00							
distance (ft)	FS (ft)	elevation	bankfull	FS top of bank	W/tpa (ft)	dmax slope (%)	Mannings 'n'	distance (ft)	FS (ft)	elevation	bankfull	FS top of bank	W/tpa (ft)	dmax slope (%)	Mannings 'n'
0	3.18	10.82	11.22	9.37	400.0	26	0.04	0	0	13	10.138	7.34	107.0	9.2	0.04
0	3.55	10.45	2.78	4.63				2	0.21	12.79	2.882	5.66			
4.2	5.11	8.89						6	2.69	10.31					
11.3	9.8	4.2	dimensions					12.7	7.12	5.88	dimensions				
18	9.92	4.08	120	x-section area	0.7	dmean	17.3	7.76	5.24	7.3	x-section area	0.6	dmean		
25.7	10.19	3.81	169	width	2.06	vet P	23.1	8.5	4.5	12.4	width	1.52	vet P		
30.7	10.67	3.33	24	dmax	0.6	hydrad	23.5	9.81	3.19	25	dmax	0.5	hydrad		
37	10.72	3.28	4.2	bankht	23.9	wdratio	30.2	10.22	2.78	5.3	bankht	21.1	wdratio		
43.5	10.77	3.23	400.0	W/lood prone area	23.7	ent ratio	31	10.3	2.7	107.0	W/lood prone area	8.7	ent ratio		
49.9	10.65	3.35	hydraulics					31.8	10.29	2.71	hydraulics				
58.4	10.63	3.37	4.2	velocity (ft/sec)			32.7	10.31	2.69	6.9	velocity (ft/sec)				
58.4	10.95	3.05	50.0	discharge rate, Q (cfs)			33.5	10.64	2.36	50.0	discharge rate, Q (cfs)				
62.7	10.82	3.18	0.94	shear stress (lb/ft ² sec)			34.6	10.75	2.25	2.74	shear stress (lb/ft ² sec)				
66.3	11.47	2.53	0.70	shear velocity (ft/sec)			34.9	11.93	1.07	1.19	shear velocity (ft/sec)				
67.4	11.95	2.05	4.795	unit stream power (lb/ft ² /sec)			35.4	12.64	0.36	23.232	unit stream power (lb/ft ² /sec)				
68.3	11.54	2.46	0.77	Froude number			36.5	10.91	2.09	2.51	Froude number				
68.9	12.08	1.92	6.0	friction factor ulf			37.7	10.71	2.29	5.8	friction factor ulf				
69.8	12.1	1.9	64.7	threshold grain size (mm)			38.7	11.19	1.81	518.6	threshold grain size (mm)				
71.5	11.18	2.82					39.8	10.39	2.61						
73.4	11.3	2.7	155.8	10.77	3.23		40.7	10.05	2.95	121	8.94	4.06			
74.4	11.24	2.76	156.2	11.35	2.65		41.6	10.28	2.72	121.5	8.36	4.64			
78.9	10.46	3.54	157.9	11.68	2.32		43.5	9.9	3.1	123.7	7.54	5.46			
82.8	10.65	3.35	158.5	10.78	3.22		44.4	10.07	2.98	125	7.36	5.64			
85.5	10.96	3.04	159	11.49	2.51		45.8	10.01	2.99	130	6.61	6.39			
86.7	12	2	159.7	11.57	2.43		47.9	10.58	2.42	136	6.02	6.98			
87.9	11.86	2.14	160.6	10.34	3.66		50.7	8.86	4.14	139.6	5.87	7.13			
88.4	13.52	0.48	161.6	10.35	3.65		53.2	8.51	4.49	139.6	5.48	7.52			
89.3	13.6	0.4	162.6	9.98	4.02		56	7.66	5.34						
90.8	13.52	0.48	163.5	9.94	4.06		58	7.56	5.44						
90.9	13.51	0.49	165.1	10.19	3.81		62	7.55	5.45						
91.2	11.89	2.11	173	9.89	4.11		62	7.565	5.435						
94	10.75	3.25	179.4	9.92	4.08		67.4	7.34	5.66						
98.3	10.21	3.79	181	10.26	3.74		72	7.72	5.28						
103.7	10.39	3.61	185.3	9.82	4.18		76	7.56	5.44						
107.4	10.13	3.87	189.7	9.76	4.24		81.5	8	5						
110.6	10.5	3.5	192	10.13	3.87		82	8.34	4.66						
113.7	10.49	3.51	194.6	9.9	4.1		83	8.48	4.52						
116.2	10.3	3.7	197.6	10.31	3.69		84.4	8.36	4.65						
117	10.63	3.37	200.3	10.09	3.91		87	8.33	4.67						
118.8	10.68	3.32	207	10.25	3.75		90	8.56	4.44						
119.6	10.44	3.56	209	10.39	3.61		90.5	8.68	4.32						
121.3	10.46	3.54	211.1	10.27	3.73		91.4	8.25	4.75						
123.3	10.95	3.05	212.7	10.49	3.51		92.8	8.52	4.48						
124.4	10.78	3.22	215	10.17	3.83		93.5	9.14	3.86						
125.8	10.84	3.16	218	10.4	3.6		93.8	9.88	3.12						
125.9	11.86	2.14	218.5	10.58	3.42		94.5	10.01	2.99						
127.4	11.37	2.63	221.2	10.45	3.55		95.4	9.83	3.17						
128.2	11.09	2.91	223.5	10.64	3.36		95.7	9.78	3.22						
129.3	11.4	2.6	225.9	10.49	3.51		96.8	9.43	3.57						
130.2	11.41	2.59	228.3	10.63	3.37		96	8.93	4.07						
130.9	11.8	2.2	229.6	10.79	3.21		98	7.98	5.02						
132.3	11.41	2.59	233.6	9.98	4.02		98.8	7.85	5.15						
133.8	11.19	2.81	237	9.6	4.40		100.6	7.97	5.03						
134.8	11.4	2.6	242	9.52	4.48		101.7	8.53	4.47						
135.3	11.04	2.96	250	9.45	4.55		103	8.53	4.47						
135.7	10.79	3.21	262	9.37	4.63		104	8.25	4.75						
137.5	10.61	3.39	281	9.97	4.03		106.3	8.44	4.55						
138.7	10.9	3.1	288	10.2	3.80		107.5	7.99	5.01						
140	10.58	3.42	300	10.39	3.61		108.5	8.07	4.98						
141.2	11.14	2.85	300	10.12	3.88		109	9.52	3.48						
142.2	10.72	3.28					111	10.58	2.42						
143	11.48	2.52					111.3	8.19	4.81						
144	10.55	3.45					112.6	7.9	5.1						
145	10.52	3.48					113.5	8.66	4.34						
145.4	10.91	3.09					114.7	8.69	4.31						
147.6	11.15	2.85					116	9.25	3.75						
149	10.79	3.21					118.6	9.18	3.82						
152.8	10.99	3.01					119.3	8.5	4.5						

Table B-2. Measurements at Cross Sections 18 and 17

Cross-section P4West, NVED18 Date 8/27/2002 height of instrument (ft): 16.00								Cross-section P4West, NVED17 Date 8/27/2002 height of instrument (ft): 24.00							
distance (ft)	FS (ft)	elevation	FS bankfull	FS top of bank	W/tpa (ft)	dramel slope (%)	Mannings 'n'	distance (ft)	FS (ft)	elevation	FS bankfull	FS top of bank	W/tpa (ft)	dramel slope (%)	Mannings 'n'
0	0.055	15.945	14.411	9.7	120	9.2	0.04	0	2.8	21.2	22.383	17.72	140	3	0.04
0	0.055	15.945	1.589	6.3				0	3.26	20.74	1.617	6.28			
12	0.65	15.35						5	5.38	18.62					
20.65	5.8	10.2	dimensions				6.3	7.01	16.99	dimensions					
21.9	5.98	10.02	6.1	x-section area	0.7	dmean	20.2	10.47	13.53	7.7	x-section area	1.0	dmean		
23.3	5.77	10.23	9.0	width	10.0	vet P	35.6	17.18	6.82	7.3	width	7.5	vet P		
27	5.99	10.01	1.2	dmax	0.6	hydrad	35.4	17.57	6.43	1.3	dmax	1.0	hydrad		
27.6	6.35	9.65	6.0	bankht	13.2	wdratio	39.7	17.34	6.65	5.9	bankht	7.0	wdratio		
32.2	6.79	9.21	120	W/lood prone area	1.3	ent ratio	45.9	17.16	6.84	14.0	W/lood prone area	1.9	ent ratio		
38.1	7.51	8.49	hydraulics				48.5	17.72	6.28	hydraulics					
42.6	8.34	7.66	8.1	velocity (ft/sec)			54.2	18.02	5.98	6.5	velocity (ft/sec)				
47.8	8.54	7.46	50.0	discharge rate, Q (cfs)			62.9	17.71	6.29	50.0	discharge rate, Q (cfs)				
51.7	8.99	7.01	3.51	shear stress (lbs/ft sq)			67.2	18.62	5.38	1.91	shear stress (lbs/ft sq)				
54.9	9.73	6.27	1.35	shear velocity (ft/sec)			68.7	18.83	5.17	0.99	shear velocity (ft/sec)				
55.9	11.18	4.82	31.901	unit stream power (lbf/ft/sec)			70.8	19.44	4.55	12.813	unit stream power (lbf/ft/sec)				
60.35	11.5	4.5	3.00	Froude number			74.6	19.21	4.79	1.26	Froude number				
63.1	12.24	3.76	6.0	friction factor ulf			75.2	19.89	4.11	6.6	friction factor ulf				
64.45	12.71	3.29	8406	threshold grain size (mm)			76.4	19.94	4.05	255.9	threshold grain size (mm)				
64.9	13.74	2.26					76.8	20.69	3.31						
67.65	14.7	1.3					78.4	21.34	2.66						
71.55	15.1	0.9					79.9	21.06	2.94						
73.5	15.46	0.54					82.8	22.14	1.85						
74.25	15.65	0.35					83.4	23	1						
75.6	15.44	0.55					83.7	23.25	0.75						
75.65	14.51	1.49					84.4	23.39	0.61						
76.95	13.72	2.28					85.9	23.49	0.51						
78.8	12.14	3.86					87.8	23.64	0.36						
80.75	10.57	5.43					88.8	23.44	0.55						
81.55	10.4	5.6					90.2	23.32	0.68						
82.1	9.7	6.3					90.7	23.04	0.95						
88.1	10.1	5.9					91.5	20.9	3.1						
91.3	10.31	5.69					94.7	19.79	4.21						
94.15	10.03	5.97					97.4	18.54	5.46						
96.1	10.41	5.59					99.7	15.44	8.55						
96.5	11.71	4.29					102.2	13.76	10.24						
97.45	13.63	2.37					104.2	13.44	10.55						
98.55	13.26	2.74					108	13.46	10.54						
100.2	13.38	2.62					111	13.2	10.8						
101.6	13.33	2.67					115.6	13.57	10.43						
102.4	13.4	2.6					122	13.69	10.31						
103.15	13.23	2.77					130	13.69	10.31						
104.05	13	3					140	14.01	9.99						
104.55	12.08	3.92					152	13.55	10.44						
105.6	11.03	4.97					158	13.95	10.05						
106.8	10.22	5.78					165	13.77	10.23						
108.2	9.9	6.1					179	13.81	10.19						
110.9	9.12	6.88					183	14.03	9.97						
111.85	10.64	5.35					187	13.72	10.28						
114	8.29	7.71					199	13.87	10.13						
115.8	7.36	8.64					204	14.2	9.8						
117.9	5.96	10.04					206	14.01	9.99						
120	5.91	10.09					210	13.94	10.05						
123	6.07	9.93					221	13.4	10.6						
125	6.4	9.6					226	14	10						
136	6.27	9.73					235	13.9	10.1						
147	6.75	9.25					241	13.69	10.31						
158	6.59	9.41					245	13.63	10.37						
165	6.7	9.3					245.4	13.8	10.2						
170	6.67	9.33					248	13.78	10.22						
170	6.33	9.67					250	13.82	10.18						
							252	13.95	10.05						
							254	13.61	10.39						
							258	13.37	10.63						
							260	13.05	10.95						
							263	12.77	11.23						
							263	12.37	11.63						

Table B-3. Measurements at Cross Sections 16 and 15

Cross-section P4West, NVED16 Date 8/27/2002 height of instrument (ft): 24.50								Cross-section P4West, NVED15 Date 8/26/2002 height of instrument (ft): 23.00							
distance (ft)	FS (ft)	elevation	FS bankfull	FS top of bank	W/tpa (ft)	dramel slope (%)	Mannings 'n'	distance (ft)	FS (ft)	elevation	FS bankfull	FS top of bank	W/tpa (ft)	dramel slope (%)	Mannings 'n'
0	2.79	21.71	22.5	17.93	150	2.03	0.04	0	2.8	20.2	19.743	15.35	160	22	0.04
0	3.24	21.26	2	6.57				0	3.81	19.19	3.257	7.65			
2	3.17	21.33						1.8	4.59	18.41					
4	4.9	19.6	dimensions						14.2	13.48	9.52	dimensions			
6	5.93	18.57	8.1	x-section area	1.5	dmean		18.8	14.13	8.87	8.8	x-section area	1.1	dmean	
7	7.5	17	5.5	width	6.4	wet P		20.6	14.64	8.36	7.8	width	8.3	wet P	
13.8	12.59	11.91	1.8	dmax	1.3	hydrad		22.7	15.08	7.92	1.6	dmax	1.1	hydrad	
22	17.09	7.41	6.4	bankht	3.7	wdratio		31.6	15.07	7.93	6.0	bankht	7.0	wdratio	
27.4	17.86	6.64	150	W/lood prone area	27	ent ratio		33.6	15.66	7.34	160	W/lood prone area	20	ent ratio	
33.8	17.67	6.83	hydraulics						36.3	16.37	6.63	hydraulics			
38.1	17.72	6.78	6.2	velocity (ft/sec)				38.8	16.89	6.11	5.7	velocity (ft/sec)			
45.8	18.7	5.8	50.1	discharge rate, Q (cfs)				40.8	17.12	5.88	50.0	discharge rate, Q (cfs)			
46.7	19.07	5.43	1.60	shear stress (lbs/ft sq)				43.3	17.24	5.76	1.44	shear stress (lbs/ft sq)			
48.6	18.72	5.78	0.91	shear velocity (ft/sec)				45.5	16	7	0.86	shear velocity (ft/sec)			
50.85	18.21	6.29	11.537	unit stream power (lbf/ft/sec)				49.6	15.35	7.65	8.765	unit stream power (lbf/ft/sec)			
54.7	18.13	6.37	0.81	Froude number				52.8	15.78	7.22	0.90	Froude number			
60.1	17.96	6.54	6.8	friction factor ulf				56.8	16.22	6.78	148.6	threshold grain size (mm)			
62.7	17.93	6.57	181.9	threshold grain size (mm)				59.8	16.27	6.73					
63.9	18.49	6.01						61.2	16.53	6.47					
68.5	19.22	5.28						62.8	17.07	5.93					
69.5	20.03	4.47						65.4	17.49	5.51					
71.2	20.34	4.16						67.3	17.88	5.12					
74	20.09	4.41						68.8	18.01	4.99					
75.6	20.58	3.92						70.5	18.37	4.63					
78	20.65	3.85						72.2	19.16	3.84					
80.2	22.65	1.85						72.5	18.38	4.62					
81.2	22.83	1.67						73.4	18.73	4.27					
82.2	22.35	2.15						76	20.41	2.59					
83.4	21.03	3.47						76.5	20.69	2.31					
85.6	21.48	3.02						78	20.83	2.17					
87.5	23.89	0.61						78.5	21.23	1.77					
88.1	24.28	0.22						80	21.36	1.64					
89.5	24.32	0.18						80.8	21.1	1.9					
91.8	23.91	0.59						82.8	20.72	2.28					
91.9	23.78	0.72						82.8	18.92	4.03					
93	20.34	4.16						84.8	17.65	5.35					
94.7	19.74	4.76						87.2	16.89	6.11					
95.7	18.38	6.12						91.8	14.35	8.65					
100	14.73	9.77						96.8	11.02	11.98					
102	13.82	10.68						97.3	10.38	12.62					
115	13.9	10.6						99.8	10.17	12.83					
132	14.32	10.18						116.8	10.74	12.26					
138	14.54	9.96						116.8	10.47	12.53					
140	14.31	10.19													
145	14.32	10.18													
153	14.89	9.61													
155	14.85	9.65													
155	14.27	10.23													

Table B-4. Measurements at Cross Sections 14 and 13

Cross-section P4West, NVED14 Date 8/25/2002 height of instrument (ft): 22.00								Cross-section P4West, NVED13 Date 8/23/2002 height of instrument (ft): 23.50							
distance (ft)	FS (ft)	elevation	FS bankfull	FS top of bank	W/tpa (ft)	dmax slope(%)	Mannings 'n'	distance (ft)	FS (ft)	elevation	FS bankfull	FS top of bank	W/tpa (ft)	dmax slope(%)	Mannings 'n'
0	5.18	16.82	18.807	14.57	50.0	1.7	0.04	0	1.79	21.71	20.321	14.39	36.0	1.6	0.04
0	5.37	16.63	3.193	7.43				0	3.05	20.45	3.179	9.11			
7	5.86	16.14						2.5	4.21	19.29					
12	6.77	15.23	dimensions				9	5.18	18.32	dimensions					
14	7.56	14.44	130	x-section area	0.8	dmean	18	5.93	17.57	5.8	x-section area	2.5	dmean		
19	10.72	11.28	156	width	18.4	vet P	22	8.32	15.18	23	width	2.4	vet P		
26.4	14.57	7.43	27	dmax	0.7	hydrad	25	9.2	14.3	26	dmax	2.5	hydrad		
30	15.49	6.51	6.9	bankht	18.7	wdratio	27	12.02	11.48	8.6	bankht	0.9	wdratio		
35.3	16.47	5.53	500	W/lood prone area	3.2	ent ratio	36.4	15.85	7.65	36.0	W/lood prone area	15.7	ent ratio		
36.3	17.01	4.99	hydraulics				38.5	15.45	8.05	hydraulics					
37.4	17.69	4.31	3.8	velocity (ft/sec)			41.5	15.67	7.83	8.6	velocity (ft/sec)				
43	17.6	4.4	50.0	discharge rate, Q(dfs)			42.4	17.08	6.42	50.0	discharge rate, Q(dfs)				
46.7	17.7	4.3	0.75	shear stress (lbs/ft sq)			46	17.95	5.55	2.46	shear stress (lbs/ft sq)				
50.2	17.89	4.11	0.62	shear velocity (ft/sec)			51	18.08	5.42	1.13	shear velocity (ft/sec)				
51	18.34	3.66	3.400	unit stream power (lbs/ft/sec)			53.7	18.67	4.83	21.714	unit stream power (lbs/ft/sec)				
53.4	18.62	3.38	0.55	Froude number			57.7	19.1	4.4	0.90	Froude number				
54.7	18.76	3.24	6.2	friction factor ulu ²			63.7	19.46	4.04	7.6	friction factor ulu ²				
55.2	18.62	3.38	482	threshold grain size (mm)			64.8	19.32	4.18	4200	threshold grain size (mm)				
55.5	18.76	3.24					66.7	19.26	4.24						
57.7	18.73	3.27					67.7	19.88	3.92						
59.2	18.91	3.09					68	22.7	0.8						
60.6	18.48	3.52					68.8	22.88	0.62						
63.2	18.94	3.06					69.7	22.87	0.63						
63.7	18.84	3.16					69.9	22.97	0.53						
67	19.5	2.5					70.3	22.85	0.65						
67.7	20.19	1.81					70.7	20.14	3.36						
68.1	20.26	1.74					71.8	19.42	4.08						
68.4	20.99	1.01					73.2	19.41	4.09						
69	21.48	0.52					74	19.03	4.47						
69.7	21.46	0.54					75.6	18.84	4.66						
70.3	21.04	0.96					77	18.95	4.55						
70.7	21.15	0.85					79.5	18.05	5.45						
70.8	19.71	2.29					82	17.69	5.81						
71.6	19.88	2.42					84.2	17.77	5.73						
72.5	19.41	2.59					92.5	16.6	6.9						
73.5	19.5	2.5					97.7	15.89	7.61						
74.8	19.16	2.84					99	15.35	8.15						
75.9	19.43	2.57					102	14.75	8.75						
76.8	19.35	2.65					102.5	14.39	9.11						
77.5	19.01	2.99					115	14.66	8.84						
78.9	18.49	3.51					128	14.92	8.88						
80.3	17.89	4.11					136	14.98	8.52						
81.1	17.86	4.14					141	14.06	9.44						
81.6	17.25	4.75					144	13.6	9.9						
83.1	16.89	5.41					148	13.34	10.16						
84.3	16.32	5.68					155.5	13.61	9.89						
85.1	14.57	7.43					155.5	13.16	10.34						
92.3	14.47	7.53													
96.3	14.21	7.79													
98.7	13.37	8.63													
101	13.06	8.94													
104	13.11	8.89													
106	12.88	9.12													
113	13.25	8.75													
118	12.77	9.23													
123	11.83	10.17													
131	11.47	10.53													
131	11.15	10.85													

Table B-5. Measurements at Cross Sections 12 and 11A

Cross-section P4West, NWED12 Date 8/16/2002 height of instrument (ft): 20.50								Cross-section P4West, NWED11A Date 8/20/2002 height of instrument (ft): 16.50							
distance (ft)	FS (ft)	elevation	bankfull	FS top of bank	W/tpa (ft)	dramel slope (%)	Mannings 'n'	distance (ft)	FS (ft)	elevation	FS bankfull	FS top of bank	W/tpa (ft)	dramel slope (%)	Mannings 'n'
0	0.32	20.18	17.16	13.75	21.0	1.2	0.04	0	2.8	13.7	13.232	9.8	4.50	1.8	0.04
0	0.88	19.62	3.34	6.75				0	3.05	13.45	3.288	6.7			
11.3	5.42	15.08						12	4.61	11.89					
18	5.57	14.93	dimensions						12.2	7.14	9.36	dimensions			
19	5.81	14.69	11.5	x-section area	1.8	dmean		17.9	10.37	6.13	13.2	x-section area	0.8	dmean	
22.5	7.25	13.25	6.4	width	10.5	wet P		21	11.76	4.74	16.3	width	199	wet P	
23.6	7.27	13.23	2.7	dmax	1.1	hydrad		22.6	12.47	4.03	2.9	dmax	0.7	hydrad	
24.6	7.09	13.41	6.1	bankht	3.5	wdratio		23.9	12.6	3.9	6.3	bankht	20.3	wdratio	
28	8.79	11.71	21.0	W/lood prone area	3.3	ent ratio		24.4	12.52	3.98	4.50	W/lood prone area	2.8	ent ratio	
32.2	16.32	4.18	hydraulics						25.7	12.59	3.91	hydraulics			
41.6	17.52	2.98	4.3	velocity (ft/sec)				26.2	12.9	3.6	3.8	velocity (ft/sec)			
42.7	17.62	2.88	50.0	discharge rate, Q (cfs)				27.8	13.08	3.42	50.0	discharge rate, Q (cfs)			
42.8	17.82	2.68	0.82	shear stress (lbf/ft ²)				29.7	13.54	2.96	0.74	shear stress (lbf/ft ²)			
44.2	17.92	2.58	0.65	shear velocity (ft/sec)				31.9	13.77	2.73	0.62	shear velocity (ft/sec)			
46	18.05	2.45	5.855	unit stream power (lbf/ft ² /sec)				32.6	13.66	2.84	3.432	unit stream power (lbf/ft ² /sec)			
47.3	17.66	2.84	0.32	Froude number				33.1	13.52	2.98	0.55	Froude number			
48.9	17.29	3.21	6.7	friction factor ul ²				34.4	13.62	2.88	6.1	friction factor ul ²			
50.9	17.44	3.05	49.6	threshold grain size (mm)				35	13.95	2.55	47.7	threshold grain size (mm)			
51.2	19.54	0.96						36	13.41	3.09					
52.2	19.87	0.63						36.2	13.46	3.04					
54.2	19.83	0.67	312.7	12.19	8.31			37.3	13.26	3.24					
55.2	19.81	0.69	318	12.19	8.31			39.2	14.28	2.22					
55.3	17.49	3.01	321.5	12.54	7.95			39.4	16.09	0.41					
56.2	16.91	3.59	322.3	12.08	8.42			40	16.1	0.4					
57.2	16.3	4.2	330	12.01	8.49			41	16.07	0.43					
57.9	16.14	4.36	330.6	12.5	8			41.4	15.22	1.28					
61	14.17	6.33	331.8	12.45	8.05			42.2	14.51	1.99					
63	13.75	6.75	332.7	12.14	8.36			42.9	14.23	2.27					
71	13.94	6.55	338.6	12.21	8.29			43.4	14.35	2.15					
77.6	13.9	6.6	340	12.03	8.47			44	13.55	2.95					
80.3	14.16	6.34	355	12.76	7.74			45.1	13.1	3.4					
83.1	14.39	6.11	368	11.83	8.67			45.2	11.95	4.55					
85.6	14.36	6.14	373	11.9	8.6			47.3	11.73	4.77					
86.4	14.01	6.49	376	12.11	8.39			50.2	11.36	5.14					
93.3	13.82	6.68	379	12.12	8.38			52.2	11.53	4.97					
95.7	13.62	6.88	380	12.21	8.29			53.2	11.45	5.05					
98	12.88	7.62	382	12.17	8.33			55.8	10.9	5.6					
102	12.54	7.95	382.3	12.17	8.33			57.8	10.72	5.78					
108	12.56	7.94	384	12.34	8.16			63	9.8	6.7					
115	12.29	8.21	384.1	12.36	8.14			75.8	9.59	6.91					
123	12.11	8.39	388	12.21	8.29			80.5	9.95	6.55					
137	12.44	8.05	393	12.33	8.17			84	9.67	6.83					
156	12.54	7.95	395.4	12.21	8.29			87	9.76	6.74					
161	12.63	7.87	399	11.38	9.12			91	9.74	6.76					
174	12.29	8.21	406	11.26	9.24			95.5	9.59	6.91					
191	12.34	8.16	416	11.33	9.17			99	8.86	7.64					
204	12.42	8.08	439	11.74	8.76			101	8.57	7.93					
210	12.56	7.94	436	11.7	8.8			115	8.38	8.12					
213	12.32	8.18	461	10.59	9.91			127	8.57	7.93					
219	11.86	8.64	477	9.34	11.16			128.5	8.41	8.09					
228	11.79	8.71	499.5	6.84	13.65			128.5	8.32	8.18					
254	11.84	8.65	501	5.92	14.58										
266	12.15	8.35	507	4.54	15.95										
280	12.13	8.37	508	3.8	16.70										
284	11.96	8.54	510	3.34	17.16										
286	11.9	8.6													
287	12.08	8.42													
288.9	11.87	8.63													
290.2	11.96	8.54													
291.8	12.27	8.23													
294	12.13	8.37													
296	11.97	8.53													
297	11.89	8.61													
303.4	11.98	8.52													
304.8	12.22	8.28													
307	12.26	8.24													
308	12.08	8.42													
309	11.89	8.61													

Table B-6. Measurements at Cross Sections 11C and 10

Cross-section P4West, NVED11c Date 8/21/2002 height of instrument (ft): 16.50								Cross-section P4West, NVED10 Date 8/14/2002 height of instrument (ft): 18.00							
distance (ft)	FS (ft)	elevation	FS bankfull	FS top of bank	W/tpa (ft)	dramel slope(%)	Mannings 'n'	distance (ft)	FS (ft)	elevation	FS bankfull	FS top of bank	W/tpa (ft)	dramel slope(%)	Mannings 'n'
0	0	16.5	14.046	10.27	23.0	23	0.04	-1	3.73	14.27	16.345	10.02	11.0	1.6	0.04
4	0.82	15.68	2.462	6.23				0	3.96	14.04	1.655	7.98			
8	1.43	15.07						7	6.79	11.21					
19	4.45	12.05	dimensions						8.5	7.05	10.95	dimensions			
27	5.53	10.97	8.6	x-section area	1.5	dmean			13	7.55	10.45	10.2	x-section area	1.1	dmean
38	5.13	11.37	5.5	width	8.2	wet P			21	7.6	10.4	9.4	width	9.7	wet P
41	5.09	11.41	2.0	dmax	1.0	hydrad			26	7.32	10.68	1.2	dmax	1.1	hydrad
44	6	10.5	5.8	bankht	3.6	wdratio			35	6.87	11.13	7.6	bankht	8.6	wdratio
46	5.8	10.7	23.0	W/lood prone area	4.1	entratio			46	7.48	10.52	11.0	W/lood prone area	1.2	entratio
53	6.42	10.08	hydraulics						55	7.57	10.43	hydraulics			
62.9	6.21	10.29	5.8	velocity (ft/sec)					58	8.19	9.81	4.9	velocity (ft/sec)		
63	7.4	9.1	50.0	discharge rate, Q(cfs)					64	8.66	9.34	50.0	discharge rate, Q(cfs)		
67.8	10.44	6.06	1.51	shear stress (lbs/ft sq)					69	8.55	9.45	1.05	shear stress (lbs/ft sq)		
68.2	11.17	5.33	0.88	shear velocity (ft/sec)					73	8.37	9.63	0.74	shear velocity (ft/sec)		
68.5	11.55	4.95	12.932	unit stream power (lbs/ft/sec)					78	8.57	9.43	5.308	unit stream power (lbs/ft/sec)		
70	11.97	4.53	0.68	Froude number					82	8.37	9.63	6.6	friction factor ulf		
70.1	13.49	3.01	1609	threshold grain size (mm)					85	8.49	9.51	80.5	threshold grain size (mm)		
71.8	13.51	2.99							91	8.79	9.21				
72.1	12.9	3.6							97	8.4	9.6				
73	12.94	3.56							104	7.86	10.14				
74.6	15.25	1.25							107	8.65	9.35	267.1	10.02	7.98	
74.8	15.58	0.92							111.4	10.35	7.65	270	9.75	8.25	
75.3	15.63	0.87							115	11.09	6.91	272.5	9.33	8.67	
76	15.65	0.85							120	11.45	6.55	277	8.89	9.11	
77	15.82	0.68							121.6	11.8	6.2	279.5	8.69	9.31	
78.2	16.01	0.49							123.3	12.05	5.95	280.3	8.1	9.9	
79.1	16.05	0.45							124	12.25	5.75	283.3	7.97	10.03	
79.4	13.26	3.24							126	13.23	4.77	286	7.36	10.64	
80.2	12.82	3.68							129.2	14.16	3.84	290	6.28	11.72	
81.7	13.07	3.43							129.8	14.91	3.09	293	5.77	12.23	
83.8	13.43	3.07							131.7	13.37	4.63	300	5.72	12.28	
84.5	13.06	3.44							132	16.22	1.78	310	5.89	12.11	
85.5	12.85	3.65							132.7	16.28	1.72	324	6.24	11.76	
86.1	13.08	3.42							133.2	16.31	1.69	333	6.06	11.94	
86.8	12.9	3.6							134	17.13	0.87	336	6.03	11.97	
88.5	13.39	3.11							134.8	17.48	0.52	345.6	5.65	12.35	
89.5	12.46	4.04							135.4	17.59	0.41	353	6.16	11.84	
92.6	11.65	4.85							136.7	17.54	0.46	357.2	6.33	11.67	
95	10.82	5.68							138.9	17.52	0.48	360.4	6.84	11.16	
97	10.27	6.23							140.5	17.59	0.41	362	6.45	11.55	
101.6	10.38	6.12							141.5	17.58	0.42	366	6.78	11.22	
106.5	10.28	6.22							141.9	17.15	0.85	368.4	7.03	10.97	
107.5	10.17	6.33							143.4	16.86	1.14	370	6.19	11.81	
109.7	9.75	6.75							144	16.33	1.67	370.9	7.08	10.92	
112.6	9.6	6.9							144.4	14.12	3.88	376	6.35	11.65	
114.8	8.86	7.64							146.4	13.6	4.4	384	6.07	11.93	
121	9	7.5							147.6	12.54	5.46	388	6.54	11.46	
127	9.61	6.89							148	12.5	5.5	390.4	7.33	10.67	
133	8.66	7.84							150.4	12.33	5.67	394.7	8.36	9.64	
136	8.35	8.15							152.4	12.66	5.34	396.8	8.34	9.66	
142	8.27	8.23							154.6	10.68	7.32	401	6.76	11.24	
149	7.47	9.03							156	10.02	7.98	406	6.8	11.2	
155.5	7.81	8.69							157.5	9.97	8.03	414	6.4	11.6	
158.5	8.24	8.26							167	10.21	7.79	421	6.35	11.65	
163	8.51	7.99							174	11.14	6.86	425	5.91	12.09	
167	8.24	8.26							180.3	11.63	6.37	429	6.09	11.91	
173.8	7.77	8.73							183.4	11.81	6.19	437.4	6.46	11.54	
176	7.51	8.99							186.9	11.43	6.57	445	6.19	11.81	
181	7.52	8.98							191	11.86	6.14	448	5.97	12.03	
185	7.08	9.42							194.6	11.01	6.99	451.5	5.39	12.61	
192	7.13	9.37							195.5	10.63	7.37	456	4.65	13.35	
200	7.1	9.4							199.9	10.24	7.76	459	4.66	13.34	
200	6.84	9.66							203.3	10.35	7.65	464	4.88	13.12	
									207	10.61	7.39	473	3.24	14.76	
									213	9.74	8.26	479	2.48	15.52	
									223	9.79	8.21	481	2.31	15.69	
									234	9.86	8.14	481	2.03	15.97	
									238	9.78	8.22				

Table B-7. Measurements at Cross Sections 11 and 8

Cross-section P4West, NVED11 Date height of instrument (ft): 18.00								Cross-section P4West, NVED8 Date 8/8/2002 height of instrument (ft): 17.50							
distance (ft)	FS (ft)	elevation	FS bankfull	FS top of bank	W/tpa (ft)	dramel slope (%)	Mannings 'n'	distance (ft)	FS (ft)	elevation	FS bankfull	FS top of bank	W/tpa (ft)	dramel slope (%)	Mannings 'n'
-1	9.15	8.85	15.975	11.36	160	1.4	0.04	-1	2.48	15.02	14.63	7.95	280	1.4	0.04
0	9.71	8.29	2.025	6.64				0	2.81	14.69	2.87	9.55			
2	9.66	8.34						13	7.88	9.62					
3.3	9.81	8.19	dimensions						26	9.3	8.2	dimensions			
6	10.15	7.85	10.2	x-section area	1.4	dmean		38	8.56	8.94	7.4	x-section area	2.1	dmean	
11	10.96	7.04	7.5	width	8.7	wet P		69	8.72	8.78	3.5	width	3.9	wet P	
14	10.92	7.08	1.6	dmax	1.2	hydrad		86	8.79	8.71	2.4	dmax	1.9	hydrad	
17	11.27	6.73	6.3	bankht	5.6	wdratio		100	8.36	9.14	9.1	bankht	1.6	wdratio	
19.4	10.63	7.37	16.0	W/lood prone area	2.1	ent ratio		105	8.77	8.73	28.0	W/lood prone area	8.0	ent ratio	
20.3	11.32	6.68	hydraulics						114	8.66	8.84	hydraulics			
21.5	12.4	5.6	4.9	velocity (ft/sec)				128	8.08	9.42	6.8	velocity (ft/sec)			
27	12.65	5.35	50.0	discharge rate, Q (cfs)				141	7.85	9.65	50.3	discharge rate, Q (cfs)			
30	12.54	5.46	1.03	shear stress (lbs/ft sq)				146	7.91	9.59	1.67	shear stress (lbs/ft sq)			
34	11.77	6.23	0.73	shear velocity (ft/sec)				155	8.87	8.63	0.93	shear velocity (ft/sec)			
38	11.49	6.51	5.797	unit stream power (lb/ft/sec)				175	8.6	8.9	12.50	unit stream power (lb/ft/sec)			
43.6	11.29	6.71	0.55	Froude number				196	8.42	9.03	0.67	Froude number			
48.4	11.36	6.64	6.7	friction factor ul*f				209	8.23	9.27	7.3	friction factor ul*f			
49.9	12.17	5.83	76.1	threshold grain size (mm)				230	8.1	9.4	197.2	threshold grain size (mm)			
50.9	12.85	5.15						234	7.93	9.57					
52.6	13.29	4.71	225	4.97	13.03			237	7.91	9.59	385	7.15	10.35		
53.5	13.71	4.29	235	4.81	13.19			241	7.95	9.55	389	6.27	11.23		
54.7	13.9	4.1	243.2	4.66	13.34			243	8.27	9.23	393	6.15	11.35		
56.4	14.73	3.27	248	4.81	13.19			248	10.4	7.1	396	6.24	11.26		
57	15.06	2.94	251.3	4.93	13.07			250.8	11.29	6.21	398	5.77	11.73		
57.7	15.22	2.78	252.7	4.99	13.01			252.5	11.97	5.53	402	5.16	12.34		
58	15.61	2.39	256	4.93	13.07			255.2	12.35	5.15	412	4.91	12.59		
58.8	16.43	1.57	260	5	13			258.2	12.28	5.22	415	4.99	12.51		
59.4	16.99	1.01	263	4.76	13.24			262.5	12.73	4.77	417.3	4.78	12.72		
60	17.61	0.39	266.7	4.62	13.38			264.5	12.41	5.09	419.2	4.68	12.82		
61.9	17.51	0.49	276	3.85	14.15			266	12.5	5					
63.5	17.6	0.4	285	3.91	14.09			270	11.33	6.17					
64.8	17.47	0.53	285	3.5	14.5			275	10.57	6.93					
65.1	17.3	0.7						281	11.5	6					
66.2	16.41	1.59						282.8	11.83	5.67					
66.4	15.78	2.22						284.3	11.85	5.65					
68	14.69	3.31						288.6	12.43	5.07					
71.5	14.42	3.88						291	11.99	5.51					
74	14.08	3.92						292.4	12.5	5					
76.7	13.6	4.4						293.5	12.54	4.95					
77.2	12.91	5.09						294.1	12.45	5.05					
77.7	12.37	5.63						295.9	13.05	4.45					
79.3	11.71	6.29						298	13.16	4.34					
80.6	10.55	7.45						298.7	14.55	2.94					
84.1	10.51	7.49						299.6	14.29	3.21					
87.5	10.55	7.45						300.7	14.65	2.85					
89.4	11.16	6.84						302	14.28	3.22					
92	11.64	6.36						303	14.84	2.66					
95	11.65	6.35						303.4	15.18	2.32					
98	11.49	6.51						304.1	14.93	2.57					
101	11.49	6.51						304.8	13.99	3.51					
104	11.04	6.96						305.6	13.83	3.67					
106.9	11.25	6.75						307.8	13.87	3.63					
112	11	7						308.5	14.28	3.22					
117.7	10.68	7.32						308.6	16.72	0.78					
121.4	11.36	6.64						309.7	17.03	0.47					
126.7	9.92	8.08						311.3	16.72	0.78					
132.4	9.55	8.45						312.1	15.95	1.55					
136.2	9.76	8.24						312.3	15.04	2.46					
137.2	9.45	8.55						312.8	14.82	2.68					
138.2	9.23	8.77						313.5	14.12	3.38					
139.5	9.63	8.37						314.5	13.86	3.64					
140.4	9.61	8.39						315.4	13.79	3.71					
140.8	9.74	8.26						316.5	13.41	4.09					
148	8.5	9.5						318.1	12.87	4.63					
155	7.95	10.05						319.2	12.82	4.68					
163.4	7.14	10.86						319.8	12.24	5.26					
177	6.55	11.45						320.4	6.56	10.94					
179.3	6.73	11.27						320.9	5.84	11.66					

Table B-8. Measurements at Cross Sections 9 and 7

Cross-section P4West, NVED9 Date 8/8/2002 height of instrument (ft): 16.00								Cross-section P4West, NVED7 Date 8/7/2002 height of instrument 14.00							
distance (ft)	FS (ft)	elevation	FS bankfull	FS top of bank	W/tpa (ft)	channel slope(%)	Mannings "n"	distance (ft)	FS (ft)	elevation	FS bankfull	FS top of bank	W/tpa (ft)	channel slope(%)	Mannings "n"
-1	3.93	12.07	12.624	8.29	20.0	0.8	0.04	-1	4.97	9.03	10.83	6.94	46.0	1.9	0.04
0	4.48	11.52	3.376	7.71				0	5.65	8.35	3.17	7.06			
10	4.82	11.18						5.5	5.64	8.36					
12	5.26	10.74	dimensions					13.4	5.43	8.57	dimensions				
17	6.13	9.87	10.6	x-section area	1.9	d mean	18.7	5.65	8.35	10.4	x-section area	1.2	d mean		
23	8.54	7.46	5.7	width	6.2	wet P	24	5.65	8.35	9.0	width	11.4	wet P		
27	8.81	7.19	2.3	d max	1.7	hydrad	32.4	4.93	9.07	2.5	d max	0.9	hydrad		
30.5	9.16	6.84	6.6	bank ht	3.1	wd ratio	37.7	4.51	9.49	6.4	bank ht	7.8	wd ratio		
32.5	9.17	6.83	20.0	W/flood prone area	3.5	ent ratio	48.8	4.66	9.34	46.0	W/flood prone area	5.1	ent ratio		
35.7	9.8	6.2	hydraulics					57.2	4.81	9.19	hydraulics				
37.3	9.69	6.31	4.7	velocity (ft/sec)			57.9	6.02	7.98	4.8	velocity (ft/sec)				
39.2	9.82	6.18	50.0	discharge rate, Q(cfs)			62	8.76	5.24	50.0	discharge rate, Q(cfs)				
42.6	8.52	7.48	0.85	shear stress ((lbs/ft sq)			64.5	9.53	4.47	1.08	shear stress ((lbs/ft sq)				
47	8.17	7.83	0.66	shear velocity (ft/sec)			65.2	10.3	3.7	0.75	shear velocity (ft/sec)				
52	8.23	7.77	4.381	unit stream power (lbf/ft/sec)			66.9	10.48	3.52	6.590	unit stream power (lbf/ft/sec)				
53.9	8.73	7.27	0.37	Froude number			68.5	10.84	3.16	0.62	Froude number				
57.7	10.04	5.96	7.2	friction factor u/u*			69.4	11	3	6.5	friction factor u/u*				
59	10.45	5.55	52.6	threshold grain size (mm)			69.9	11.43	2.57	84.4	threshold grain size (mm)				
65	10.39	5.61					71.7	11.14	2.86						
68	10.78	5.22					72.7	11.39	2.61						
70	11.27	4.73					73.3	13.29	0.71						
71.3	11.45	4.55					74.2	13.36	0.64						
72.2	11.98	4.02					74.8	13.34	0.66						
72.7	12.98	3.02					75.4	13.25	0.75						
72.9	14.88	1.12					76	12.08	1.92						
74.3	14.8	1.2					77.5	11.73	2.27						
75.1	14.65	1.35					78.2	10.99	3.01						
76	14.72	1.28					80.9	10.81	3.19						
76.6	14.71	1.29					82.4	10.68	3.32						
77	14.4	1.6					84.1	11.2	2.8						
77.7	13.91	2.09					85.6	9.9	4.1						
78.6	13.2	2.8					88.2	10.51	3.49						
79.1	12.21	3.79					90.8	10.88	3.12						
79.5	11.96	4.04					95.4	10.57	3.43						
80.2	12.01	3.99					97.8	10.26	3.74						
81.1	11.84	4.16					99.5	10.5	3.5						
81.6	11.68	4.32					100.9	10.26	3.74						
82.2	11.52	4.48					103	10.15	3.85						
83.5	11.08	4.92					108	7.96	6.04						
84.6	10.95	5.05					112	6.94	7.06						
86.8	9.11	6.89					121.1	6.49	7.51						
87.1	8.09	7.91					123.7	5.91	8.09						
89	8	8					128.3	4.88	9.12						
92	7.68	8.32					133	4.43	9.57						
95	6.96	9.04					136.5	4.14	9.86						
98	6.92	9.03													
102	6.67	9.33													
105	6.78	9.22													
107	6.53	9.47													
109	5.67	10.33													
110.9	5.49	10.51													
110.9	5.06	10.94													

Table B-9. Measurements at Cross Sections 6B and 5D

Cross-section F4 West, NVED6b							Cross-section F4 West, NVED5D								
Date 8/7/2002							Date 9/4/2002								
height of instrument (ft): 17.5							height of instrument (ft): 16								
distance (ft)	FS (ft)	FS elevation	FS bankfull	FS top of bank	Wfpa (ft)	channel slope (%)	Mannings "n"	distance (ft)	FS (ft)	FS elevation	FS bankfull	FS top of bank	Wfpa (ft)	channel slope (%)	Mannings "n"
-1	4.3	13.2	14.605	10.83	6.20	1.3	0.04	0	4.85	11.15	13.18	9.63	51.0	1.3	0.04
0	4.65	12.85	2.855	6.67				0	5.26	10.74	2.82	6.37			
9	4.9	12.6						12.7	5.3	10.7					
21.2	11.75	5.75	dimensions					17.3	4.51	11.49	dimensions				
70	12.11	5.39	12.8	x-section area	1.0	dmean		30	4.85	11.15	7.7	x-section area	2.0	dmean	
116.2	11.82	5.68		width	14.5	wet P		40	5.63	10.37	3.9	width	4.0	wet P	
120.8	11.16	6.34	2.5	dmax	0.9	hydrad		51.5	5.97	10.03	2.1	dmax	1.9	hydrad	
125.4	10.79	6.71	6.3	bank ht	11.8	w/d ratio		56	5.8	10.2	5.7	bank ht	2.0	w/d ratio	
151.1	11.01	6.49	6.20	Wflood prone area	5.0	entratio		64	6.39	9.61	51.0	Wflood prone area	13.1	entratio	
157	11.12	6.38						89	6.61	9.39					
161	11.61	5.89	hydraulics					114	6.99	9.01	hydraulics				
192.8	11.7	5.8	3.9	velocity (ft/sec)				121	6.48	9.52	6.5	velocity (ft/sec)			
209.1	11.16	6.34	50.1	discharge rate, Q (cfs)				129	6.69	9.31	50.0	discharge rate, Q (cfs)			
222.6	11.09	6.41	0.72	shear stress (lb/ft ²)				133	7.05	8.95	1.55	shear stress (lb/ft ²)			
250	11.19	6.31	0.61	shear velocity (ft/sec)				140	7.01	8.99	0.89	shear velocity (ft/sec)			
275	11.21	6.29	3.301	unit stream power (lb/ft ² /sec)				147.2	9.09	6.91	10.397	unit stream power (lb/ft ² /sec)			
285	10.62	6.88	0.46	Froude number				152.1	10.96	5.04	0.67	Froude number			
297	10.64	6.86	6.4	friction factor u [*]				154.9	11.27	4.73	7.3	friction factor u [*]			
299	10.83	6.67	45.7	threshold grain size (mm)				161.1	11.92	4.08	17.06	threshold grain size (mm)			
309	13.01	4.49						165.4	11.99	4.01					
315.5	13.39	4.11						168.1	12.23	3.77					
321.8	13.74	3.76						169.7	12.98	3.02					
325.2	14.21	3.29						172	13.37	2.63					
327.4	14.57	2.93						175.2	12.93	3.07					
329.8	14.66	2.84						178.9	12.94	3.05					
330.5	14.96	2.54						179.9	12.66	3.34					
332	15.15	2.35						181.7	12.47	3.53					
334.4	17.15	0.35						182.3	12.83	3.17					
336.4	15.12	2.38						182.4	14.74	1.26					
337.8	14.95	2.55						183.8	15.23	0.77					
339.8	15.24	2.26						184.9	15.32	0.68					
340.7	15.01	2.49						185.5	15.22	0.78					
341.7	14.91	2.59						186.3	15.08	0.92					
342.5	15.01	2.49						186.6	13.56	2.44					
343.8	14.74	2.76						186.8	13.19	2.81					
344.7	14.7	2.8						187.8	13.01	2.99					
346.6	14.87	2.63						188.5	12.82	3.18					
347.7	15.01	2.49						189.3	12.9	3.1					
348.4	16.13	1.37						190.1	12.79	3.21					
349	16.44	1.05						191.9	12.97	3.03					
349.4	16.31	1.19						196.4	12.33	3.67					
349.9	16.3	1.2						196.7	13.03	2.97					
350.8	15.2	2.3						197.8	13.02	2.98					
352	14.87	2.63						197.9	12.16	3.84					
353.1	15.22	2.28						201.3	11.51	4.49					
355.4	15.06	2.44						203.2	10.96	5.04					
357.1	14.81	2.69						207.4	10.71	5.29					
359.4	14.35	3.15						212	10.95	5.05					
362.5	13.57	3.93						220.2	10.25	5.75					
364.8	12.48	5.02						223.8	9.9	6.1					
370.5	11.81	5.69						228.6	9.63	6.37					
374.5	11.37	6.13						236	9.94	6.05					
378.6	6.17	11.33						241.5	10.08	5.92					
387.4	4.68	12.82						248.9	10.41	5.59					
389	5.33	12.17						259.8	10.54	5.46					
405.2	5.47	12.03						264.7	10.44	5.56					
407.6	5.76	11.74						269.2	8.01	7.99					
412	6.18	11.32						272	7.52	8.48					
415.3	6.29	11.21						277	5.95	10.05					
420.3	5.49	12.01						283.3	4.77	11.23					
428.2	3.68	13.82						283.3	4.37	11.63					
431	3.08	14.42													
435.7	2.61	14.89													
435.7	2.36	15.14													

Table B-10. Measurements at Cross Sections 5C and 6

Cross-section R4West, R4WNMED5C								Cross-section R4West, NMED6									
Date								Date									
height of instrument (ft): 145								height of instrument (ft): 12									
distance (ft)	FS (ft)	elevation	FS bankfull	FS top of bank	Wfipa (ft)	channel slope(%)	Mannings "n"	distance (ft)	FS (ft)	elevation	FS bankfull	FS top of bank	Wfipa (ft)	channel slope(%)	Mannings "n"		
0	3.53	10.97	10.649	7.54	50.0	1.1	0.04	-1	3.51	8.49	8.515	5.54	47.0	1.4	0.04		
0	3.92	10.58	3.851	6.96				0	3.64	8.36	3.485	6.46					
17	4.09	10.41						9	3.72	8.28							
27	4.11	10.39						18.4	3.66	8.34							
30	3.4	11.1	dimensions						19.3	5.01	6.99	dimensions					
33	3.19	11.31	15.2	x-section area	1.0	dmean		24	7.68	4.32	15.7	x-section area	0.7	dmean			
36	3.31	11.19		width	19.5	wet P		26.5	8.88	3.12	22.5	width	2.55	wet P			
39	3.64	10.86	3.1	dmax	0.8	hydrat		27.9	8.94	3.05	2.6	dmax	0.6	hydrat			
74	4.81	9.69	6.2	bank ht	15.7	w/d ratio		28.3	10.45	1.55	5.5	bank ht	3.23	w/d ratio			
92	5.28	9.22	50.0	Wflood prone area	3.2	entratio		29.2	11.07	0.98	47.0	Wflood prone area	2.1	entratio			
99	5.6	8.9	hydraulics						30.7	10.89	1.11	hydraulics					
110	5.36	9.14	3.3	velocity (ft/sec)				31.6	10.47	1.53	3.2	velocity (ft/sec)					
129	5.69	8.81	50.0	discharge rate, Q(cfs)				32.1	9.24	2.76	50.0	discharge rate, Q(cfs)					
135	5.85	8.65	0.53	shear stress (lb/ft ²)				33.5	8.88	3.12	0.54	shear stress (lb/ft ²)					
141	5.56	8.94	0.52	shear velocity (ft/sec)				34.8	9.33	2.67	0.53	shear velocity (ft/sec)					
145	5.83	8.67	2.221	unit stream power (lb/ft ² /sec)				35.8	9.01	2.99	1.940	unit stream power (lb/ft ² /sec)					
152.6	5.91	8.59	0.34	Froude number				36.3	9.02	2.98	0.46	Froude number					
155	7.4	7.1	6.3	friction factor u/f				37	9.33	2.67	6.0	friction factor u/f					
156.6	8.38	6.12	32.9	threshold grain size (mm)				37.4	8.96	3.04	33.3	threshold grain size (mm)					
157.4	10.64	3.85						38.9	8.7	3.3							
159.5	11.07	3.43						40.4	8.66	3.34							
161.9	11.08	3.42						42.5	8.82	3.18							
163.4	11.56	2.94						44.6	8.84	3.16							
164.2	11.39	3.11						44.9	8.56	3.44							
166.5	11.28	3.22						46	8.97	3.03							
167.2	11.59	2.91						48.4	8.82	3.18							
167.3	13.63	0.87						49.2	8.43	3.57							
168	13.76	0.74						51.3	8.33	3.67							
168.6	13.66	0.84						54.4	7.49	4.51							
169	13.66	0.84						57.6	6.86	5.14							
169.2	13.88	0.92						62.4	6.73	5.27							
169.5	13.35	1.15						64.1	6.52	5.48							
170.3	13.22	1.28						65.3	6.61	5.39							
170.4	11.54	2.96						67.4	6.38	5.62							
171.7	10.78	3.72						69.6	6.32	5.68							
172.6	10.82	3.68						71	5.83	6.17							
172.9	10.72	3.78						72.6	5.54	6.46							
174.6	10.69	3.81						81	5.57	6.43							
175.8	10.64	3.86						84	5.42	6.58							
176.6	11.27	3.23						97.7	5.63	6.37							
177.5	10.45	4.05						100	4.73	7.27							
178.9	10.32	4.18						102.2	3.63	8.37							
182.1	11.01	3.49						104	3.6	8.4							
183.4	11.27	3.23						110	6.26	5.74							
184.7	11.41	3.09						113.5	7.09	4.91							
185.9	11.17	3.33						115.4	7.29	4.71							
187.4	11.04	3.46						117.3	7.19	4.81							
189.4	11.66	2.84						121.4	6.6	5.4							
191.2	9.93	4.57						127	6.97	5.03							
194.8	8.55	5.95						133.2	6.86	5.14							
199	8.08	6.42						137.2	6.91	5.09							
205.3	7.64	6.86						140.4	6.66	5.34							
218	7.39	7.11						145.6	3.16	8.84							
225.4	7.55	6.95						149	2.71	9.29							
232	8.42	6.03						149	2.43	9.57							
234	8.75	5.75															
236.1	8.56	5.94															
241.5	9.22	5.28															
255	9.57	4.93															
261	9.77	4.73															
265	10.12	4.38															
278.5	10.05	4.45															
280.7	8.94	5.55															
283	7.2	7.3															
285.3	6.52	7.98															
285.3	6.11	8.39															

Table B-11. Measurements at Cross Sections 5B and 5

Cross-section F4 West, NVED 5B Date 9/22/02 Height of instrument (ft): 16							Cross-section F4 West, NVED 5 Date 8/6/2002 Height of instrument (ft): 18								
distance (ft)	FS (ft)	FS elevation	FS bankfull	FS top of bank	Wfipa (ft)	channel slope (%)	Mannings "n"	distance (ft)	FS (ft)	FS elevation	FS bankfull	FS top of bank	Wfipa (ft)	channel slope (%)	Mannings "n"
0	6.94	9.05	12.666	8.96	540	1	0.04	0	5.56	12.44	13.735	8.7	980	0.3	0.04
0	7.28	8.72	3.334	7.04				0	5.95	12.05	4.255	9.3			
14	7.03	8.97						25	6.05	11.95					
18	5.83	10.17	dimensions				6	6.87	11.13	dimensions					
32	5.91	10.09	126	x-section area	1.7	dmean	12	8.56	9.44	222	x-section area	1.4	dmean		
54	6.6	9.4	7.5	width	11.4	wet P	17.5	8.78	9.22	156	width	190	wet P		
67	6.97	9.03	28	dmax	1.1	hydrad	37	8.86	9.14	3.3	dmax	1.2	hydrad		
68.1	7.28	8.72	6.5	bank ht	4.5	w/d ratio	70.4	8.69	9.31	8.4	bank ht	10.9	w/d ratio		
68.5	9.33	6.67	540	Wflood prone area	7.2	entratio	73.5	8.46	9.54	980	Wflood prone area	6.3	entratio		
69.1	9.6	6.4					85.2	8.45	9.55						
69.4	10.78	5.22	hydraulics				87.5	7.8	10.2	hydraulics					
72.9	11.6	4.4	40	velocity (ft/sec)			94.3	7.4	10.6	2.3	velocity (ft/sec)				
73.7	11.85	4.15	50.0	discharge rate, Q (cfs)			110.5	7.4	10.6	50.1	discharge rate, Q (cfs)				
75.2	11.59	4.11	0.69	shear stress (lb/ft ²)			128	8.13	9.87	0.22	shear stress (lb/ft ²)				
75.8	11.67	4.33	0.60	shear velocity (ft/sec)			143.2	8.7	9.3	0.34	shear velocity (ft/sec)				
76.6	11.81	4.19	4.161	unit stream power (lb/ft ² /sec)			143.9	11.13	6.87	0.602	unit stream power (lb/ft ² /sec)				
78.4	12.19	3.81	0.29	Froude number			144.6	11.38	6.62	0.11	Froude number				
80.1	12.86	3.14	6.7	friction factor uL*			144.7	12.56	5.44	6.7	friction factor uL*				
81.5	13.22	2.78	439	threshold grain size (mm)			147.3	13.12	4.88	125	threshold grain size (mm)				
82	14.34	1.66					149.6	13.78	4.22						
82.3	14.85	1.15					151.1	13.43	4.57						
84	15.05	0.95					153	13.75	4.25						
85.5	15.45	0.55					154.7	14.24	3.76						
86	15.45	0.55					155.3	14.55	3.45						
86.5	13.5	2.5					156.2	14.77	3.23						
87.4	13.21	2.79					157.1	14.59	3.41						
87.6	14.58	1.42					157.5	14.76	3.24						
88	12.72	3.28					158	16.64	1.36						
90.4	12.19	3.81					159.6	16.95	1.05						
93.5	11.9	4.1					161.1	17.05	0.95						
98.9	11.59	4.41					161.7	17.01	0.99						
98.1	11.83	4.17					162.5	16.5	1.5						
99.7	11.66	4.34					163	16.295	1.705						
104	11.28	4.72					163.1	14.72	3.28						
109.6	10.36	5.64					166.3	14.15	3.85						
117.3	10.48	5.52					168.4	13.69	4.31						
121.6	9.96	6.04					169.1	13.79	4.21						
122.9	9.57	6.43					169.6	13.79	4.21						
123.8	9.33	6.67					170.1	13.54	4.46						
129.4	9.44	6.55					173.5	13.46	4.54						
132.2	8.95	7.05					174.9	13.43	4.57						
136.3	8.96	7.04					176.9	13.05	4.95						
138.8	9.31	6.69					177.8	13.24	4.76						
143.4	9.79	6.21					179	13.22	4.78						
145.5	10.42	5.98					179.7	12.97	5.03						
146.8	10.58	5.42					181	12.82	5.18						
164.8	10.08	5.92					182.9	12.36	5.64						
166.8	9.79	6.21					187.9	12.18	5.82						
176.9	9.2	6.8					191.4	12.54	5.46						
179.4	8.83	7.17					194.6	12.42	5.58						
181.8	8.62	7.38					195.6	11.96	6.04						
183.1	7.86	8.14					196.4	11.99	6.01						
185.5	5.56	10.44					197.3	11.77	6.23						
191.2	4.93	11.07					201	11.71	6.29						
191.2	4.53	11.47					204	11.91	6.09						
							206.7	12.6	5.4						
							210	12.71	5.29						
							212.7	12.47	5.53						
							214.2	12.45	5.55						
							216.2	12.62	5.38						
							224.5	12.21	5.79						
							230.5	12.06	5.94						
							234.5	11.7	6.3						
							240.6	9.66	8.34						
							242.8	9.32	8.68						
							245.2	8.27	9.73						
							251.6	7.08	10.92						

Table B-12. Measurements at Cross Sections 5A and 4

Cross-section F4 West, NVED5A Date 9/2/2002 height of instrument (ft): 15							Cross-section F4 West, NVED4 Date 8/5/2002 height of instrument (ft): 13								
distance (ft)	FS (ft)	FS elevation	FS bankfull	FS top of bank	Wfipa (ft)	channel slope (%)	Mannings "n"	distance (ft)	FS (ft)	FS elevation	FS bankfull	FS top of bank	Wfipa (ft)	channel slope (%)	Mannings "n"
0	4.39	10.61	12.915	7.68	71.0	1.1	0.04	-1	2.6	10.4	9.762	5.84	740	1.7	0.04
0	4.72	10.28	2.085	7.32				0	2.78	10.22	3.238	7.16			
11	5.1	9.9						11	3.15	9.85					
14	5.83	9.17	dimensions					20	3.34	9.66	dimensions				
20	7.54	7.46	11.1	x-section area	1.4	dmean		24	3.95	9.05	11.7	x-section area	0.9	dmean	
37	7.73	7.27	7.8	width	8.9	wet P		29	4.71	8.29	124	width	14.3	wet P	
58	7.77	7.23	1.8	dmax	1.2	hydrad		35.4	5.08	7.92	2.5	dmax	0.8	hydrad	
63.8	7.01	7.99	7.0	bank ht	5.5	w/d ratio		43	4.75	8.25	64	bank ht	131	w/d ratio	
69	7.62	7.38	71.0	W/wood pore area	9.1	er ratio		47	4.51	8.49	740	W/wood pore area	6.0	er ratio	
83	7.43	7.57	hydraulics					51	4.43	8.57	hydraulics				
88	7.76	7.24	4.5	velocity (ft/sec)				52.5	4.05	8.95	4.3	velocity (ft/sec)			
95	7.68	7.32	50.0	discharge rate, Q (cfs)				54	4.19	8.81	50.0	discharge rate, Q (cfs)			
99	7.16	7.84	0.85	shear stress (lb/ft ²)				57	4.7	8.3	0.87	shear stress (lb/ft ²)			
106	6.61	8.39	0.66	shear velocity (ft/sec)				61.2	5.22	7.78	0.67	shear velocity (ft/sec)			
112	6.45	8.55	4.399	unit stream power (lb/ft ² /sec)				65	5.33	7.67	4.280	unit stream power (lb/ft ² /sec)			
117	6.76	8.24	0.44	Froude number				66.9	5.2	7.8	0.59	Froude number			
120	7.7	7.3	6.8	friction factor u/u*				78	5.07	7.93	55.8	friction factor u/u*			
127	9.72	5.28	53.2	threshold grain size (mm)				84.5	5.01	7.99					
129.5	10.29	4.71						89.5	5.05	7.95					
133	10.49	4.51						91.5	5.33	7.67					
136	11.01	3.99						97	4.47	8.53	270	3.42	9.58		
141	11.44	3.56						99	4.46	8.54	273.6	2.42	10.58		
147	11.85	3.15						104	4.47	8.53	275.9	4.84	8.16		
150.6	12.28	2.72						107	4.6	8.4	276.4	5.53	7.47		
152.7	11.9	3.1						113.8	7	6	280.2	5.91	7.09		
155.3	12.38	2.62						118.5	8.31	4.69	286.1	5.76	7.24		
155.9	12.28	2.72						120.2	8.62	4.38	288.8	4.32	8.68		
157	12.36	2.64						123.6	8.51	4.49	289.2	3.1	9.9		
158.1	13.02	1.98						126	8.84	4.16	290	2.43	10.57		
159.2	14.33	0.67						128.4	8.53	4.47	293	1.65	11.35		
161.2	14.39	0.61						130	8.76	4.24	296.7	1.39	11.61		
163.6	14.67	0.33						135	8.57	4.43	296.7	1.23	11.77		
165.4	14.43	0.57						136	8.81	4.19					
165.9	13.89	1.41						141	8.84	4.16					
166.3	13.02	1.98						144.5	8.97	4.03					
167	12.88	2.12						148.3	8.57	4.43					
168.3	12.7	2.3						150.7	8.5	4.5					
169	12.83	2.17						153	8.74	4.26					
171.4	12.54	2.46						154	8.98	4.02					
172.7	12.59	2.41						155.3	8.87	4.13					
173.8	12.42	2.58						156.4	8.91	4.09					
175	12.52	2.48						157	9.42	3.58					
177.1	12.26	2.74						157.8	9.49	3.51					
177.8	12.37	2.63						158.5	9.34	3.66					
179	12.3	2.7						160.3	9.44	3.56					
180	12.12	2.88						161.1	9.35	3.65					
181.5	11.89	3.11						162	9.48	3.52					
182.1	12.67	2.33						162.7	9.62	3.38					
183.3	11.7	3.3						163.5	10.12	2.88					
185.4	11.91	3.09						164.1	10.26	2.74					
186.9	11.69	3.31						165.7	10.26	2.74					
190.7	11.71	3.29						167.2	10.24	2.76					
196.7	11.38	3.62						169.3	10.49	2.51					
199.7	11.34	3.66						170	11.12	1.88					
203.3	12.1	2.9						171.6	10.07	2.93					
208	11.5	3.5						172.5	9.95	3.05					
212	10.58	4.42						173.3	9.78	3.22					
217.4	7.67	7.33						174.8	9.8	3.2					
220	7.37	7.63						175.6	9.81	3.19					
234	7.45	7.55						176.3	11.48	1.52					
239	6.99	8.01						177.1	11.19	1.81					
247.3	7.28	7.72						178	12.23	0.77					
250	7.61	7.39						179.1	11.29	1.71					
256.3	7.3	7.7						180.6	10.13	2.87					
262.9	4.96	10.04						181.3	10.06	2.94					
263.7	4.83	10.17						182	9.49	3.51					
263.7	4.45	10.55						183.7	8.86	4.14					

Table B-13. Measurements at Cross Sections 3 and 2

Cross-section F4 West, NMED3 Date 8/20/02 height of instrument (ft): 14							Cross-section F4 West, NMED2 Date 7/30/2002 height of instrument (ft): 12								
distance (ft)	FS (ft)	elevation	FS bankfull	FS top of bank	Wfipa (ft)	channel slope (%)	Mannings "n"	distance (ft)	FS (ft)	elevation	FS bankfull	FS top of bank	Wfipa (ft)	channel slope (%)	Mannings "n"
-1	7.08	6.92	10.854	7.21	56.0	1.8	0.04	-1	3.61	8.39	8.5	5.08	125.0	1.1	0.04
0	7.32	6.68	3.146	6.79				0	4	8	3.5	6.92			
5	7.48	6.52						9	4.32	7.68					
10	7.48	6.52	dimensions						18	5.22	6.78	dimensions			
15	7.5	6.5	108	x-section area	1.2	dmean		25	5.54	6.46	195	x-section area	0.6	dmean	
20	7.52	6.48	92	width	120	wet P		33	5.72	6.28	314	width	364	wet P	
25	7.27	6.73	20	dmax	0.9	hydrad		51	5.54	6.46	26	dmax	0.5	hydrad	
35	7.4	6.6	57	bank ht	7.8	w/d ratio		74.3	5.29	6.71	60	bank ht	504	w/d ratio	
45	7.61	6.39	550	W/wood prone area	6.1	entratio		87	5.01	6.99	1250	W/wood prone area	4.0	entratio	
55	7.77	6.23	hydraulics						108.3	5.08	6.92	hydraulics			
65	7.6	6.4	4.6	velocity (ft/sec)				112.5	5.08	6.92	26	velocity (ft/sec)			
734	7.04	6.96	50.0	discharge rate, Q (cfs)				112.7	7.79	4.21	50.1	discharge rate, Q (cfs)			
78.5	7.54	6.46	1.01	shear stress (lb/ft ²)				113.5	8.06	3.94	0.37	shear stress (lb/ft ²)			
88.7	6.77	7.23	0.72	shear velocity (ft/sec)				114.6	7.77	4.23	0.44	shear velocity (ft/sec)			
99	6.9	7.1	6.103	unit stream power (lb/ft ² /sec)				117.3	8.67	3.33	1.038	unit stream power (lb/ft ² /sec)			
101	7.01	6.99	0.57	Froude number				118.7	8.57	3.43	0.33	Froude number			
104.7	7.21	6.79	64	friction factor u/f				121.7	8.8	3.2	5.9	friction factor u/f			
106.5	7.4	6.6	734	threshold grain size (mm)				123.8	9.09	2.91	21.8	threshold grain size (mm)			
109.8	8.28	5.72						124.3	9.31	2.69					
111.6	8.8	5.2						124.7	9.57	2.43					
115	9.86	4.14						125.7	9.12	2.88	243	486	7.14		
116.7	9.96	4.04						126.8	8.92	3.03	254.6	499	7.01		
117.7	9.8	4.2						127.2	9.07	2.93	263	439	7.61		
120	10.28	3.72						127.7	10.83	1.17					
123.6	10.01	3.99						128.6	11.08	0.92					
127.5	10.15	3.85						130	10.77	1.23					
129.5	10.48	3.52						130.3	8.72	3.28					
132.2	10.79	3.21						131.3	8.55	3.45					
133.5	10.98	3.02						135	8.98	3.02					
135	10.8	3.2						136.4	8.79	3.21					
137	10.86	3.14						137.8	9.01	2.99					
138.6	10.73	3.27						140.7	8.76	3.24					
139.3	10.84	3.16						141.9	8.35	3.65					
140.6	10.65	3.35						142.6	8.45	3.55					
142.8	10.72	3.28						143.7	8.63	3.37					
143.8	11.07	2.93						144.6	8.55	3.45					
144.2	11.37	2.63						147.1	8.73	3.27					
144.6	11.36	2.64						148	8.86	3.14					
146.5	11.16	2.84						150	8.76	3.24					
149	11.04	2.96						152.9	8.98	3.02					
151.1	10.83	3.17						154.4	9.36	2.64					
152.1	11.04	2.96						155.3	9.58	2.42					
152.6	11.99	2.01						155.9	9.3	2.7					
153.7	12.53	1.47						156.4	9.76	2.24					
154.3	12.3	1.7						157.3	9.44	2.56					
154.5	10.89	3.11						158	8.94	3.06					
155.6	10.6	3.4						159	8.79	3.21					
157	10.68	3.32						159.6	9.53	2.47					
158.1	11.71	2.29						160.6	9.08	2.92					
158.2	11.75	2.25						161.4	9.23	2.77					
159.9	12.86	1.14						162.1	8.89	3.11					
161.8	12.66	1.34						163.4	8.86	3.14					
162.3	12.75	1.25						163.7	9.27	2.73					
163.3	10.9	3.1						164.5	9.19	2.81					
163.9	10.48	3.52						164.9	8.74	3.26					
165	10.4	3.6						165.7	8.54	3.46					
166	10.05	3.95						167.2	8.46	3.54					
168.3	8.93	5.07						168.3	8.42	3.58					
170.2	7.71	6.29						169.4	8.59	3.41					
170.7	6.06	7.94						170.3	8.5	3.5					
176	5.95	8.05						172	8.35	3.65					
183	5.86	8.14						173	8.43	3.57					
188	5.54	8.46						173.7	8.58	3.42					
188	5.13	8.87						175	8.56	3.44					
193.3	5.62	8.38						176.3	8.44	3.55					
195	5.85	8.15						179.3	7.81	4.19					
203	6.01	7.99						181.3	8.16	3.84					

Table B-14. Measurements at Cross Section 1

Cross-section F4 West, NVED1							
Date 7/29/2002							
Height of instrument (ft): 14							
distance (ft)	FS (ft)	elevation	FS bankfull	FS top of bank	W/tpa (ft)	channel slope(%)	Manning's "n"
-1	5.53	8.47	11.519	8.605	76.0	1.2	0.04
0	5.89	8.11	2.481	5.335			
8	6.3	7.7					
15.4	6.8	7.2					
28	7.23	6.77					
43	7.45	6.55					
47.6	7.75	6.25					
50.7	8.23	5.77					
53.4	7.71	6.29					
58	7.59	6.41					
74	7.59	6.41					
86	7.67	6.33					
86	7.705	6.295					
102	7.765	6.235					
104.5	8.175	5.825					
109	8.425	5.575					
115	8.165	5.835					
121	8.105	5.895					
125.6	8.455	5.545					
140.6	9.935	4.065					
143	10.275	3.725	300	9.325	4.675		
146	11.335	2.665	304	9.325	4.675		
147.4	11.605	2.395	310	7.285	6.715		
152.7	11.815	2.185	318	3.735	10.235		
154.5	12.145	1.855					
156.1	12.125	1.875					
157.3	11.925	2.075					
157.9	12.025	1.975					
158.9	12.015	1.985					
159.5	11.905	2.095					
160.9	11.965	2.035					
161.9	11.815	2.185					
164	12.145	1.855					
167.2	11.765	2.235					
169	12.205	1.795					
171	11.655	2.345					
172.3	11.915	2.085					
175	11.855	2.145					
176.5	11.755	2.245					
179	11.665	2.335					
180.6	11.705	2.295					
181.5	11.545	2.455					
182.4	11.815	2.185					
183.4	11.485	2.515					
185	11.815	2.185					
186.7	11.945	2.055					
187.8	11.645	2.355					
188.8	11.835	2.165					
189.2	13.355	0.645					
190	13.185	0.815					
191	12.905	1.095					
192.2	12.015	1.985					
193.5	11.395	2.615					
194.5	12.105	1.895					
195.2	11.805	2.195					
196.8	11.815	2.185					
198	11.935	2.065					
198.7	11.825	2.175					
200.3	11.985	2.005					
201.5	11.825	2.175					
203.1	12.125	1.875					
203.9	11.625	2.375					
205.5	11.965	2.035					
206.3	11.875	2.125					
207	12.145	1.855					
207.7	11.785	2.215					
208.3	11.685	2.315					

dimensions			
239	x-section area	0.4	dmean
61.9	width	64.6	wet P
1.8	dmax	0.4	hydrat
4.8	bank ht	160.2	w/d ratio
76.0	W/wood pore area	1.2	er ratio

hydraulics	
2.1	velocity (ft/sec)
50.1	discharge rate, Q (cfs)
0.28	shear stress (lb/ft ²)
0.38	shear velocity (ft/sec)
0.607	unit stream power (lb/ft ² /sec)
0.35	Froude number
5.6	friction factor u/u*
15.2	threshold grain size (mm)

Appendix C. Stream Classification, Dimension, and Hydraulic Summaries

Description of terms for “Dimension and classification summaries” in Table C-1

Cross Sections are ordered from the most downstream location, cross section P4W-1, upstream to P4W-20.

Distance on longitude (from upstream x-sec 20) is the distance from the western extent of this study, approximately 60 feet above cross section P4W-20 to the cross section being reviewed.

Entrenchment Ratio (W_{fpa} / W_{bkf}) is the flood prone width divided by the bankfull width.

Width to depth ratio Width / Depth Ratio (W_{bkf} / d_{bkf}) is the channel width at bankfull stage divided by the mean depth.

Channel Slope (S) is the “rise over run” for a reach approximately 20 to 30 bankfull channel widths in length with the “riffle to riffle” surface slope representing the gradient at bankfull stage. Slope is determined from longitudinal profile data.

Sinuosity (Stream Length / Valley Distance) is the measure of stream pattern geometry

Classification of streams from dimension, pattern, and profile parameters based on Rosgen (1996),

Classification Key for 8 stream types (Rosgen, 1996)

Stream Type	Entrenchment Ratio	W / D Ratio	Sinuosity	Slope
A	<1.4	<12	1.0 to 1.2	0.04 to 0.10
B	1.4 to 2.2	>12	1.0 to 1.2	0.02 to 0.039
C	>2.2	>12	>1.2	<0.02
D	N/A	>40	N/A	<0.04
DA	>2.2	Highly variable	Highly variable	<0.005
E	>2.2	<12	>1.5	<0.02
F	<1.4	>12	>1.2	<0.02
G	<1.4	<12	<1.2	0.02 to 0.039

Entrenchment Ratio (W_{fpa} / W_{bkf})

Width / Depth Ratio (W_{bkf} / d_{bkf})

Sinuosity (Stream Length / Valley Distance)

Slope (Vertical Distance, Ft. / Linear Distance, Ft)

where:

Width of Flood prone Area (W_{fpa})

Bankfull Width (W_{bkf})

Bankfull Mean Depth (d_{bkf})

Table C-1. Summary table of cross section classifications and stream dimensions

Cross Section	Distance on longitude (from Entrenchment upstream x-sec 20)	W/d ratio	W/d ratio	Slope	Sinuosity (braided)*	Classification
P4W-1	2935.0	1.2	160.2	0.012	Multi chan*	(DA) F
P4W-2	2627.0	4.0	50.4	0.011	Multi chan*	(DA) C
P4W-3	2318.0	6.1	7.8	0.018	Multi chan*	(DA) E
P4W-4	1882.0	6.0	13.1	0.017	Multi chan*	(DA) C
P4W-5a	1604.0	9.1	5.5	0.011	1.03	E
P4W-5	1568.0	6.3	10.9	0.003	1.12	E
P4W-5b	1563.0	7.2	4.5	0.010	1.12	E
P4W-6	1503.0	2.1	32.3	0.014	1.13	Bc
P4W-5c	1445.0	3.2	15.7	0.011	1.14	C
P4W-5d	1385.0	13.1	2.0	0.013	1.01	E
P4W-6b	1260.0	5.0	11.8	0.013	1.15	E
P4W-7	1175.0	5.1	7.8	0.019	1.15	E
P4W-9	997.0	3.5	3.1	0.008	1.11	E
P4W-8	965.0	8.0	1.6	0.014	1.38	E
P4W-11	871.0	2.1	5.6	0.014	1.10	E?
P4W-10	718.0	1.2	8.6	0.016	1.03	G
P4W-11c	618.0	4.1	3.6	0.023	1.08	Eb
P4W-11a	537.0	2.8	20.3	0.018	1.05	C
P4W-12	465.0	3.3	3.5	0.012	1.07	E
P4W-13	405.0	15.7	0.9	0.016	1.06	E
P4W-14	367.0	3.2	18.7	0.017	oblique x-sec	C?
P4W-15	302.0	2.0	7.0	0.022	1.14	Eb?
P4W-16	277.0	2.7	3.7	0.020	1.04	E-Eb?
P4W-17	255.0	1.9	7.0	0.030	1.04	B? Eb?
P4W-18	233.0	1.3	13.2	0.092	Falls	F
P4W-19	208.0	8.7	21.1	0.092	Multi chan*	(DA) C
P4W-20	60.0	23.7	23.9	0.026	Multi chan*	(DA) C
Mean		5.7	17.2	0.021	1.11	
Median		4.0	7.8	0.016	1.10	
Std Deviation		5.1	30.6	0.021	0.08	
Minimum		1.2	0.9	0.003	1.01	
Maximum		23.7	160.2	0.092	1.38	

*Multiple braided channels

Description of terms for “Dimension summaries” in Table C-2.

The Cross Section and distance column references are the same as Table C-1.

Bankfull Cross-Section Area (A_{bkf}) is the area of the stream channel cross section at bankfull stage in riffle sections of the stream.

Bankfull Width (W_{bkf}) is the width of the stream channel at bankfull stage in riffle sections of a stream.

Maximum Bankfull Depth (d_{mbkf}) is the maximum depth of flow at bankfull stage.

Bank Height is the height of the lowest bank, measured from the channel bed (thalweg) to the top of the bank.

Bank Height helps describe entrenchment. Over-bank flow begins at this stage defined by bank height.

Width of the flood prone area (W_{fpa}) is the flooded width at flood prone height.

It is used to define entrenchment and forms the entrenchment ratio when divided by the bankfull width

Bankfull Mean Depth (d_{bkf}) = $(A_{bkf}) / (W_{bkf})$
 (A_{bkf}) = cross section area (square feet)
 (W_{bkf}) = width at bankfull stage (feet)

This is the area of the stream channel cross section at bankfull stage in a riffle cross-section.

Wetted Perimeter (P) (feet) is the perimeter of the channel cross section formed by the bed and banks.

Hydraulic Radius (R) (feet) = $(A_{bkf}) / P$ is one functional parameter used to describe resistance to flow

(A_{bkf}) = cross section area (ft²)
P = wetted perimeter (ft)

Hydraulic functions in Summary Table C-3

The Cross Section and distance column references are the same as Table C-1.

Discharge rate (Q) (cfs) = V (A_{bkf})

Velocity (V) (ft / sec) = $(1.487 \times R^{2/3} \times (S / 100)^{1/2}) / n$
n = Mannings “n” coefficient

$$\text{Shear Stress (pounds / ft}^2\text{)} = 62.4 \times R \times S$$

62.4 = density of water (lbs / ft³)

$$\text{Shear Velocity} = (32.2 \times R \times S)^{1/2}$$

32.2 = gravitational acceleration (ft / sec²)

$$\text{Unit stream power (lbs/ft/sec)} = \text{power / unit area} = \text{density of water} \times Q \times S/W = \text{Shear Stress} \times V$$

Density of water = lbs / ft³

$$\text{Froude number} = V^2 / 32.2 \times \text{Maximum Bankfull Depth (d}_{\text{mbkf}})$$

This is a dimensionless number expressing the ratio of inertial to gravitational forces. Values less than 1 are termed sub critical and are characteristic of relatively deep, slow stream flow. Values of 2q denote “critical” flow. Values greater than 1 are termed supercritical and are characteristic of shallow fast streams.

$$\text{Friction Factor } u/u^* = V / \text{shear velocity}$$

Values vary from about 2 for rough streambeds to 16 for smooth.

Threshold grain size (mm) is the size particles predicted to be at “the threshold of motion” at the shear stress calculated. It is found from Shield’s curve, which is a plot of particle size against the critical shear stress or the shear stress required to initiate movement.

Table C-2. Summary table of cross section stream dimensions

Cross Section	Distance on longitude (from upstream x-sec 20)	X-section area	Width	D max	Bank ht	W flood prone area	Depth mean	Wetted perimeter	Hydraulic radius
P4W-1	2935.0	23.9	61.9	1.8	4.8	76.0	0.4	64.6	0.4
P4W-2	2627.0	19.5	31.4	2.6	6.0	125.0	0.6	36.4	0.5
P4W-3	2318.0	10.8	9.2	2.0	5.7	56.0	1.2	12.0	0.9
P4W-4	1882.0	11.7	12.4	2.5	6.4	74.0	0.9	14.3	0.8
P4W-5a	1604.0	11.1	7.8	1.8	7.0	71.0	1.4	8.9	1.2
P4W-5	1568.0	22.2	15.6	3.3	8.4	98.0	1.4	19.0	1.2
P4W-5b	1563.0	12.6	7.5	2.8	6.5	54.0	1.7	11.4	1.1
P4W-6	1503.0	15.7	22.5	2.6	5.5	47.0	0.7	25.5	0.6
P4W-5c	1445.0	15.2	15.5	3.1	6.2	50.0	1.0	19.5	0.8
P4W-5d	1385.0	7.7	3.9	2.1	5.7	51.0	2.0	4.0	1.9
P4W-6b	1260.0	12.8	12.3	2.5	6.3	62.0	1.0	14.5	0.9
P4W-7	1175.0	10.4	9.0	2.5	6.4	46.0	1.2	11.4	0.9
P4W-9	997.0	10.6	5.7	2.3	6.6	20.0	1.9	6.2	1.7
P4W-8	965.0	7.4	3.5	2.4	9.1	28.0	2.1	3.9	1.9
P4W-11	871.0	10.2	7.5	1.6	6.3	16.0	1.4	8.7	1.2
P4W-10	718.0	10.2	9.4	1.2	7.6	11.0	1.1	9.7	1.1
P4W-11c	618.0	8.6	5.5	2.0	5.8	23.0	1.5	8.2	1.0
P4W-11a	537.0	13.2	16.3	2.9	6.3	45.0	0.8	19.9	0.7
P4W-12	465.0	11.5	6.4	2.7	6.1	21.0	1.8	10.5	1.1
P4W-13	405.0	5.8	2.3	2.6	8.6	36.0	2.5	2.4	2.5
P4W-14	367.0	13.0	15.6	2.7	6.9	50.0	0.8	18.4	0.7
P4W-15	302.0	8.8	7.8	1.6	6.0	16.0	1.1	8.3	1.1
P4W-16	277.0	8.1	5.5	1.8	6.4	15.0	1.5	6.4	1.3
P4W-17	255.0	7.7	7.3	1.3	5.9	14.0	1.0	7.5	1.0
P4W-18	233.0	6.1	9.0	1.2	6.0	12.0	0.7	10.0	0.6
P4W-19	208.0	7.3	12.4	2.5	5.3	107.0	0.6	15.2	0.5
P4W-20	60.0	12.0	16.9	2.4	4.2	NM*	0.7	20.6	0.6
Mean		11.6	12.6	2.3	6.4	60.1	1.2	14.7	1.0
Median		10.8	9.0	2.4	6.3	47.0	1.1	11.4	1.0
Std Deviation		4.5	11.7	0.6	1.1	74.4	0.5	12.4	0.5
Minimum		5.8	2.3	1.2	4.2	11.0	0.4	2.4	0.4
Maximum		23.9	61.9	3.3	9.1	125.0	2.5	64.6	2.5

* Not measured, > 200 feet

Table C-3. Summary table of cross section stream hydraulics

Cross Section	Distance on longitude (from upstream x-sec 20)	Discharge rate, Q (cfs)	Velocity (ft/sec)	Shear stress (lbs/ft sq)	Shear velocity (ft/sec)	Unit stream power (lbs/ft/sec)	Froude number	Friction factor u/u*	Threshold grain size (mm)
P4W-1	2935.0	50.1	2.1	0.3	0.4	0.6	0.4	5.6	15.2
P4W-2	2627.0	50.1	2.6	0.4	0.4	1.1	0.3	5.9	21.8
P4W-3	2318.0	50.0	4.6	1.0	0.7	6.1	0.6	6.4	73.4
P4W-4	1882.0	50.0	4.3	0.9	0.7	4.3	0.6	6.3	55.8
P4W-5a	1604.0	50.0	4.5	0.9	0.7	4.4	0.4	6.8	53.2
P4W-5	1568.0	50.1	2.3	0.2	0.3	0.6	0.1	6.7	12.5
P4W-5b	1563.0	50.0	4.0	0.7	0.6	4.2	0.3	6.7	43.9
P4W-6	1503.0	50.0	3.2	0.5	0.5	1.9	0.5	6.0	33.3
P4W-5c	1445.0	50.0	3.3	0.5	0.5	2.2	0.3	6.3	32.9
P4W-5d	1385.0	50.0	6.5	1.6	0.9	10.4	0.7	7.3	170.6
P4W-6b	1260.0	50.1	3.9	0.7	0.6	3.3	0.5	6.4	45.7
P4W-7	1175.0	50.0	4.8	1.1	0.7	6.6	0.6	6.5	84.4
P4W-9	997.0	50.0	4.7	0.8	0.7	4.4	0.4	7.2	52.6
P4W-8	965.0	50.3	6.8	1.7	0.9	12.6	0.7	7.3	197.2
P4W-11	871.0	50.0	4.9	1.0	0.7	5.8	0.5	6.7	76.1
P4W-10	718.0	50.0	4.9	1.1	0.7	5.3	0.7	6.6	80.5
P4W-11c	618.0	50.0	5.8	1.5	0.9	12.9	0.7	6.6	160.9
P4W-11a	537.0	50.0	3.8	0.7	0.6	3.4	0.6	6.1	47.7
P4W-12	465.0	50.0	4.3	0.8	0.7	5.9	0.3	6.7	49.6
P4W-13	405.0	50.0	8.6	2.5	1.1	21.7	0.9	7.6	421.0
P4W-14	367.0	50.0	3.8	0.8	0.6	3.4	0.6	6.2	48.2
P4W-15	302.0	50.0	5.7	1.4	0.9	8.8	0.9	6.6	148.6
P4W-16	277.0	50.1	6.2	1.6	0.9	11.5	0.8	6.8	181.9
P4W-17	255.0	50.0	6.5	1.9	1.0	12.8	1.3	6.6	255.9
P4W-18	233.0	50.0	8.1	3.5	1.3	31.9	3.0	6.0	840.6
P4W-19	208.0	50.0	6.9	2.7	1.2	23.2	2.5	5.8	518.6
P4W-20	60.0	50.0	4.2	0.9	0.7	4.8	0.8	6.0	64.7
Mean		50.0	4.9	1.2	0.7	7.9	0.7	6.5	140.2
Median		50.0	4.6	0.9	0.7	5.3	0.6	6.6	64.7
Std Deviation		0.3	1.7	0.8	0.2	7.5	0.6	0.5	184.8
Minimum		48.6	2.1	0.2	0.3	0.6	0.1	5.6	12.5
Maximum		50.3	8.6	3.5	1.3	31.9	3.0	7.6	840.6

Appendix D. Latitude-Longitude Coordinates for Cross Section End Points

The coordinates for features used in this report were measured with a handheld Trimble GeoExplorer III[®] GPS data collection system, using Pathfinder Office software to differentially correct the data. The data was corrected to the base station operated by the Institute for Engineering Research and Applications (IERA) Center, located in Albuquerque, New Mexico. IERA is part of the New Mexico Institute of Mining and Technology.

Table D1. Cross section end point coordinates

<i>Pueblo Canyon P-4 West Cross-Section end-point coordinates</i>				
<i>Cross section</i>	<i>North end point (Left bank)</i>		<i>South end point (Right bank)</i>	
	<i>dd mm ss.sss</i>	<i>ddd mm ss.sss</i>	<i>dd mm ss.sss</i>	<i>ddd mm ss.sss</i>
P4-W 20	35 52 39.10	106 13 35.66	35 52 36.30	106 13 36.53
P4-W 19	35 52 37.44	106 13 35.17	35 52 38.66	106 13 34.44
P4-W 18	35 52 38.57	106 13 33.98	35 52 37.05	106 13 34.90
P4-W 17	35 52 38.05	106 13 33.39	35 52 36.67	106 13 36.10
P4-W 16	35 52 38.05	106 13 33.39	35 52 36.90	106 13 34.65
P4-W 15	35 52 37.93	106 13 33.24	35 52 36.99	106 13 34.13
P4-W 14	35 52 37.64	106 13 32.65	35 52 36.58	106 13 33.68
P4-W 13	35 52 37.68	106 13 32.36	35 52 36.32	106 13 33.25
P4-W 12	35 52 37.18	106 13 31.91	35 52 32.75	106 13 34.54
P4-W 11b	35 52 36.82	106 13 31.14	35 52 35.65	106 13 32.05
P4-W 11c	35 52 36.42	106 13 30.04	35 52 35.06	106 13 31.87
P4-W 10	35 52 35.92	106 13 29.37	35 52 32.55	106 13 33.64
P4-W 11	35 52 33.31	106 13 29.88	35 52 34.41	106 13 33.06
P4-W 8	35 52 34.52	106 13 27.43	35 52 32.00	106 13 31.54
P4-W 9	35 52 33.31	106 13 29.88	35 52 32.27	106 13 30.07
P4-W 7	35 52 32.20	106 13 27.69	35 52 31.63	106 13 29.44
P4-W 6b	35 52 32.08	106 13 24.27	35 52 30.84	106 13 29.35
P4-W 5d	35 52 32.41	106 13 26.60	35 52 29.70	106 13 27.30
P4-W 5c	35 52 32.16	106 13 25.81	35 52 29.44	106 13 26.69
P4-W 6	35 52 30.55	106 13 25.46	35 52 29.39	106 13 26.60
P4-W 5b	35 52 30.24	106 13 24.55	35 52 29.21	106 13 26.25
P4-W 5	35 52 30.83	106 13 23.99	35 52 29.07	106 13 26.34
P4-W 5a	35 52 30.72	106 13 23.78	35 52 28.79	106 13 25.97
P4-W 4	35 52 29.10	106 13 21.92	35 52 26.58	106 13 23.75
P4-W 3	35 52 25.95	106 13 18.36	35 52 24.54	106 13 19.94
P4-W 2	35 52 25.23	106 13 15.86	35 52 23.01	106 13 16.56
P4-W 1	35 52 24.80	106 13 12.09	35 52 22.14	106 13 13.69

Geographic Latitude/Longitude North American Datum 1983 State Plane New Mexico Central FIPS 3002 feet. Cross Section order; upstream (west) to downstream (east)

Appendix E. Cross Section Charts, Dimensions, and Remarks For P-4 West

The cross sections presented in this appendix are from the most upstream cross section 20 to the last downstream cross section 1. The distances to each cross section are measured along the stream channel from cross section 20. Refer to Plate 3 for reference.

By convention, distance at each cross section is measured from left to right when facing down stream and is presented as such. In the east to west oriented Pueblo Canyon, the left bank is generally to the north.

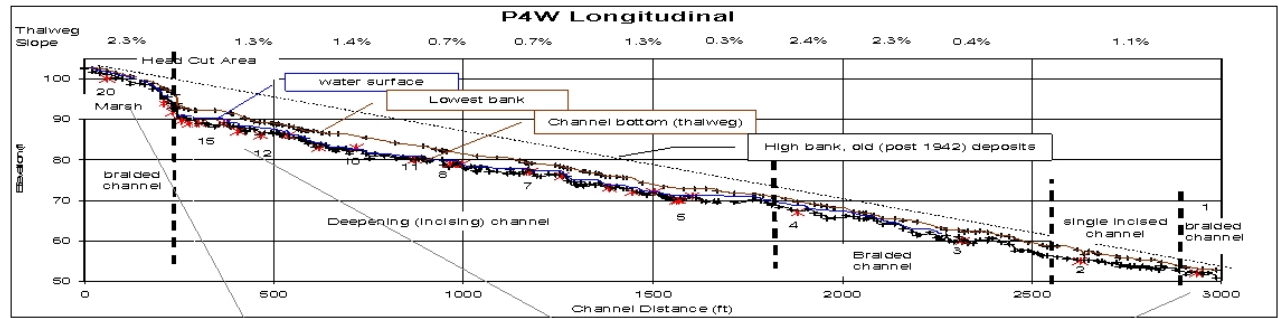
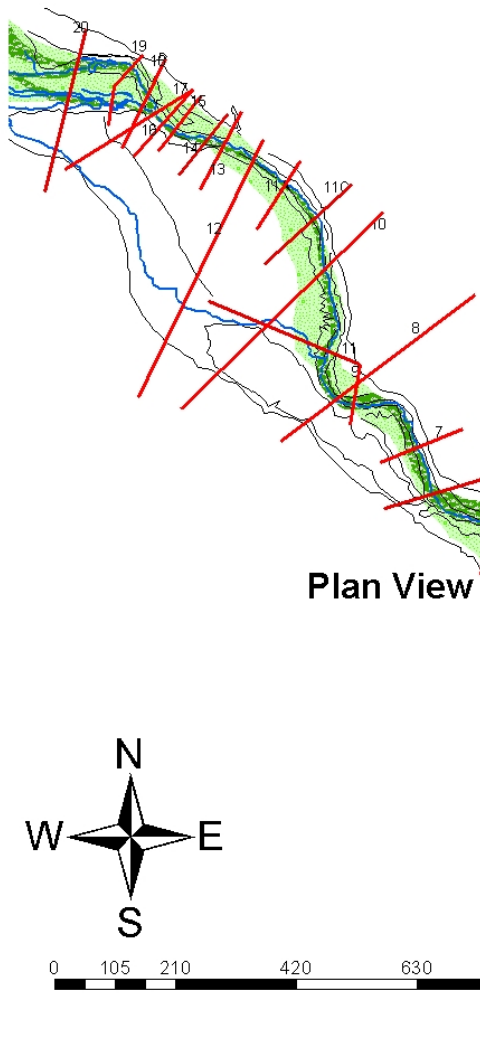
The horizontal and vertical scales have been normalized to 150 and 15 feet to present consistent scales between all cross sections. At cross sections that exceed 150 feet, the full cross section is presented on the right side of the page. At these cross sections, the ER geomorphic units are related to the cross section shape on the bottom scale.

The horizontal blue line delineates the channel banks at the maximum bankfull depth. The bankfull stage flow was estimated to be approximately 50 cfs.

The horizontal red line delineates the flood prone height, or approximately twice the maximum bankfull depth in a riffle or straight stream section. It generally includes the active floodplain and low terraces, and in most streams is associated with a < 50 year return period flood rather than with a very rare flood. This feature is used to determine entrenchment.

The comment section reflects field observations. The comments include descriptions of potential remediation efforts that could be considered, but is not inclusive of all efforts that should be considered.

C type channel

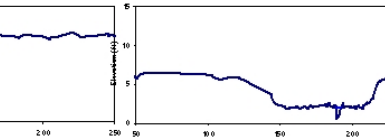
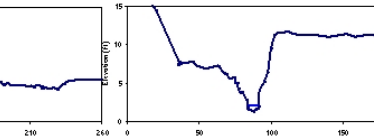
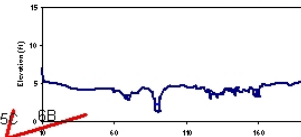


Profile

Cross Section 20, 8/20/03

Cross Section 17, 8/27/02

Cross Section 1, 7/29/02



Dimensions

Plan View

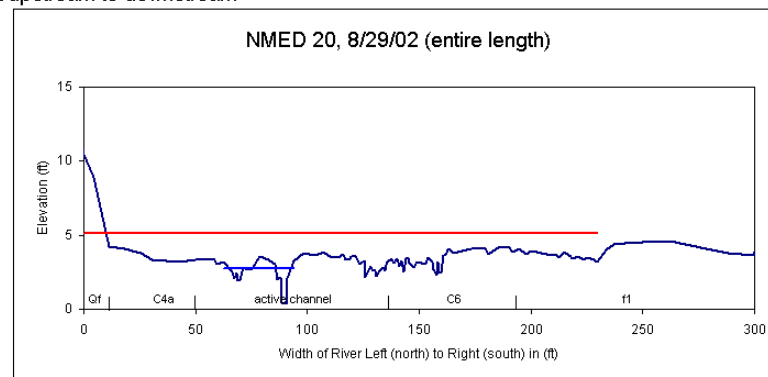
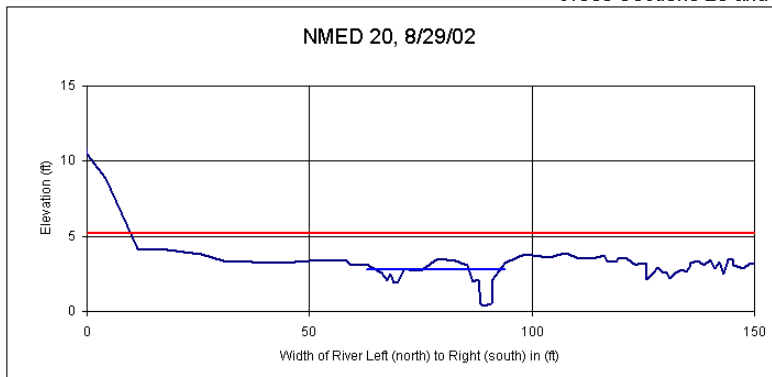
E type channel

Plate 3. Plan View, Profile, and Channel Dimensions of P4W in Pueblo Canyon

C type channel

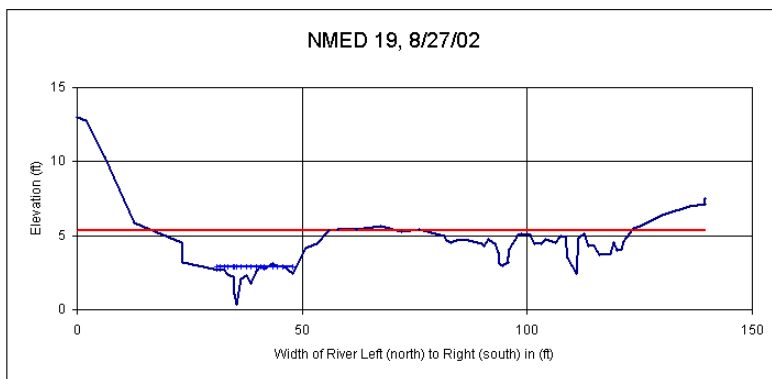
— NMED cross sections
— terrace and channel banks

Cross Sections 20 and 19, first upstream to downstream



dimensions			
12.0	x-section area	0.7	d mean
16.9	width	20.6	wet P
2.4	d max	0.6	hyd radi
4.2	bank ht	23.9	w/d ratio
400.0	W flood prone are	23.7	ent ratio

Remarks: Western upstream most cross section, C (DA) type channel, in marshy flood plain. Parallel channel appears to be cutting into northern edge of C6 unit. Depression at 229 conveys storm water during moderately high flood stage. Upstream of Cross section 20, water flows overbank characterized by features at 161. Consider sediment controls across C6 unit (terrace plains) to drop out sediments over geomorph units with high plutonium concentrations. South bank along this reach to cross section 11 should be armored (C6, c5 units exposed along high unstable banks). Flood plain units (C4a) should be protected, particularly on down stream edge where flows reenter active channel sections and erosion intensified.

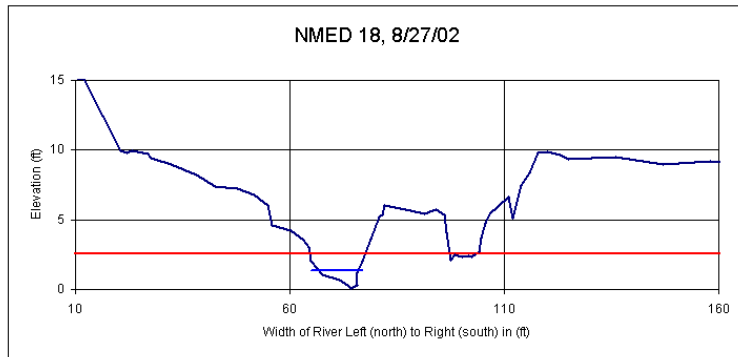


dimensions			
7.3	x-section area	0.6	d mean
12.4	width	15.2	wet P
2.5	d max	0.5	hyd radi
5.3	bank ht	21.1	w/d ratio
107.0	W flood prone are	8.7	ent ratio

Remarks: 148' downstream of cross section 20, DA type channel transitioned to C, water accelerating through channels from 94' to 124' deepening and widening channel. They are within C6 unit and should be redirected away from bank, possibly with engineered structures or natural structures (i.e. root wads).

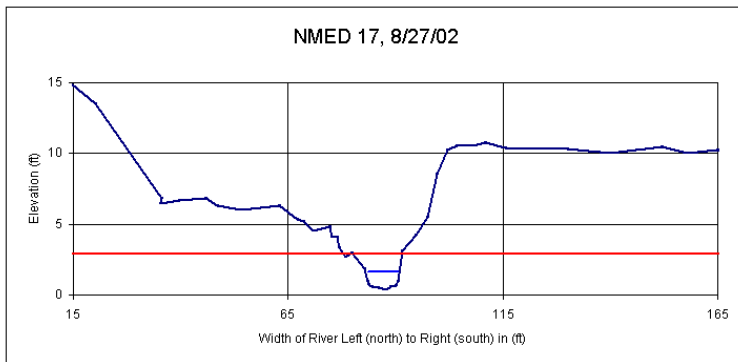
Figure E1. Cross Sections 20 and 19

Cross Sections 18 and 17, upstream to downstream



dimensions			
6.1	x-section area	0.7	d mean
9.0	width	10.0	wet P
1.2	d max	0.6	hyd radi
6.0	bank ht	13.2	w/d ratio
12.0	W flood prone are	1.3	ent ratio

Remarks: 173' downstream, F type channel, nickpoint eroded to bedrock area eroding south bank along C6 unit. South C6 bank at 106' should be armored. High banks confine channel and restricts ability to meander, creating high erosion potential in unit of large plutonium inventory.



dimensions			
7.7	x-section area	1.0	d mean
7.3	width	7.5	wet P
1.3	d max	1.0	hyd radi
5.9	bank ht	7.0	w/d ratio
14.0	W flood prone are	1.9	ent ratio

Remarks: 195' downstream, B? or Eb? (transitional) type channel, deepening and widening, particularly against high C6 unit at south bank. Sediment dampening efforts should be made on C6 terrace. C2 floodplain unit eroding at downstream edge.

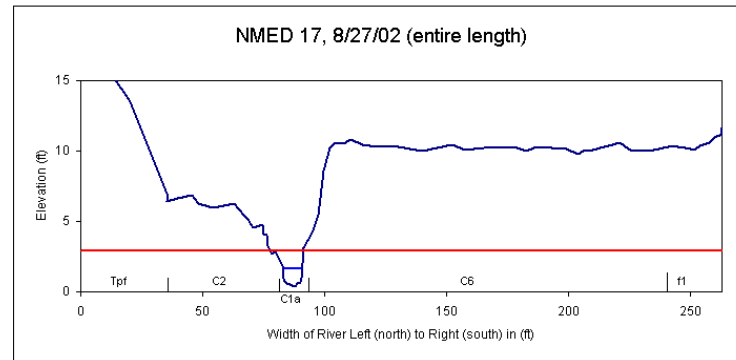
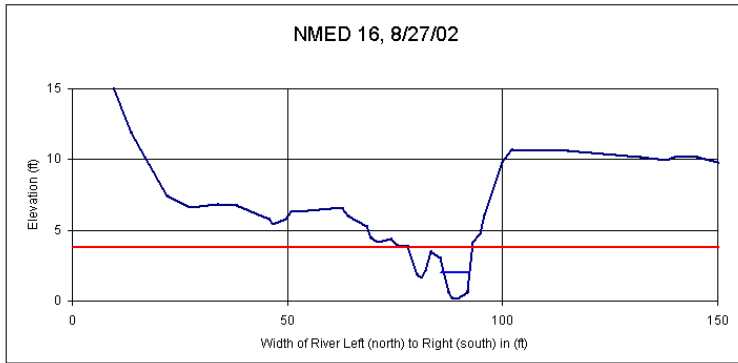


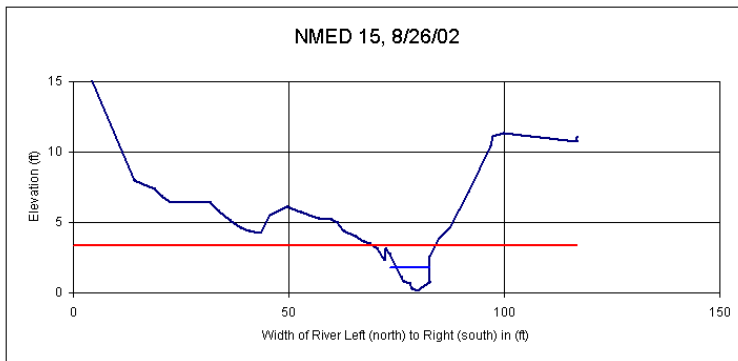
Figure E2. Cross sections 18 and 17

Cross Sections 16 and 15, upstream to downstream



dimensions			
8.1	x-section area	1.5	d mean
5.5	width	6.4	wet P
1.8	d max	1.3	hyd radi
6.4	bank ht	3.7	w/d ratio
15.0	W flood prone are	2.7	ent ratio

Remarks: 217' downstream, E or Eb? (transitional) Type channel, deepening and widening, particularly against south C6 unit bank. Same as above for terrace and lower C4 floodplain

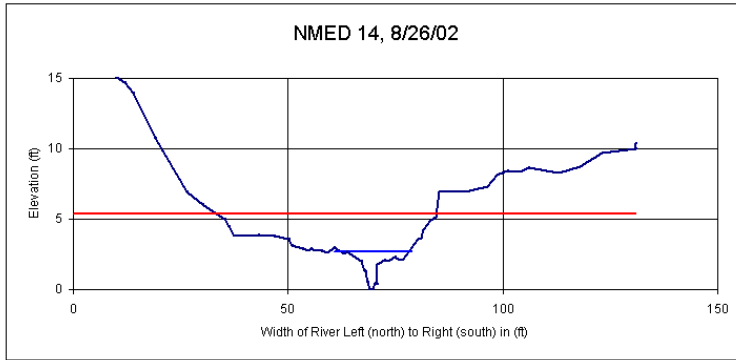


dimensions			
8.8	x-section area	1.1	d mean
7.8	width	8.3	wet P
1.6	d max	1.1	hyd radi
6.0	bank ht	7.0	w/d ratio
16.0	W flood prone are	2.0	ent ratio

Remarks: 242' downstream, Eb? (transitional) Type channel, deepening and widening, particularly against south C6 unit bank. Same as above for terrace and floodplain

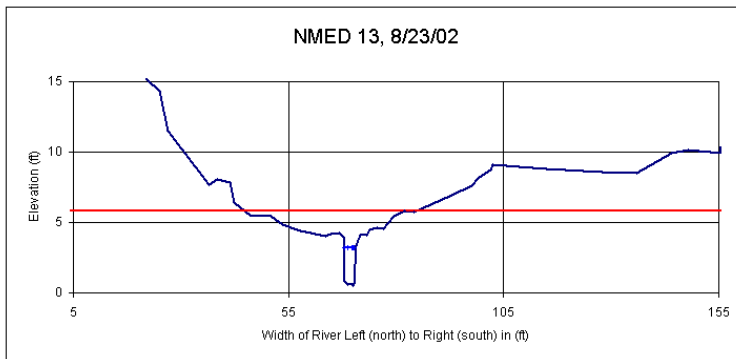
Figure E3. Cross sections 16 and 15

Cross Sections 14 and 13, upstream to downstream



dimensions			
13.0	x-section area	0.8	d mean
15.6	width	18.4	wet P
2.7	d max	0.7	hyd radi
6.9	bank ht	18.7	w/d ratio
50.0	W flood prone are	3.2	ent ratio

Remarks: 307' downstream, C type channel, deepening and widening, particularly against south C6 unit bank. Same as above for terrace

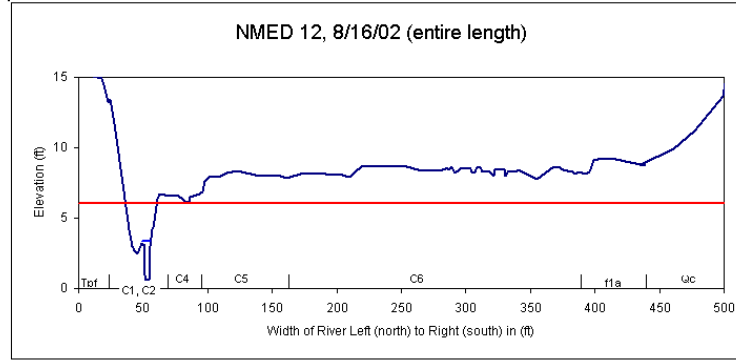
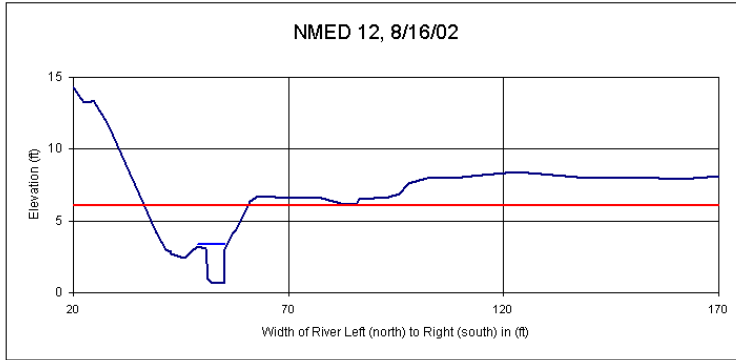


dimensions			
5.8	x-section area	2.5	d mean
2.3	width	2.4	wet P
2.6	d max	2.5	hyd radi
8.6	bank ht	0.9	w/d ratio
36.0	W flood prone are	15.7	ent ratio

Remarks: 345' downstream, E type channel, deepening channel, C4 and 5 units vulnerable to erosion from runoff in channel and overland flow across C6 unit from above cross section 20. Bank should be armored as well as sediment control measures on the C6 floodplain.

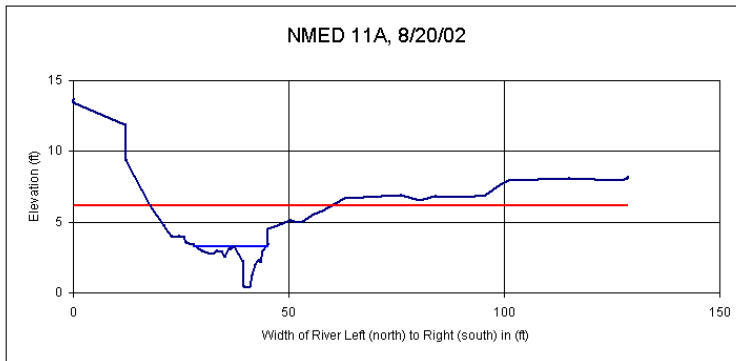
Figure E4. Cross sections 14 and 13

Cross Sections 12 and 11A, upstream to downstream



dimensions			
11.5	x-section area	1.8	d mean
6.4	width	10.5	wet P
2.7	d max	1.1	hyd radi
6.1	bank ht	3.5	w/d ratio
21.0	W flood prone are	3.3	ent ratio

Remarks: 405' downstream, E type, deepening channel, C4 and 5 units vulnerable to erosion from runoff in channel and overland flow across C6 unit from above cross section 20 (see developing channels between 300 and 350) Bank should be armored as well as sediment control measures on the C6 floodplain.

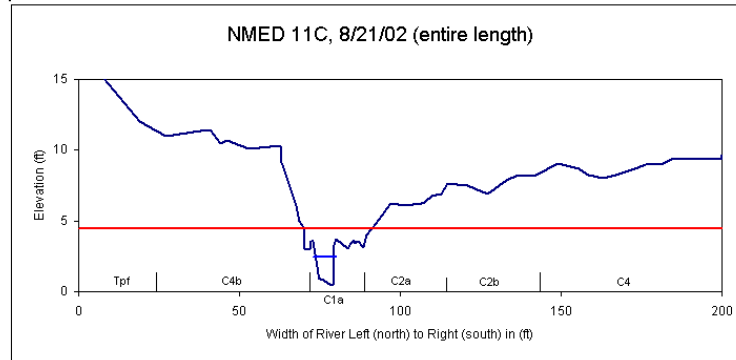
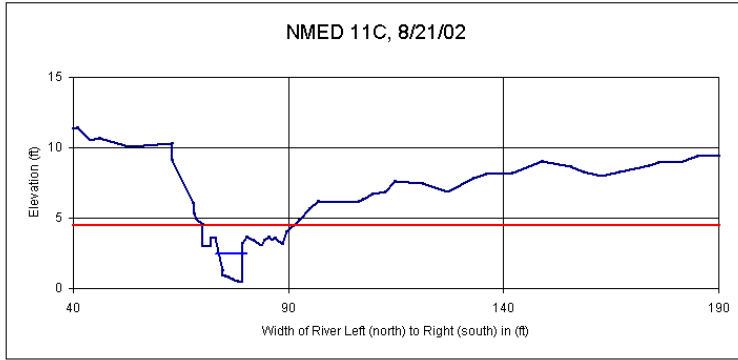


dimensions			
13.2	x-section area	0.8	d mean
16.3	width	19.9	wet P
2.9	d max	0.7	hyd radi
6.3	bank ht	20.3	w/d ratio
45.0	W flood prone are	2.8	ent ratio

Remarks: 477' downstream, C type, deepening channel, C4 and 5 units vulnerable to erosion from runoff in channel and overland flow across C6 unit from above cross section 20. Bank should be armored as well as sediment control measures on the C6 floodplain.

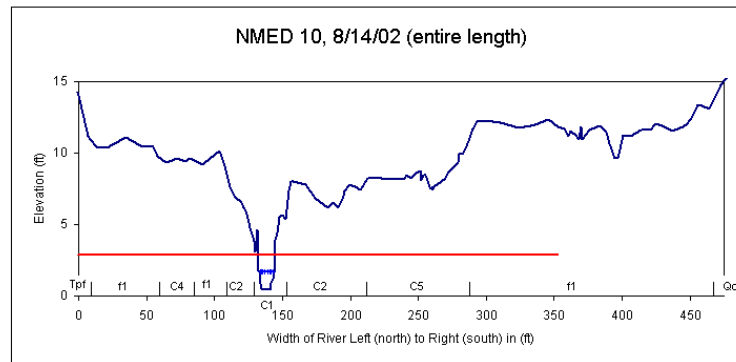
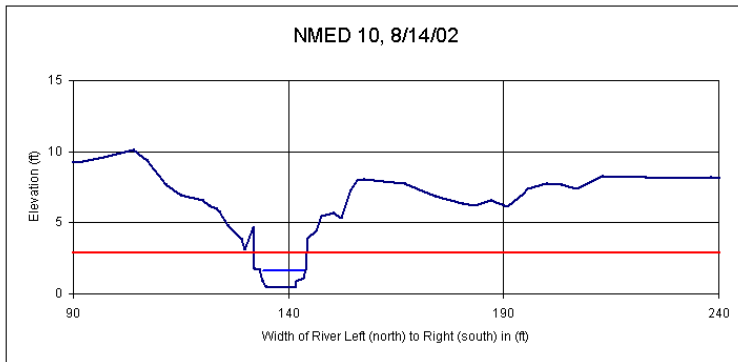
Figure E5. Cross sections 12 and 11a

Cross Sections 11C and 10, upstream to downstream



dimensions			
8.6	x-section area	1.5	d mean
5.5	width	8.2	wet P
2.0	d max	1.0	hyd radi
5.8	bank ht	3.6	w/d ratio
23.0	W flood prone are	4.1	ent ratio

Remarks: 558' downstream, Eb type, deepening channel, C4 and 5 units vulnerable to erosion from runoff in channel and overland flow across C6 unit from above cross section 20. Bank should be armored as well as sediment control measures on the C6 floodplain.

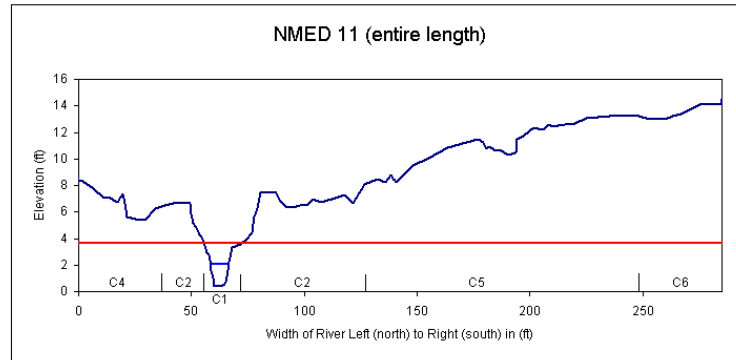
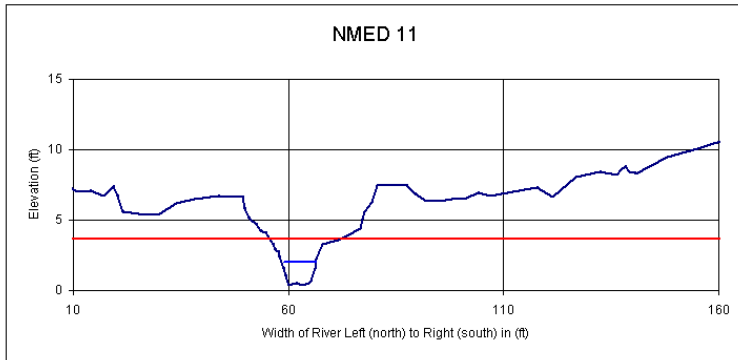


dimensions			
10.2	x-section area	1.1	d mean
9.4	width	9.7	wet P
1.2	d max	1.1	hyd radi
7.6	bank ht	8.6	w/d ratio
11.0	W flood prone are	1.2	ent ratio

Remarks: 658' downstream, G (gully) type channel, deepening and widening channel, C2 and 5 units vulnerable to erosion from runoff in channel and overland flow across C6 unit from above cross section 20. Overbank flows bifurcate into channel at 260 and 400. Flows accelerating as they reenter main channel, intensifying erosion along banks (see channel at 180 and along steepened banks). South bank should be armored as well as sediment control

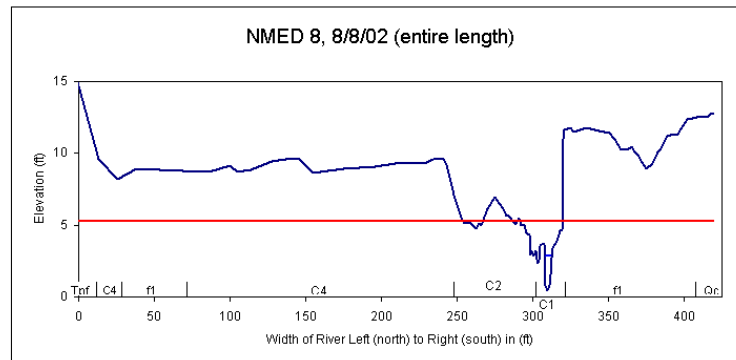
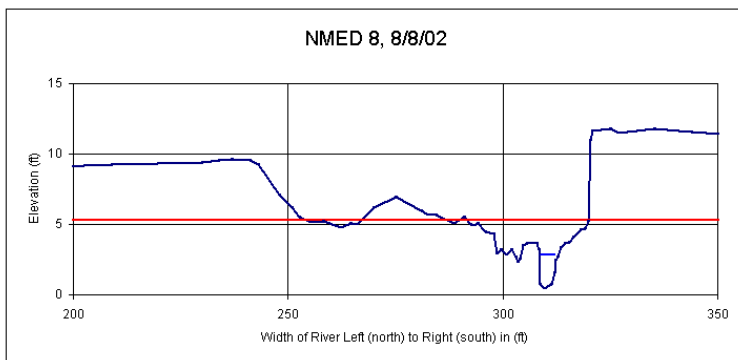
Figure E6. Cross sections 11c and 10

Cross Sections 11 and 8, upstream to downstream



dimensions			
10.2	x-section area	1.4	d mean
7.5	width	8.7	wet P
1.6	d max	1.2	hyd radi
6.3	bank ht	5.6	w/d ratio
16.0	W flood prone are	2.1	ent ratio

Remarks: 811' downstream, E? type channel, deepening channel, C2, 5, and 6 units vulnerable to erosion from runoff in channel and overland flow across C6 unit from above cross section 20. South bank should be armored as well as sediment control measures on the C6 floodplain. Rills, channels, and headcuts developing on C5 and C6 units before flowing back into main channel upstream of this section. Downstream edge of C2 floodplain eroding.

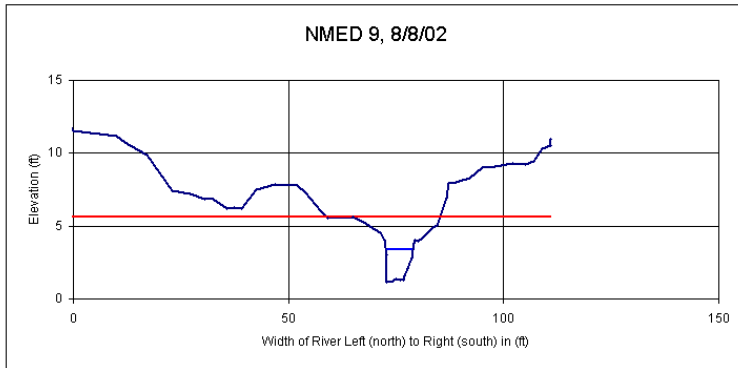


dimensions			
7.4	x-section area	2.1	d mean
3.5	width	3.9	wet P
2.4	d max	1.9	hyd radi
9.1	bank ht	1.6	w/d ratio
28.0	W flood prone are	8.0	ent ratio

Remarks: 905' downstream, E type channel, deepening and widening channel, C2 unit and C4 bank on north side of channel exposed to increased erosion, flow should be directed away from the north bank or dampened (?). Channel at 375 carries floodwaters from above cross section 20 to below cross section 6b, where reentry intensifies erosion.

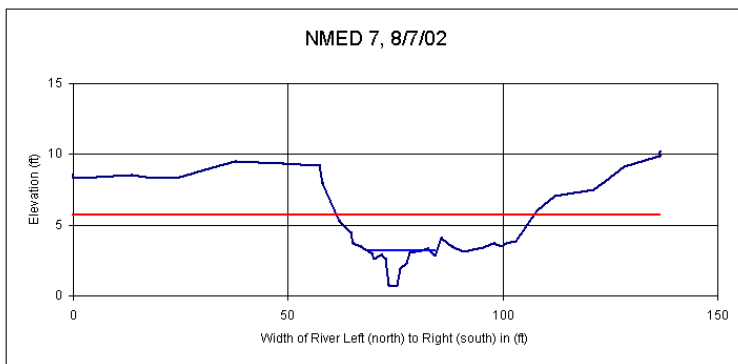
Figure E7. Cross sections 11 and 8

Cross Sections 9 and 7, upstream to downstream



dimensions			
10.6	x-section area	1.9	d mean
5.7	width	6.2	wet P
2.3	d max	1.7	hyd radi
6.6	bank ht	3.1	w/d ratio
20.0	W flood prone are	3.5	ent ratio

Remarks: 937' downstream, E type channel, deepening and widening channel, north side of channel and C4 floodplain unit exposed to main shear stress of storm water flow, downstream of cross section south bank appears impacted from overbank flows.

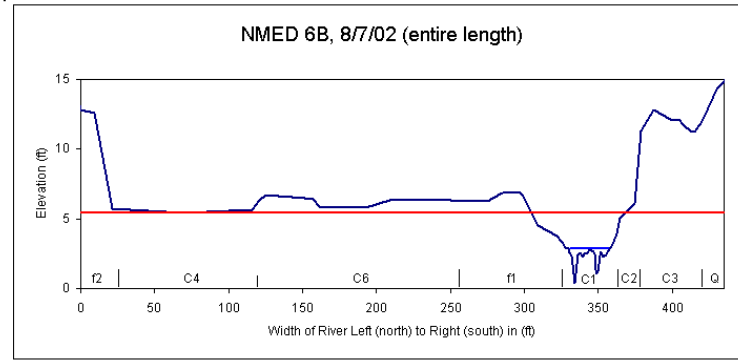
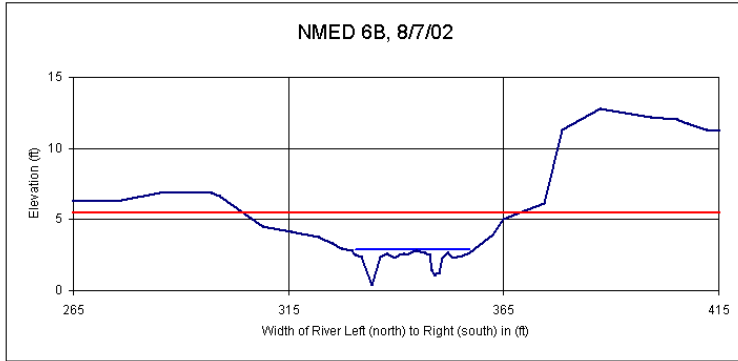


dimensions			
10.4	x-section area	1.2	d mean
9.0	width	11.4	wet P
2.5	d max	0.9	hyd radi
6.4	bank ht	7.8	w/d ratio
46.0	W flood prone are	5.1	ent ratio

Remarks: 1115' downstream, E type channel, deepening and widening channel. Main impact within active channel and overflow onto floodplain.

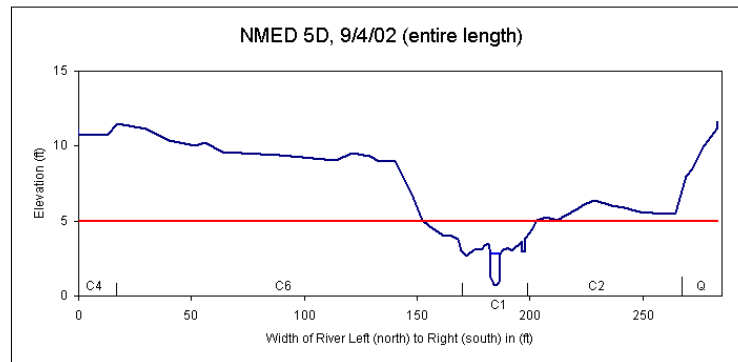
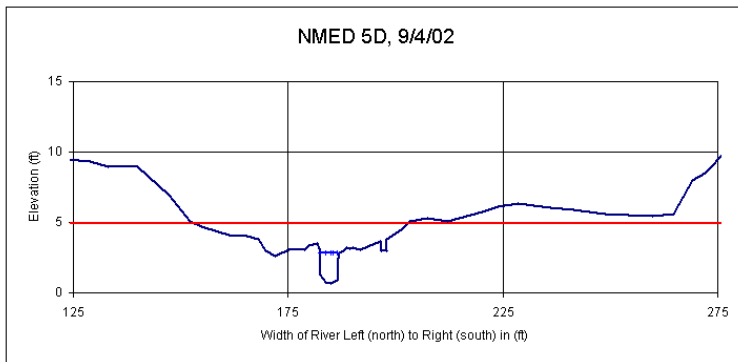
Figure E8. Cross sections 9 and 7

Cross Sections 6B and 5D, upstream to downstream



dimensions			
12.8	x-section area	1.0	d mean
12.3	width	14.5	wet P
2.5	d max	0.9	hyd radi
6.3	bank ht	11.8	w/d ratio
62.0	W flood prone are	5.0	ent ratio

Remarks: 1200' downstream, E type channel, 10' bank on south side of channel from above cross section 6b to 5b in c3 and c2 units vulnerable to high erosion potential, channel at 415 conveys flow from overflow above cross section 20. Place grade controls within channel (feature at 415) to prevent bank impacts when overflow reenters main channel.

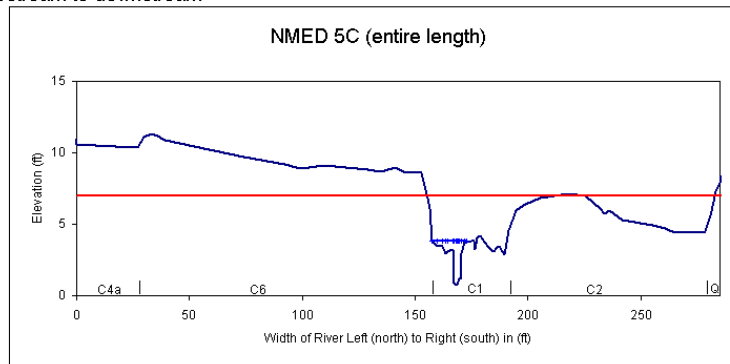
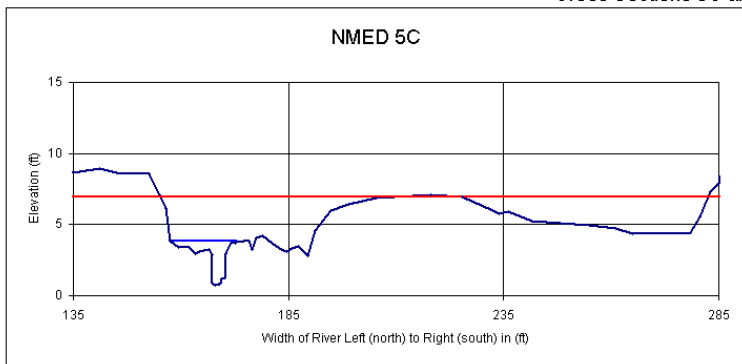


dimensions			
7.7	x-section area	2.0	d mean
3.9	width	4.0	wet P
2.1	d max	1.9	hyd radi
5.7	bank ht	2.0	w/d ratio
51.0	W flood prone are	13.1	ent ratio

Remarks: 1325' downstream, E type channel, south side of channel in younger C2 unit most exposed. C6 unit on north side of channel. Old channel at 250 feet conveys high waters onto floodplain units impacting downstream edge of floodplain.

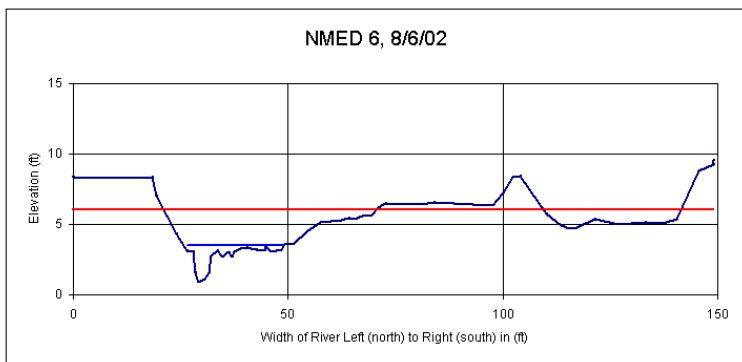
Figure E9. Cross sections 6b and 5d

Cross Sections 5C and 6, upstream to downstream



dimensions			
15.2	x-section area	1.0	d mean
15.5	width	19.5	wet P
3.1	d max	0.8	hyd radi
6.2	bank ht	15.7	w/d ratio
50.0	W flood prone are	3.2	ent ratio

Remarks: 1385' downstream, C type channel, deepening and widening channel, 5' bank C6 bank vulnerable to increased erosion on north side of channel. Old channel at 275 feet conveys high waters onto C6 floodunits downstream.

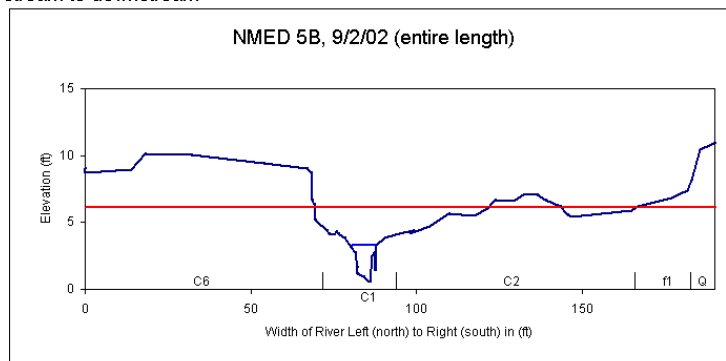
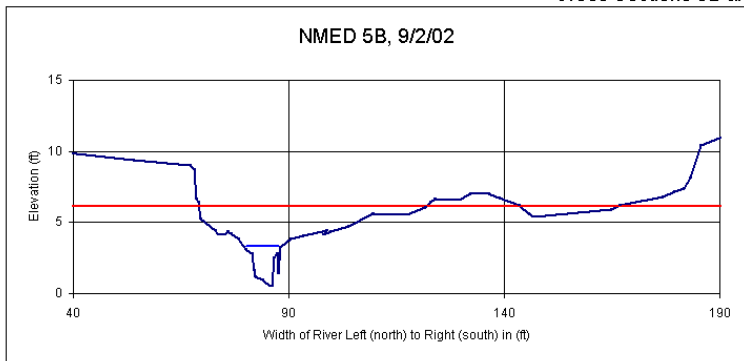


dimensions			
15.7	x-section area	0.7	d mean
22.5	width	25.5	wet P
2.6	d max	0.6	hyd radi
5.5	bank ht	32.3	w/d ratio
47.0	W flood prone are	2.1	ent ratio

Remarks: 1443' downstream, Bc type channel, deepening and widening channel, 5' bank C6 unit on north vulnerable to increased erosion, bank should be armored or flow redirected away from bank. Old channel at 125 feet conveys high waters onto C6 units downstream.

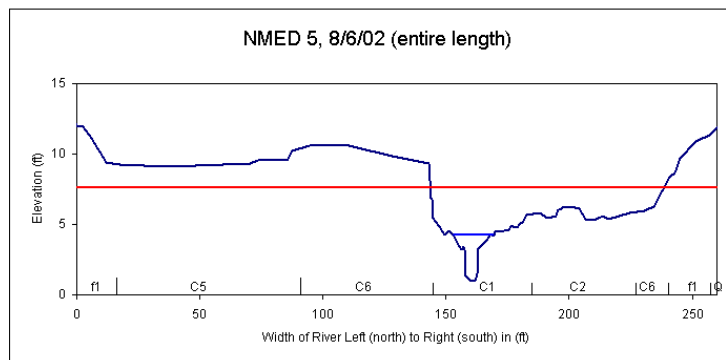
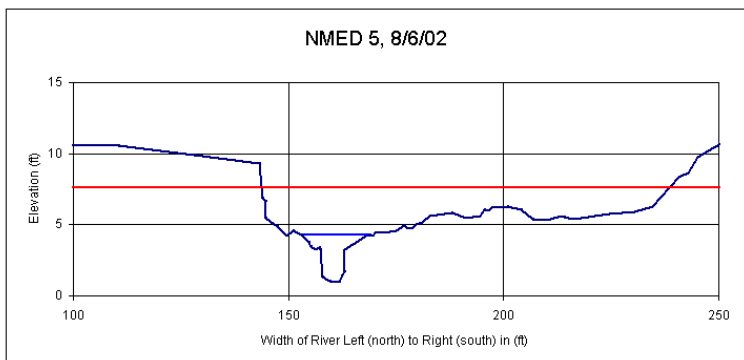
Figure E10. Cross sections 5c and 6

Cross Sections 5B and 5, upstream to downstream



dimensions			
12.6	x-section area	1.7	d mean
7.5	width	11.4	wet P
2.8	d max	1.1	hyd radi
6.5	bank ht	4.5	w/d ratio
54.0	W flood prone are	7.2	ent ratio

Remarks: 1503' downstream, E type channel, deepening and widening channel, 5' bank C6 unit on north vulnerable to increased erosion, bank should be armored or flow redirected away from bank. Channel at 150' conveys water onto C6 unit downstream.

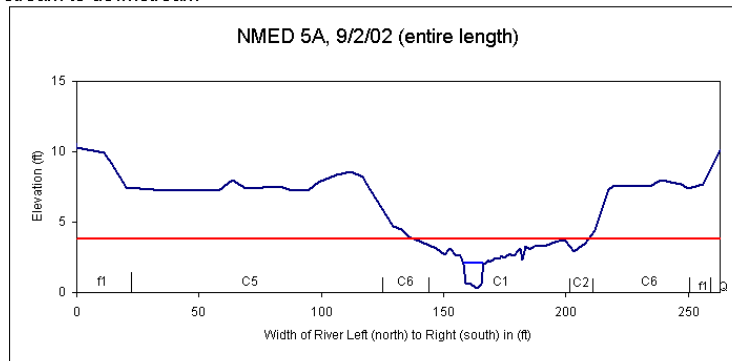
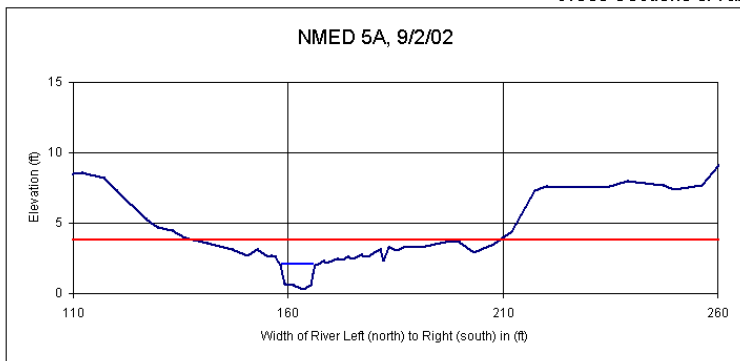


dimensions			
22.2	x-section area	1.4	d mean
15.6	width	19.0	wet P
3.3	d max	1.2	hyd radi
8.4	bank ht	10.9	w/d ratio
98.0	W flood prone are	6.3	ent ratio

Remarks: 1508' downstream, E type channel, deepening and widening channel, 5' bank C6 unit on north vulnerable to increased erosion, bank should be armored or flow redirected away from bank. Channel at 205 to 235 conveys water through C6 unit. (grade controls, structures to redirect water away from C6 unit)

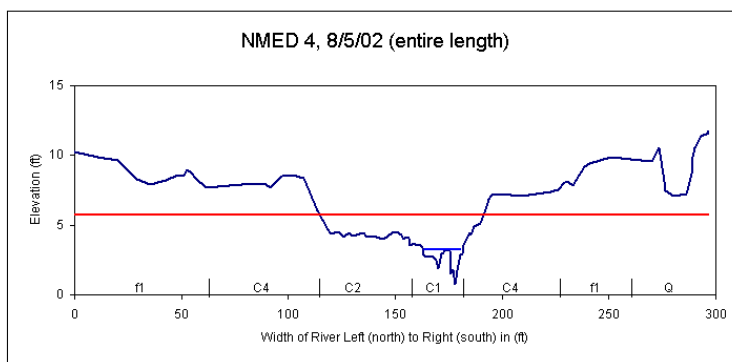
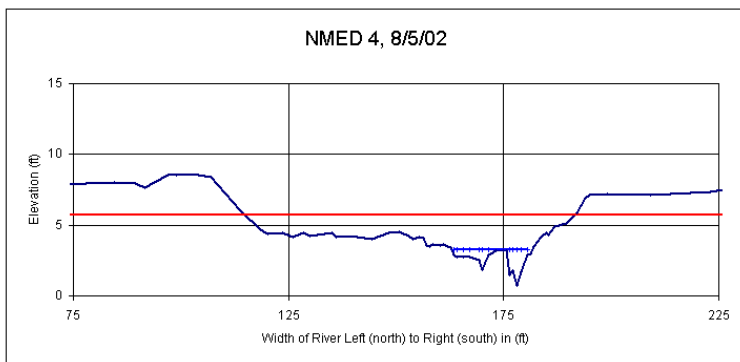
Figure E11. Cross sections 5b and 5

Cross Sections 5A and 4, upstream to downstream



dimensions			
11.1	x-section area	1.4	d mean
7.8	width	8.9	wet P
1.8	d max	1.2	hyd radi
7.0	bank ht	5.5	w/d ratio
71.0	W flood prone are	9.1	ent ratio

Remarks: 1544' downstream, E type channel, deepening and widening channel, C5 and 6 units on north bank and C6 unit on south bank, old C2 channel conveys high water through c6 unit on south bank (grade control in old channel). Downstream coarse grained sediments aggrading on active flood plain and multiple channels being sustained.

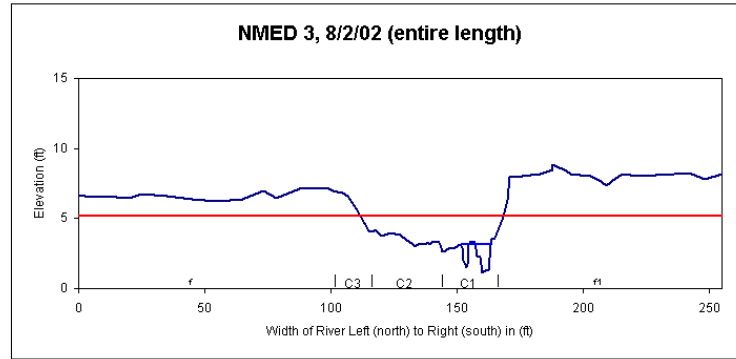
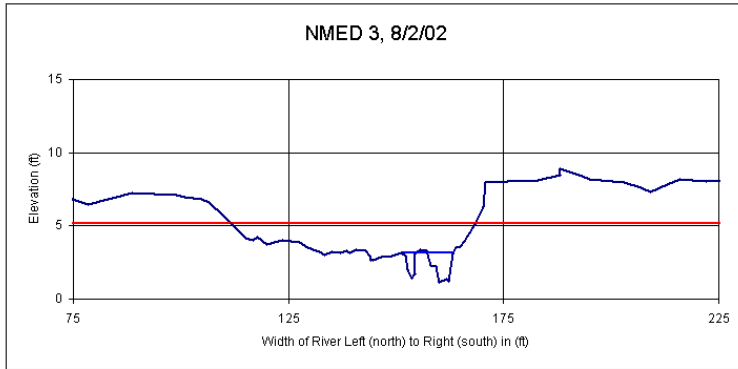


dimensions			
11.7	x-section area	0.9	d mean
12.4	width	14.3	wet P
2.5	d max	0.8	hyd radi
6.4	bank ht	13.1	w/d ratio
74.0	W flood prone are	6.0	ent ratio

Remarks: 1822' downstream, C (DA) type channel, Coarse grained sediments depositing on flood plains, multiple channels sustained (channel aggrading?). Channel on south bank just downstream of cross section 4 contributing large supply of sediments from quaternary valley wall sources. Large amount of road runoff.

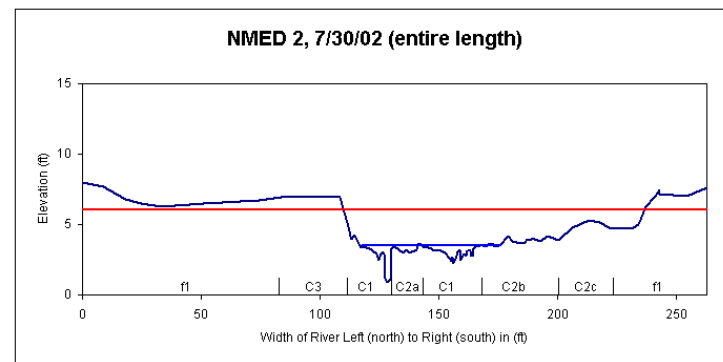
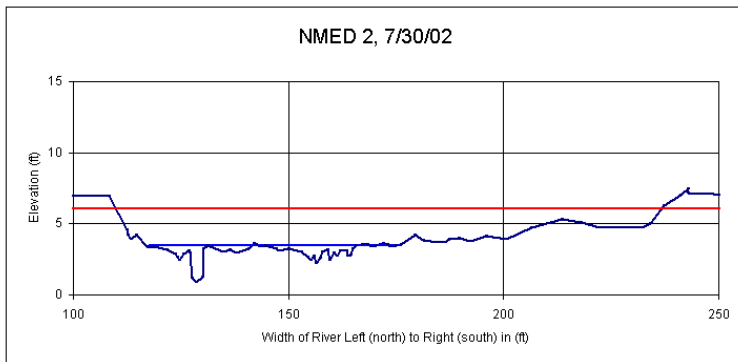
Figure E12. Cross sections 5a and 4

Cross Sections 3 and 2, upstream to downstream



dimensions			
10.8	x-section area	1.2	d mean
9.2	width	12.0	wet P
2.0	d max	0.9	hyd radi
5.7	bank ht	7.8	w/d ratio
56.0	W flood prone are	6.1	ent ratio

Remarks: 2258' downstream, E (DA) type channel, multiple channel, coarse sediments being deposited on active flood plain. C3 unit on north bank.

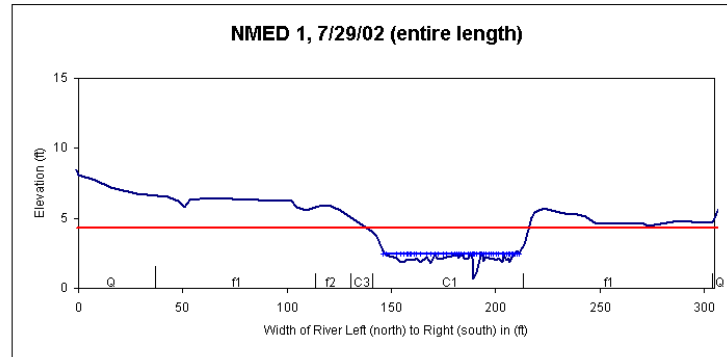
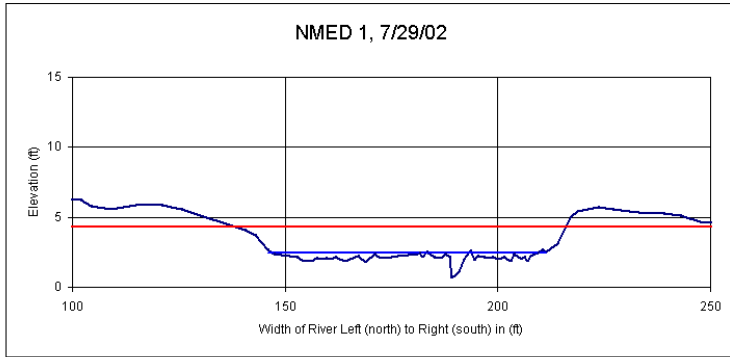


dimensions			
19.5	x-section area	0.6	d mean
31.4	width	36.4	wet P
2.6	d max	0.5	hyd radi
6.0	bank ht	50.4	w/d ratio
125.0	W flood prone are	4.0	ent ratio

Remarks: 2267' downstream, C (DA) type channel, multiple channels, coarse grained sediments being deposited on active flood plain (aggrading?, channel on north deepening). C3 unit on north bank.

Figure E13. Cross sections 3 and 2

Cross Sections 1, last downstream cross section



dimensions			
23.9	x-section area	0.4	d mean
61.9	width	64.6	wet P
1.8	d max	0.4	hyd radi
4.8	bank ht	160.2	w/d ratio
76.0	W flood prone are	1.2	ent ratio

Remarks: 2875' downstream, F (DA) type channel, Multiple channels, sediments being deposited on widening flood plain. C3 unit on north bank.

Figure E14. Cross section 1

Appendix F. DOE OB 2001 and 2002 Plutonium-239/240 and Suspended Sediment Concentrations in Pueblo Canyon Storm Water

The measured plutonium-239/240 and suspended sediment concentrations for 65 storm water samples are compiled in the following table. The samples were collected in Pueblo and Acid Canyons during 2000 through 2002. Automated ISCO[®] and grab samples were collected from 9 rainfall runoff events during 2001 and 2002. We estimated mass transport inventories at E060 for 6 of the events. Flow estimates for the remaining events were not available for this report (for example the 10/25/02, 10/26/02, and 11/1/02 storm events).

Samples collected in several Pajarito drainages during 2000 led us to focus our work in Pueblo Canyon. Further adjustments to our sampling program included particle size distribution analysis in 2002. For additional information regarding the development of our sampling program and the use of this data see Appendix A regarding developing evaluations and Appendix G for mass transport inventory representations.

Station names are listed in the first column and reflect the canyon name and mileage from its downstream confluence. For example PU-0.3 is the station at E060 stream gage in Pueblo Canyon, approximately 0.3 mile upstream from the confluence with Los Alamos Canyon. Plate 4 shows NMED storm water locations as well as LANL sediment surveillance stations. Ten year averages of LANL plutonium measurements were presented in Figure 12 for the LANL sediment stations.

For the 2001 storm water samples, concentrations of dissolved plutonium, total plutonium, and plutonium in suspended sediments were measured. Five samples were filtered, the dissolved phase measured, and designated by F in the second column. UF designates unfiltered, total, whole water sample analysis. After 2001 only total plutonium in water and plutonium in sediments were measured. Plutonium is fairly insoluble and dissolved phase measurements were regularly near detection levels

The date, time, and collection type (automated ISCO or grab sample methods) are listed in the following 3 columns. The dissolved and total plutonium-239/240 concentrations are listed in column 6 and measured in picocuries per liter. Suspended sediments were separated from the water samples, analyzed for plutonium and reported in picocuries per gram in column 7. The suspended sediment concentrations are reported as milligrams per liter in the last column.

NMED Stormwater Locations and LANL Sediment Stations

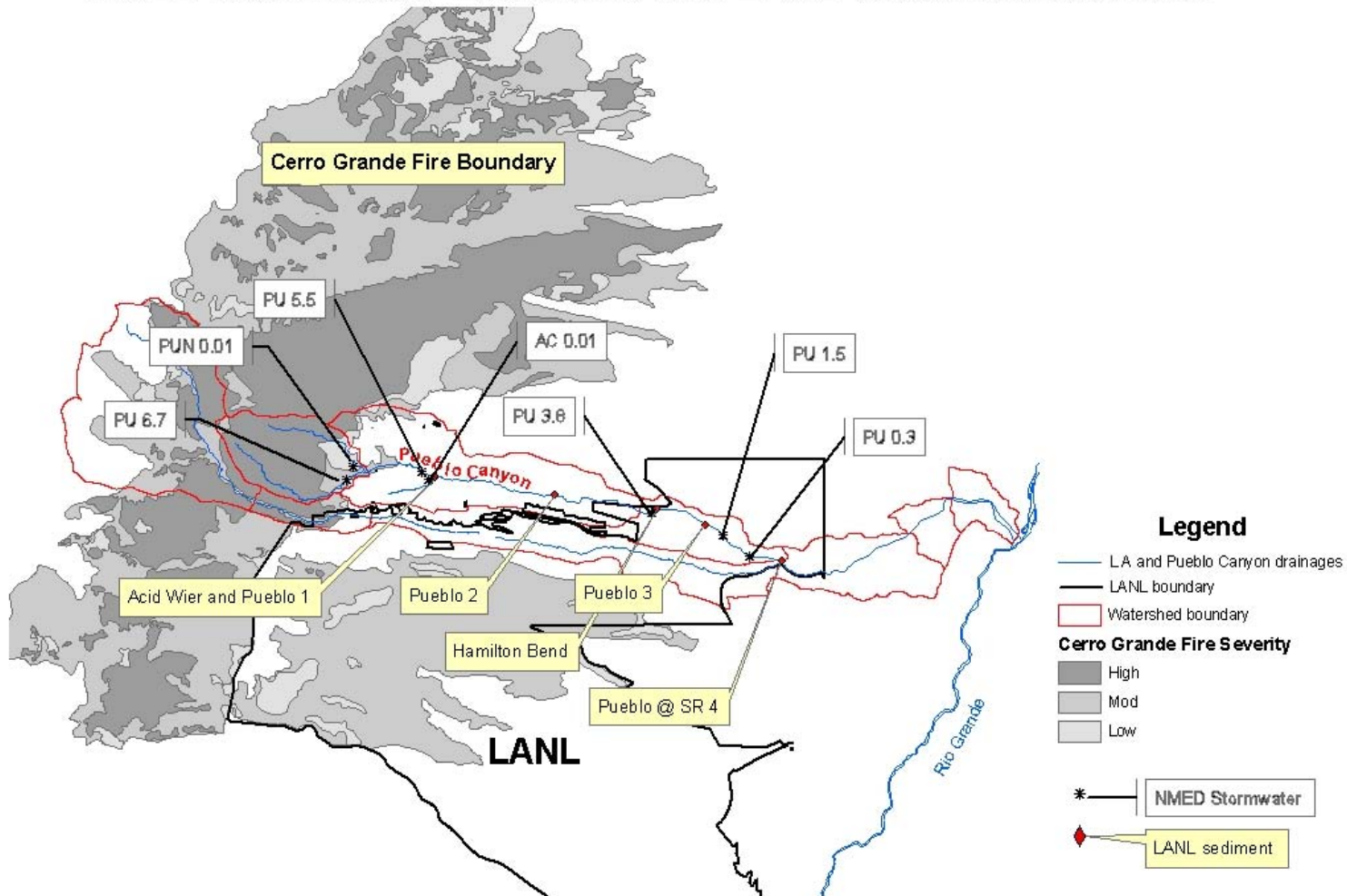


Plate 4. Project Map of P4W in Pueblo Canyon

Table F1. NMED DOE OB 2000, 2001, and 2002 Plutonium-239/240 and Suspended Sediment Concentrations in Pueblo Canyon system

STATION NAME	F/UF	DATE	TIME	Type	Pu-239/240 (pCi/L)	Pu-239/240 (pCi/g)	SSC mg/L
PUN 0.1	F	9/8/2000	16:30	Grab	0.03	0.06	NA
SFAC 0.01	F	9/8/2000	NA	Grab	2.00	107	NA
AC-0.5	F	9/8/2000	NA	Grab	0.16	0.2	NA
PU 2.0	F	9/8/2000	18:00	Grab	0.04	0.18	NA
PU 6.7	F	9/8/2000	16:50	Grab	0.04	0.06	NA
SFAC 0.01	F	10/12/2000	12:00	Grab	2.6	Commingled	NA
SFAC 0.01	F	10/13/2000	15:00	Grab	16.4		38.1
AC 0.5	F	10/12/2000	12:15	Grab	< 0.2	0.1	NA
PUN 0.1	F	10/28/2000	14:00	Grab	< 0.07	0.22	NA
PU 2.0	F	10/28/2000	11:08	Grab	0.11	3.92	NA
PU-0.3	F	8/11/2001	14:58	ISCO	0.02	NA	NA
PU-0.3	UF	8/11/2001	14:58	ISCO	55.8	1.05	53,510
PU-0.3	F	8/11/2001	15:56	ISCO	0.04	NA	NA
PU-0.3	UF	8/11/2001	15:56	ISCO	46.2	1.5	30,100
PU-0.3	F	8/11/2001	17:17	ISCO	0.037	NA	NA
PU-0.3	UF	8/11/2001	17:17	ISCO	42.8	1.96	20,100
PU-0.3 (dup)	UF	8/11/2001	17:17	ISCO	44.9	NA	NA
PU-0.3	F	8/16/2001	20:37	ISCO	0.47	6.02	NA
PU-0.3	UF	8/16/2001	20:37	ISCO	253	5.83	39,400
PU-0.3	F	8/16/2001	21:37	ISCO	0.046	NA	NA
PU-0.3	UF	8/16/2001	21:37	ISCO	103	5.16	19,400
PU-0.3	UF	6/22/2002	1:49	ISCO	161	1.67	84,500
PU-0.3	UF	6/22/2002	2:29	ISCO	197	4.82	40,800
PU-0.3	UF	6/22/2002	3:14	ISCO	151	5.52	24,200
PU-0.3	UF	6/22/2002	3:59	ISCO	123	5.63	19,500

STATION NAME	F/UF	DATE	TIME	Type	Pu-239/240 (pCi/L)	Pu-239/240 (pCi/g)	SSC mg/L
PUN-0.01	UF	7/18/2002	17:30	Grab	0.89	0.04	37,996
PU-6.7	UF	7/18/2002	17:40	Grab	0.49	0.04	13,470
PU-5.5	UF	7/18/2002	14:03	ISCO	3.4	0.02	71,200
PU-0.3	UF	7/18/2002	20:38	ISCO	147	5.88	17,300
PU-0.3	UF	7/18/2002	21:34	ISCO	124	5.3	17,900
PU-0.3	UF	7/18/2002	22:34	ISCO	84	4.07	12,900
PU-5.5	UF	7/25/2002	23:35	ISCO	10.8	0.04	153,000
PU-0.3	UF	7/26/2002	0:36	ISCO	61.4	3.12	39,780
PU-0.3	UF	7/26/2002	1:24	ISCO	85	3.96	26,120
PU-0.3	UF	7/26/2002	2:24	ISCO	61.2	4.74	17,210
PU-6.7	UF	9/10/2002	13:40	Grab	0.13	0.04	5,234
AC-0.01	UF	9/10/2002	12:55	Grab	2.64	9.1	74
PU-5.5	UF	9/10/2002	12:50	Grab	0.15	0.03	5,464
PU-3.8	UF	9/10/2002	14:30	Grab	27.2	3.48	11,621
PU-1.5	UF	9/10/2002	15:00	Grab	19.1	4.07	4,741
PU-0.3	UF	9/10/2002	15:10	ISCO	3.7	1.22	781
PU-0.3	UF	9/10/2002	15:57	ISCO	7.27	3.42	2,490
PU-0.3	UF	9/10/2002	16:52	ISCO	11	4.12	2,450
PU-0.3	UF	10/25/2002	11:37	ISCO	1.32	2.41	583
PU-0.3	UF	10/25/2002	12:37	ISCO	0.88	2.26	341
PU-0.3	UF	10/25/2002	13:37	ISCO	0.33	1.82	238
PU-0.3	UF	10/25/2002	14:37	ISCO	2.18	NA	135
PU-0.3	UF	10/25/2002	15:37	ISCO	0.15	NA	46
PU-0.3	UF	10/25/2002	16:37	ISCO	0.13	NA	111

STATION NAME	F/UF	DATE	TIME	Type	Pu-239/240 (pCi/L)	Pu-239/240 (pCi/g)	SSC mg/L
AC-0.01	UF	10/26/2002	19:50	ISCO	6.03	22.3	320
AC-0.01	UF	10/26/2002	20:50	ISCO	2.07	NA	51
AC-0.01	UF	10/26/2002	21:50	ISCO	0.17	NA	38
AC-0.01	UF	10/26/2002	22:50	ISCO	2.3	NA	21
AC-0.01	UF	10/26/2002	23:50	ISCO	1.91	NA	12
PU-5.5	UF	10/26/2002	18:48	ISCO	0.05	0.06	1,437
PU-5.5	UF	10/26/2002	19:48	ISCO	0.08	0.03	2,458
PU-5.5	UF	10/26/2002	20:48	ISCO	0.06	0.02	1,708
PU-5.5	UF	10/26/2002	21:48	ISCO	0.02 <	0.02	1,425
PU-5.5	UF	10/26/2002	22:48	ISCO	< 0.01 <	0.03	942
PU-5.5	UF	10/26/2002	23:48	ISCO	< 0.008	0.02	515
PU-0.3	UF	11/1/2002	12:52	ISCO	4.54	2.21	503
PU-0.3	UF	11/1/2002	13:52	ISCO	0.48	2.37	212
PU-0.3	UF	11/1/2002	14:52	ISCO	0.19	NA	68
PU-0.3	UF	11/1/2002	15:52	ISCO	0.15	NA	39
PU-0.3	UF	11/1/2002	16:52	ISCO	0.14	NA	27
PU-0.3	UF	11/1/2002	17:52	ISCO	0.11	NA	19

NA = not analyzed

< indicates measurement was less than minimum detectable activity

Table F2. Particle Size Distribution for Storm water Samples in Pueblo Canyon

Station	Date	Time	Percent Weight										
			Gravel	Sand (in millimeters)					Silt		total sand	total silt	clay
				2.0 - 1.0	1.0 - 0.5	0.5 - 0.25	0.25 - 0.025	.025 - 0.0625	fine silt	coarse silt			
PU 0.3 a	9/10/2002	15:10	0	0	0.4	4.2	2	1.1	46.1	8.2	6.4	54.3	37.4
PU 0.3 b	9/10/2002	15:57	0	0	0.6	2.2	1.4	0.6	54.8	6.3	4.7	61	34.2
PU 0.3 c	9/10/2002	16:52	0	0	0	1.5	2.1	1.6	50.7	1.4	5.2	52.1	42.6
PU 0.3 d	6/22/2002	1:49	0	0	0.1	0.3	0.5	0.5	57.4	13.6	1.3	71	27.7
PU 0.3 e	6/22/2002	2:29	0	0	0	0	0.1	0.1	53.2	24	0.2	77.2	22.6
PU 0.3 f	6/22/2002	3:14	3	0	0.3	0.3	0.2	0.7	57.9	14.3	1.4	72.1	25.5
PU 0.3 g	6/22/2002	3:58	0	0.1	0.1	0.3	0.2	0.9	57.4	10.7	1.6	68.2	30.3
PU 5.5 h	7/15/2002	14:03	0	0.1	1.2	0.4	5.3	6.8	33.4	36.5	16.8	69.9	13.3
PU 5.5 h dup				0.1	1.1	3.6	5.5	6.3	32	35.5	16.8	68	15.3
PU 5.5 l	7/25/2002	21:33	0	0.1	0.7	1.8	4.3	9	33.1	36.4	15.6	69.5	14.8
PU 5.5 j	7/25/2002	23:35	0	0.1	0.9	5.7	4.4	7.4	30.7	36.7	18.4	67.3	14.2
PU 5.5 j dup				0	1	0	5.4	8.5	31.5	35.5	18.1	67.1	14.6
PU 0.3 k	7/26/2002	0:36	0	0	0	0.2	0.4	0.3	59.5	4.4	1	64	35
PU 0.3 l	7/26/2002	1:24	0	0.1	0.1	0.2	0.5	0.3	52.9	4.6	1.2	57.5	45.3
PU 0.3 m	7/26/2002	2:24	11	0.1	0.1	0.3	0.3	0.1	50.9	3.5	0	54.4	44.9
PU 5.5 n	9/10/2002	12:50	0	0	0	0.1	0.9	2.8	41.3	35.5	4.1	75.9	19.1
PU 6.7 o	9/10/2002	13:40	0	0.2	0.4	0.9	3.6	5.2	42	36	11.4	70	10.6
PUN 0.01 p	7/18/2002	17:30	0	0.1	0.1	0.2	0.6	1.9	46.2	17.7	2.9	63.8	33.2
PUN 0.01 p dup				0	0.1	0.2	0.4	2	46	17.4	2.6	63.4	33.8
Pu 6.7 q	7/18/2002	17:40	0	0.2	0.4	0.6	1.5	3.5	50.1	22.8	6.3	73	20.7
Pu 0.3 r	7/18/2002	20:36	0	0	0.1	0.2	0.3	0.1	54.7	3.4	0.9	58.1	41
Pu 0.3 s	7/18/2002	21:34	7.6	0	0.1	0.3	0.3	0.1	47.6	2.6	1	50.2	48.6
Pu 0.3 t	7/18/2002	22:34	0	0.1	0.1	0.3	0.3	0.3	42	2.1	1	44.1	54.9

Appendix G. Plutonium-239/240 and Suspended Sediment vs Flow Plots For Storm Water Runoff Measured in 2001 and 2002

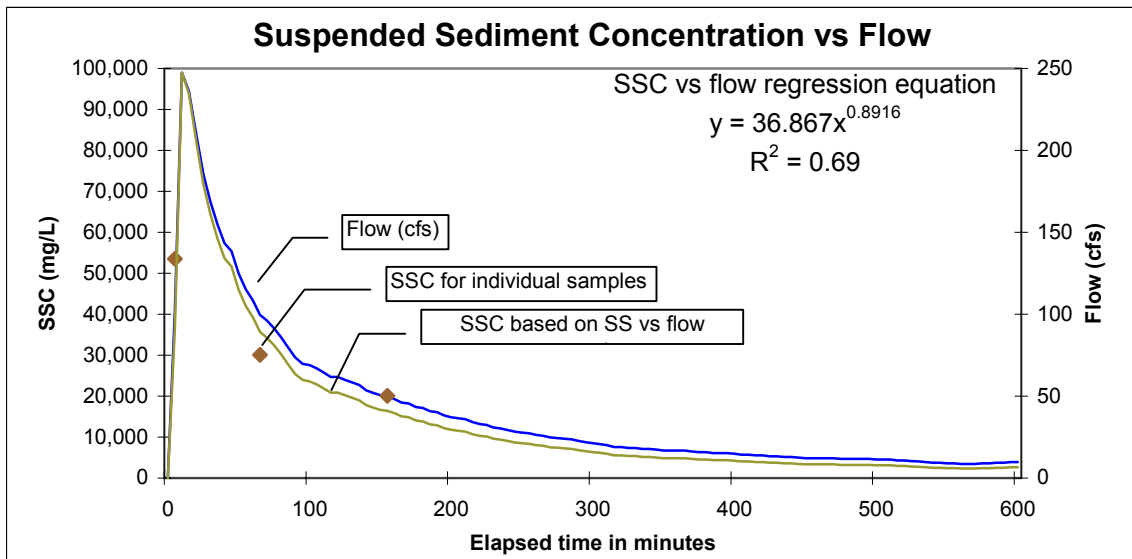
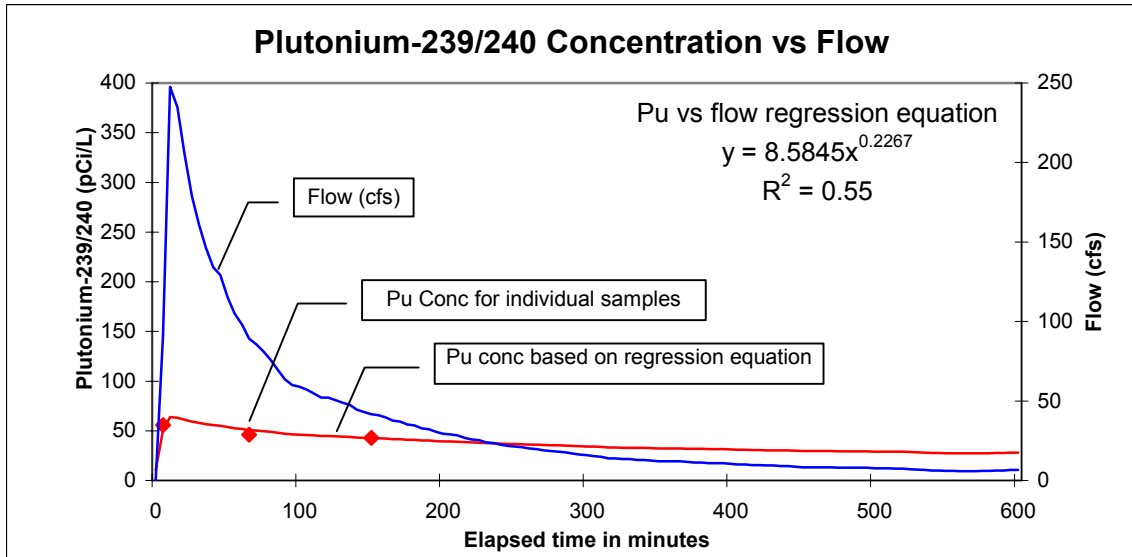
Twelve charts are presented in this appendix. They reflect the relationships of suspended sediment and plutonium-239/240 concentrations to flows measured at the E060 stream gage during 6 runoff events. For each chart, time is reflected on the bottom scale, plutonium or suspended sediment concentrations are scaled on the left, and the flow rate is presented as the blue line, scaled on the right side of the charts.

Plutonium-239/240 and flow relationships are presented in the charts on the top of each page. Suspended sediment and flow relationships are presented on the bottom. The small figures in the charts reflect the analytical measurements for storm water samples collected during the event. The lines through the small figures that represent the analytical measurements reflect the calculated concentrations throughout the runoff event and are based on the equations for the regression correlations of flow to plutonium or suspended sediment concentrations.

The maximum instantaneous flow rate or peak flow, the daily accumulative rainfall, the maximum hourly rate, as well as the time from the rainfall centroid to the beginning of the flow event are presented in the tables below the charts. The plutonium-239/240 and suspended sediment masses transported past the E060 stream gage are also presented. We presented mass transport estimates for the first hour of the runoff event, 5 hours into the event, and at 10 hours. Plutonium-239/240 mass transport is measured in mCi and suspended sediment is in tons.

The rainfall event on September 9, 2002, was a long, infiltrating, and low intensity rain over much of the state. It combined with the Bayo wastewater plant discharge (average \approx 6 cfs) generating a maximum 28 cfs flow that increased and ebbed during an approximate 10-hour period. Suspended sediment and plutonium-239/240 concentrations were low, suggesting runoff was minimal. Twenty-two of the 37 runoff events greater than 10 cfs were less than 30 cfs. This includes the July 18, 2002 event, a storm of shorter duration but greater intensity, which generated a 'flashy' runoff and 3 times more suspended sediment and plutonium-239/240 mass transported beyond E060 than the event on September 9.

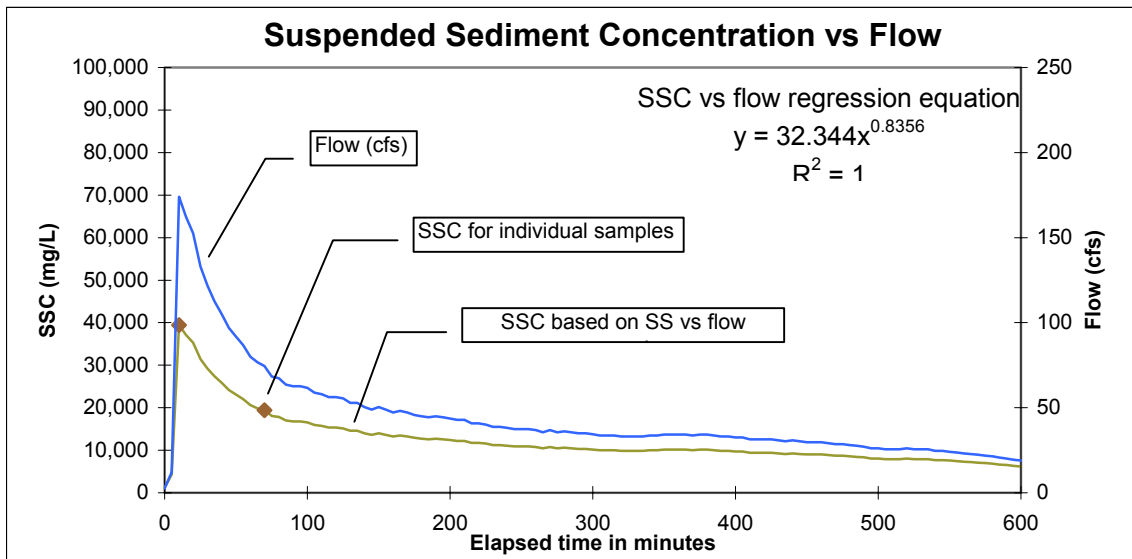
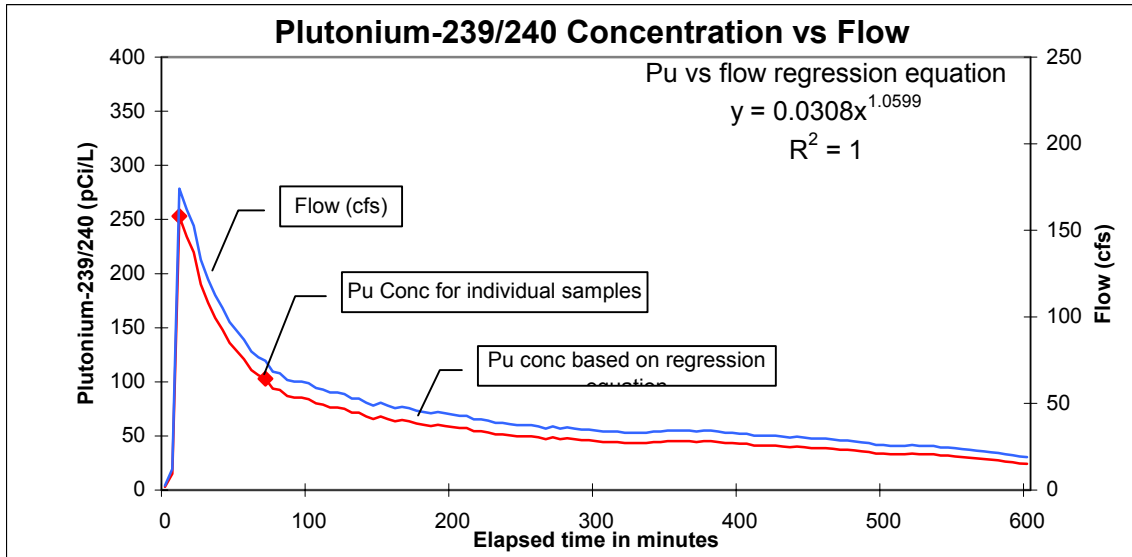
Figure G-1. Plutonium-239/240 and Suspended Sediment Concentration Relationships to Flow during August 11, 2001 Runoff Event



Daily precipitation accumulation 0.71"
 Max hourly rate 11:00-12:00 0.55"/hr
 Peak Flow Time at E060: 15:10 248 cfs
 Peak flow 3 hours 40 minutes after rain centroid

Time into event	1 hour	5 hours	10 hours
Plutonium transport inventory (mCi)	0.91	1.6	1.74
Sediment transport inventory (tons)	1223	1621	1650

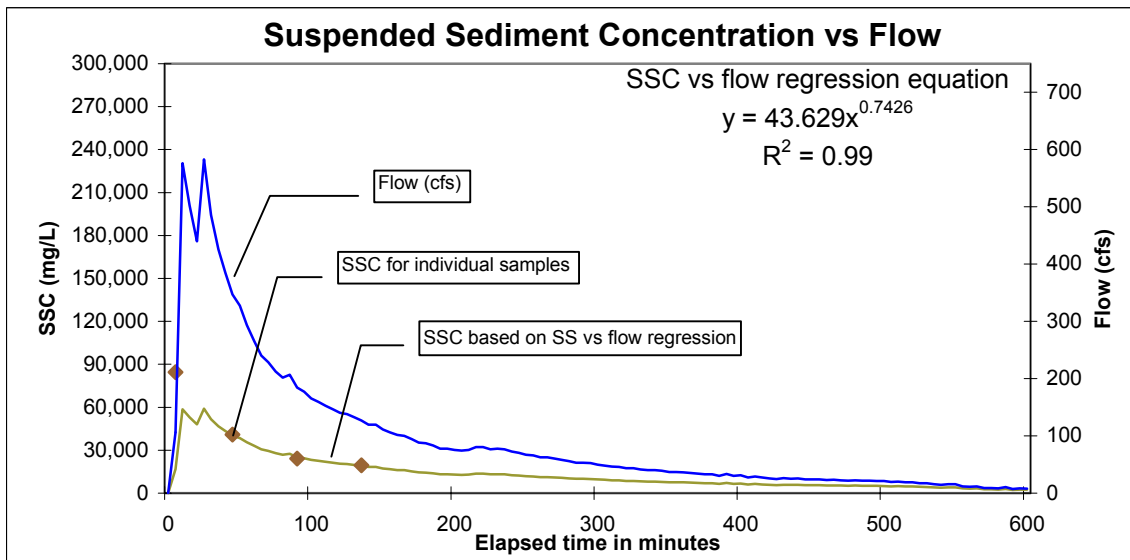
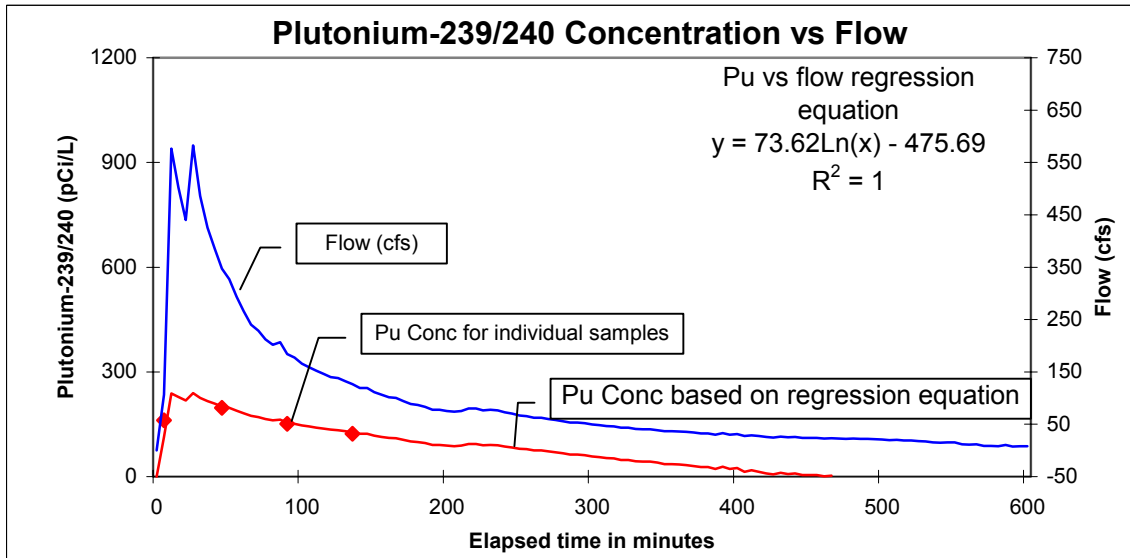
Figure G-2. Plutonium-239/240 and Suspended Sediment Concentration Relationships to Flow during August 16, 2001 Runoff Event



Daily precipitation accumulation 0.52"
 Max hourly rate 16:00-17:00 0.35"/hr
 Peak Flow Time at E060: 20:35 174 cfs
 Peak flow 4 hours 5 minutes after rain centroid

Time into event	1 hour	5 hours	10 hours
Plutonium transport inventory (mCi)	2.04	3.36	3.93
Sediment transport inventory (tons)	373	673	818

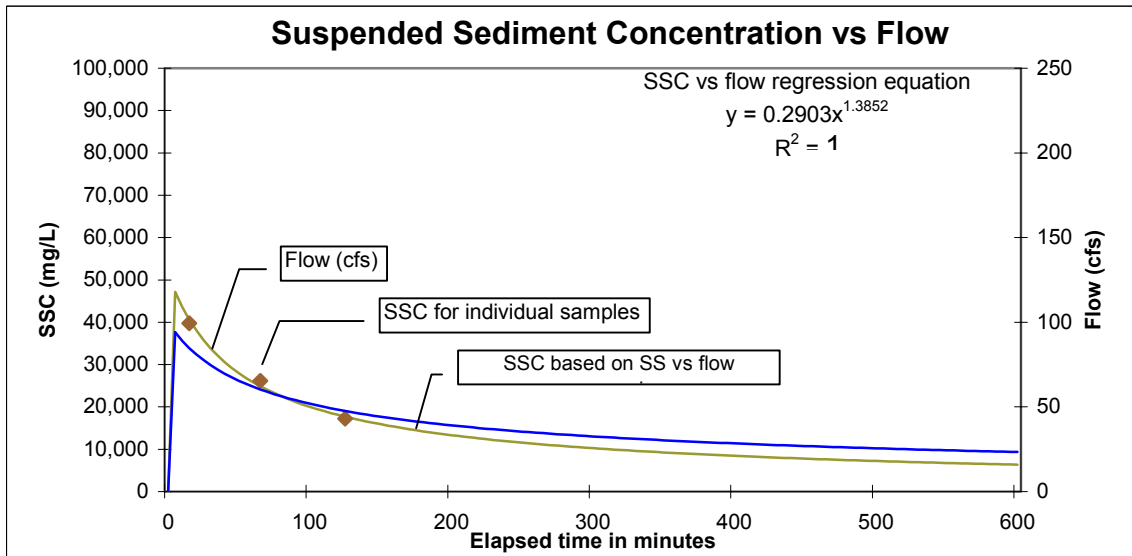
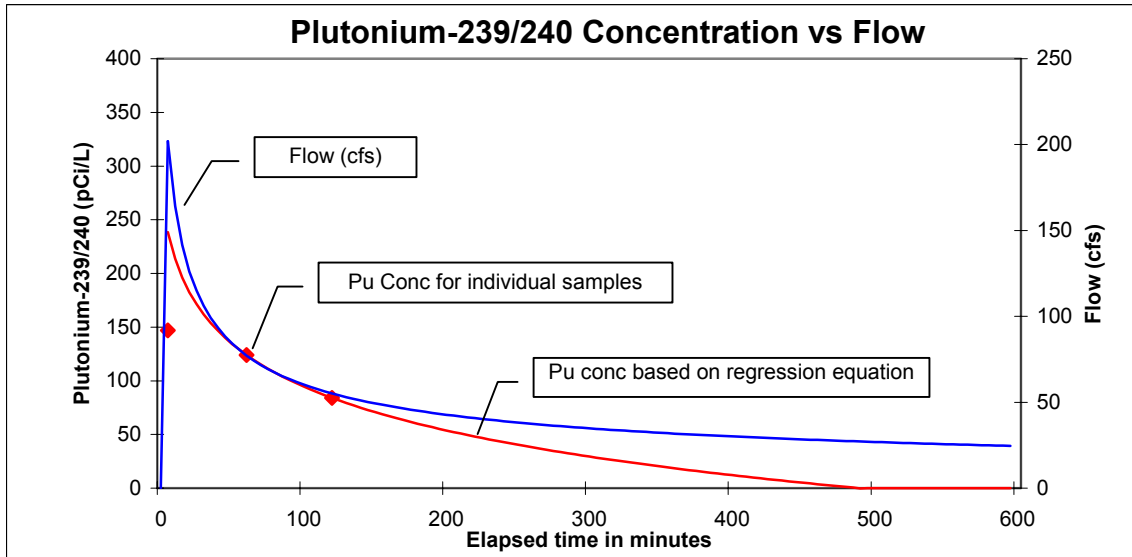
Figure G-3. Plutonium-239/240 and Suspended Sediment Concentration Relationships to Flow during June 22, 2002 Runoff Event



Daily precipitation accumulation 1.38"
 Max hourly rate 21:00-22:00 0.80"/hr
 Peak Flow Time at E060: 00:45 583 cfs
 Peak flow 3 hours 15 minutes after rain centroid

Time into event	1 hour	5 hours	10 hours
Plutonium transport inventory (mCi)	8.66	14.06	14.34
Sediment transport inventory (tons)	2109	3045	3136

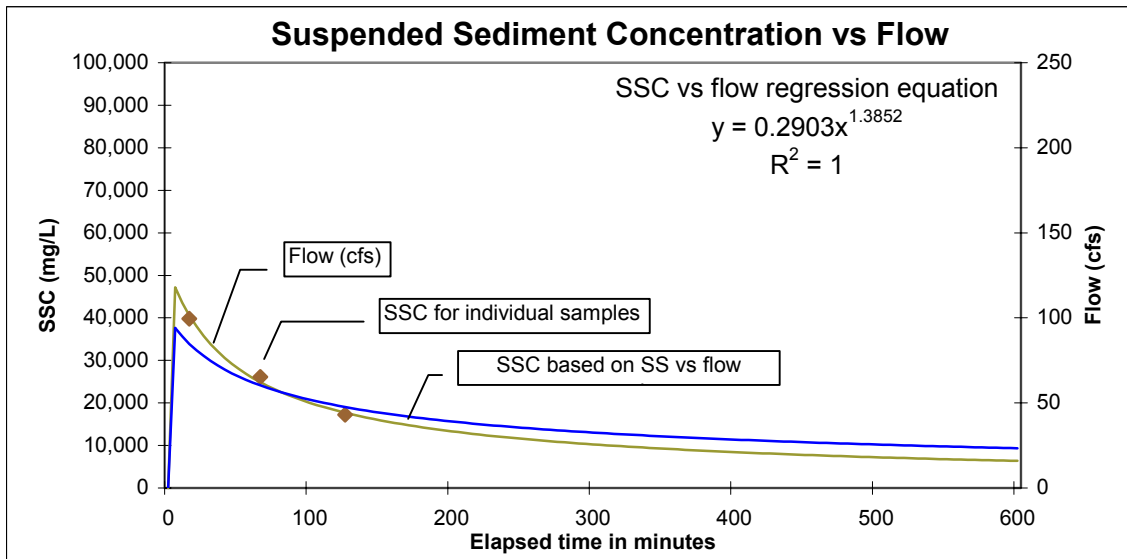
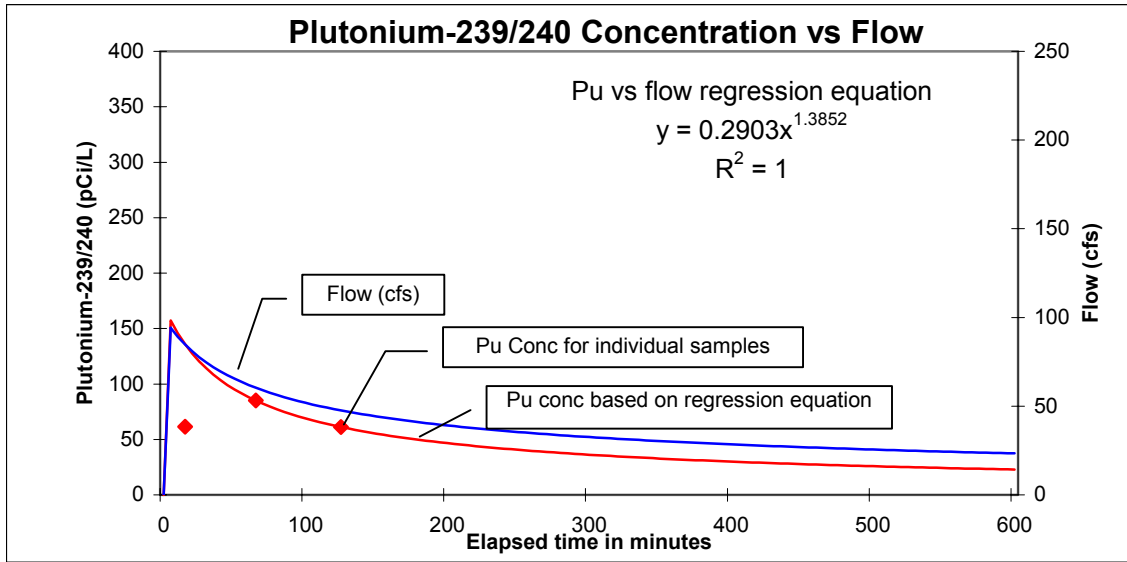
Figure G-4. Plutonium-239/240 and Suspended Sediment Concentration Relationships to Flow during July 18, 2002 Runoff Event



Daily precipitation accumulation 0.25"
 Max hourly rate 15:00-16:00 0.18"/hr
 Peak Flow Time at E060: 22:05 53 cfs
 Peak flow 6 hours 35 minutes after rain centroid

Time into event	1 hour	5 hours	10 hours
Plutonium transport inventory (mCi)	0.73	1.07	1.59
Sediment transport inventory (tons)	115	248	312

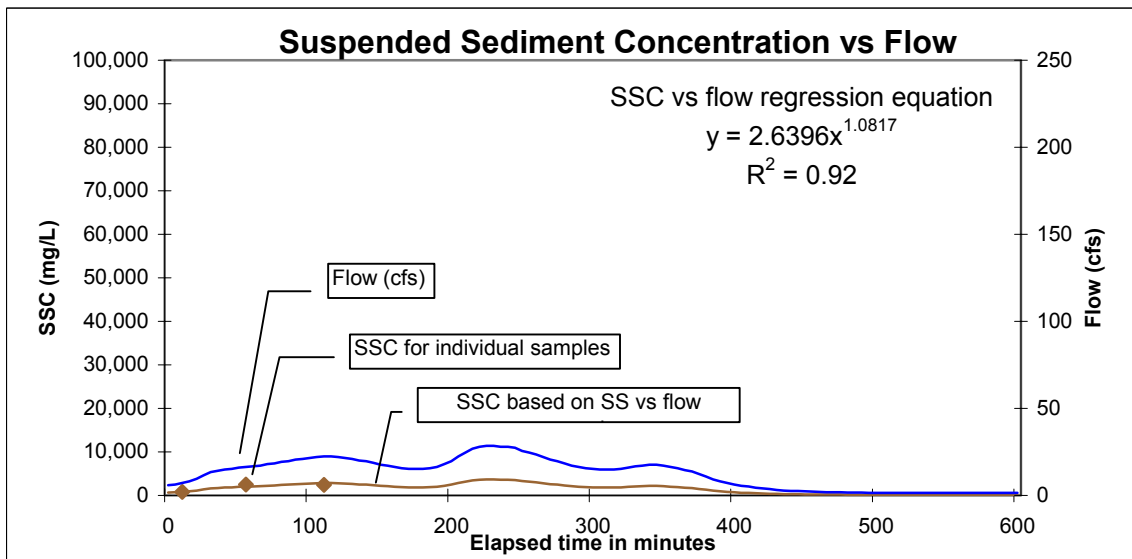
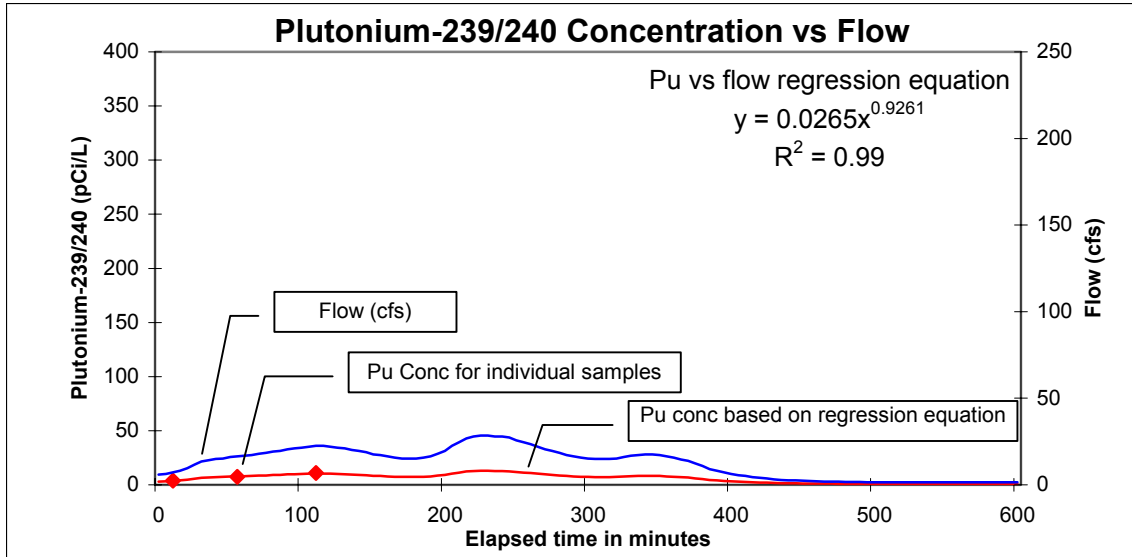
Figure G-5. Plutonium-239/240 and Suspended Sediment Concentration Relationships to Flow during July 26, 2002 Runoff Event



Daily precipitation accumulation 0.60"
 Max hourly rate 19:00-20:00 0.42"/hr
 Peak Flow Time at E060: 01:35 94 cfs
 Peak flow 6 hours after rain centroid

Time into event	1 hour	5 hours	10 hours
Plutonium transport inventory (mCi)	0.91	1.86	2.26
Sediment transport inventory (tons)	297	601	724

Figure G-6. Plutonium-239/240 and Suspended Sediment Concentration Relationships to Flow during September 10, 2002 Runoff Event



Daily precipitation accumulation 1.29''
 Max hourly rate 05:00-06:00 0.32''/hr
 Peak Flow Time at E060: 05:45 29 cfs
 Undetermined time from rain centroid to peak flow, long low intensity rainfall

Time into event	1 hour	5 hours	10 hours
Plutonium transport inventory (mCi)	0.01	0.09	0.11
Sediment transport inventory (tons)	2	27	32